

The University of Maine

DigitalCommons@UMaine

---

Electronic Theses and Dissertations

Fogler Library

---

Summer 8-12-2022

## Developing and Characterizing a Novel TEMPO CNF Hydrogel Adjuvant and Delivery System for Aquatic Vaccines

Kora Kukk

University of Maine, bajeepgirl@gmail.com

Follow this and additional works at: <https://digitalcommons.library.umaine.edu/etd>



Part of the [Aquaculture and Fisheries Commons](#), and the [Biomaterials Commons](#)

---

### Recommended Citation

Kukk, Kora, "Developing and Characterizing a Novel TEMPO CNF Hydrogel Adjuvant and Delivery System for Aquatic Vaccines" (2022). *Electronic Theses and Dissertations*. 3644.

<https://digitalcommons.library.umaine.edu/etd/3644>

This Open-Access Thesis is brought to you for free and open access by DigitalCommons@UMaine. It has been accepted for inclusion in Electronic Theses and Dissertations by an authorized administrator of DigitalCommons@UMaine. For more information, please contact [um.library.technical.services@maine.edu](mailto:um.library.technical.services@maine.edu).

**DEVELOPING AND CHARACTERIZING A NOVEL TEMPO CNF HYDROGEL  
ADJUVANT AND DELIVERY SYSTEM FOR AQUATIC VACCINES**

By

Kora Kukk

B.S University of Maine, 2021

A Thesis

Submitted in Partial Fulfillment of the  
Requirement for the Degree of  
Master of Science  
(in Biomedical Engineering)

The Graduate School

The University of Maine

August 2022

Advisory Committee:

Dr. Michael Mason, Professor of Biomedical and Chemical Engineering, Advisor

Dr. Deborah Bouchard, Aquaculture Research Institute Director, Associate Extension Professor

Dr. Karissa Tilbury, Professor of Biomedical and Chemical Engineering

© 2022 Kora Kukk

All Rights Reserved

**DEVELOPING AND CHARACTERIZING A NOVEL TEMPO CNF HYDROGEL  
ADJUVANT AND DELIVERY SYSTEM FOR AQUATIC VACCINES**

By: Kora Kukk

Thesis Advisor: Dr. Michael D. Mason

An Abstract of the Thesis Presented  
In Partial Fulfillment of the Requirements for the  
Degree of Master of Science  
(in Biomedical Engineering)  
August 2022

Aquaculture is a large part of the food production sector which is greatly expanding. One of the largest losses in aquaculture is due to pathogens. Current solutions for protecting farmed finfish from pathogens can be very expensive with variable efficiency. Current disease prevention strategies include vaccination. Types of vaccines include immersion vaccines, feed vaccines, and injectable vaccines. The most popular solution is oil-based injectable vaccines due to its protection. However, the oil-based adjuvant used in most of these formulations causes adverse reactions in the fish including reduced growth. These vaccines require multiple administrations throughout the fish's lifetime causing unwanted handling stress and additional labor costs. Preliminary trials show that cellulose nanomaterials cause minimal adverse reactions when injected into salmon and does not significantly affect their growth. The goal of this research was to create an adjuvant from cellulose nanomaterials which would increase bacterin efficacy while avoiding harmful side effects. A prolonged release formulation was also desirable, obviating the need for multiple vaccinations. Additionally, hydrogels have been used for a wide variety of applications including drug delivery, making them an attractive aquatic vaccine adjuvant. Cellulose nanomaterials were

decided as the polymer to make up the hydrogel matrix due to their biocompatibility, sustainability, high tunability, high abundance, low cost. The development of the hydrogel formulation, modifying the hydrogel for easier delivery into the salmon, measuring the diffusive properties of the hydrogel, and *in vivo* testing of the hydrogel for analysis of delivery methods and reactions to the formulation are described in this research.

## ACKNOWLEDGEMENTS

First, thank you to my advisor, Dr. Michael Mason, for introducing me to lab research back when I was an undergrad in the summer of 2018. I would also like to thank Dr. Deborah Bouchard for collaborating with Dr. Mason to obtain the grant for this research and choosing me to work on the project. Special thanks to Sarah Turner for entertaining all of my questions about finfish aquaculture and salmon, handling the salmon used in the safety studies, and performing the ELISAs. Thank you to Dr. Muhammad Hossen for being a consultant of this project and answering hydrogel formulation questions. Thank you to all the members of Mason Lab for offering advice and sharing lab equipment with me. Additional thanks go out to Dr. Mitchell Chesley for helping me find explanations for some of my data trends and when Origin misbehaved for me along with Evan Bess who helped me troubleshoot LabVIEW errors that appeared.

Additional thanks go out to Josh Hamilton and Jordan Miner for helping me create ImageJ macros and ImageJ troubleshooting for the fluorescence study. Thank you to all my undergraduate students (Jacob Holbrook, Blake Turner, Sairah Damboise, Lena Biju, and Shaun Brilliant) for helping me collect data for this research. Special thanks to Jacob Holbrook for being my right hand throughout this research and conducting some of the imaging experiments. Thank you to Dr. Emma Perry of the University of Maine Electron Microscope Laboratory for help in acquiring the SEM images.

Lastly, thank you to all my family and friends for supporting me throughout my educational journey. I wouldn't have made it here without you guys. Also thank you to my animals for being my emotional support. All the thanks in the world to my fiancé for making the long six-hour drive to visit me more times than I can count, love you!

## TABLE OF CONTENTS

ACKNOWLEDGEMENTS.....	iii
LIST OF TABLES.....	viii
LIST OF FIGURES.....	ix
LIST OF ABBREVIATIONS.....	xii
CHAPTER 1 INTRODUCTION.....	1
CHAPTER 2 LITERATURE REVIEW.....	3
2.1    Finfish Farming and Salmon.....	3
2.2    Aquaculture Vaccines.....	5
2.3    Hydrogels and Biomaterials.....	12
2.4    Cellulose Nano-Materials.....	19
CHAPTER 3 DESIGNING CITRIC ACID CROSSLINKED TEMPO CNF HYDROGELS LOADED WITH BACTERIN.....	24
3.1    Introduction.....	24
3.1.1    Crosslinking CNF.....	24
3.1.2    Considerations for Hydrogel Formulation.....	25
3.2    Materials.....	27
3.3    Methods of Formulating a TEMPO CNF and <i>Vibrio anguillarum</i> Hydrogel.....	27
3.3.1    Crosslinking TEMPO CNF with Citric Acid.....	27

3.3.2	Mixing TEMPO CNF and <i>Vibrio anguillarum</i> .....	30
3.3.3	Post Drying Addition of Antigen.....	31
3.3.4	Heating of TEMPO CNF and <i>Vibrio anguillarum</i> Mixture.....	31
3.3.5	Filtering TEMPO CNF and <i>Vibrio anguillarum</i> .....	33
3.4	Characterizing <i>Vibrio anguillarum</i> .....	35
3.5	Effects of Wash Steps on Cross-Linked Hydrogels.....	37
3.5.1	Changes in pH.....	37
3.5.2	Diffusion of Dye .....	1
 CHAPTER 4 DRYING AND REHYDRATING PROPERTIES OF		
HYDROGELS .....		
4.1	Introduction .....	4
4.2	Methods.....	5
4.2.2	Drying Methods .....	5
4.2.2	Methods of Analysis .....	6
4.3	Results and Discussion.....	8
4.3.1	Mass and Volume of Dried Hydrogels Using Different Methods .....	8
4.3.2	SEM Imaging of Different Drying Methods.....	14
4.3.3	Mechanical Properties of Dried Hydrogels.....	17
4.3.4	Mass and Volume of Rehydrated Hydrogels .....	20
4.3.5	Breakdown of Rehydrated Hydrogels over Time .....	26

4.4	Most Optimized Delivery Method .....	27
CHAPTER 5 CHARACTERIZING DIFFUSION OF BACTERIN OUT OF		
HYDROGELS .....		
		29
5.1	Introduction .....	29
5.2	Methods.....	29
5.2.1	ELISA Method.....	29
5.2.2	Coomassie Brilliant Blue Diffusion Method .....	30
5.2.3	Fluorescent <i>in vivo</i> Study Methods.....	30
5.3	Results and Discussion.....	33
5.3.1	ELISA of Bacterin in the Hydrogels.....	33
5.3.2	Diffusion of Coomassie Brilliant Blue from Rehydrated Hydrogels .....	35
5.3.3	Fluorescent <i>in vivo</i> Study.....	38
CHAPTER 6 EFFECT OF CITRIC ACID CROSSLINKED HYDROGEL		
VACCINES ON SALMON.....		
		47
6.1	Introduction .....	47
6.2	Methods.....	47
6.2.1	First Safety Study.....	47
6.2.2	Second Safety Study .....	49
6.3	Results and Discussion.....	50
6.3.1	First Safety Study.....	50

6.3.2	Second Safety Study .....	53
6.3.3	Comparison of Hydrogel Delivery Methods.....	57
CHAPTER 7 CONCLUSION.....		58
7.1	Summary .....	58
7.2	Recommendations and Future Work.....	61
REFERENCES .....		63
APPENDICES .....		70
Appendix A: Stress Strain Curves from Mechanical Testing .....		70
Appendix B: Short Term Rehydrating Data.....		72
Appendix C: Salmon Scoring Reference Sheet.....		73
AUTHOR BIOGRAPHY.....		75

## LIST OF TABLES

Table 2.2: Comparison of common natural polymers used to make hydrogels.....	18
Table 3.1: Common Cellulose Crosslinkers .....	25
Table 3.2: Desired Characteristics of Designed Aquaculture Vaccine Hydrogel.....	26
Table 4.1: Volume Comparison of Hydrogels.....	22
Table 6.1: First Safety Study Hydrogel Retention Rate in 30 Salmon after 300- Degree Days.....	51
Table 6.2: Second Safety Study Hydrogel Retention Rate in 32 Salmon after 300 Degree Days.....	54
Table C1: Scoring for Visual Appearance of Abdominal Cavity.....	73
Table C2: Scoring for Pigment (Melanin) for Viscera .....	73
Table C3: Scoring for Pigment (Melanin) for Peritoneum.....	74
Table C4: Formulation Residues in the Abdominal Cavity.....	74

## LIST OF FIGURES

Figure 2.1: Antibiotic use over time (grey bars) related to Norwegian salmon production (black line joining square dots) from 1981-2004.....	6
Figure 2.2: Cartoon depiction of the Atlantic salmon life cycle.....	8
Figure 2.3: Heat map comparing the three different kinds of aquaculture vaccine delivery methods.....	10
Figure 2.4: Hydrogel classifications and properties .....	13
Figure 2.5: Mechanism of delivery from a reservoir system hydrogel.....	15
Figure 2.6: Mechanism of delivery from a matrix system hydrogel.....	15
Figure 2.7: Cartoon depiction of the delivery of the aquaculture vaccine hydrogel into the fish and subsequent vaccination.....	19
Figure 2.8: Chemical structures of normal and modified cellulose.. .....	21
Figure 3.1: Size comparison of 5 mL, 3 mL, and 1 mL cut-off syringes used as molds for forming hydrogels.....	28
Figure 3.2: Failed attempt at mixing TEMPO CNF and bacterin where it dispersed in citric acid solution (left). Successful attempt at forming hydrogels from TEMPO CNF and bacterin mixture using a 3 mL cutoff syringe (right).....	32
Figure 3.3: Vacuum filtration trends of how the weight and weight percent of TEMPO CNF changes over time .....	34
Figure 3.4: Volume distribution of measured bacteria diameter size obtained through DLS .....	36
Figure 3.5: Distribution of measured bacteria zeta potential.....	37
Figure 3.6: Change in hydrogel wash solution pH over time. ....	1

Figure 3.7: Change in intensity of Coomassie Brilliant Blue dye over the number of wash days conducted.....	2
Figure 4.1: Changes in percent of initial hydrogel mass over time dried at different drying temperatures.....	9
Figure 4.2: Changes in hydrogel volume over time dried at different drying temperatures.....	10
Figure 4.3: Comparison of hydrogel drying rates based on the drying temperature. ....	11
Figure 4.4: Changes in hydrogel mass after being air-dried and then freeze dried. ....	13
Figure 4.5: SEM images of dried, fully wet, and freeze-dried hydrogels.....	15
Figure 4.6: Cartoon depiction of changes that occur in hydrogel matrix through drying. ....	16
Figure 4.7: Compression strength and modulus of hydrogels at different stages of drying. ....	18
Figure 4.8: Compression strength statistical analysis. ....	19
Figure 4.9: Compression modulus statistical analysis. ....	20
Figure 4.10: Changes in % of initial hydrogel mass over time as the hydrogel rehydrates after being dried at different temperatures for different lengths of time. ....	21
Figure 4.11: Comparison of dried hydrogel mass % to final rehydrated hydrogel mass %. ....	23
Figure 4.12: Comparison of changes in hydrogel size based on the extent hydrogels are dried to at different temperatures.....	25
Figure 4.13: Fluorescent images of the hydrogel before and after 8 weeks for breakdown analysis.....	26
Figure 5.1: Antibody response percentage of the bacterin isolated from the hydrogels.....	34
Figure 5.2: Antibody response percentage of the bacterin diffused from the hydrogels.....	35
Figure 5.3: Changes in absorbance due to presence of CBB dye over time.....	37

Figure 5.4: Green and red fluorescence intensities of the hydrogels over time in the salmon.....	39
Figure 5.5: Hydrogel red and green fluorescence intensities analyzed for statistical significance. ....	41
Figure 5.6: Merged red, green, and white images of hydrogels over time .....	42
Figure 5.7: Merged red, green, and white images of injected bacterin over time .....	43
Figure 5.8: Chemistry of the procedure to label CNF with FITC.....	44
Figure 6.1: First safety study Fulton’s condition factor based on treatment group. ....	52
Figure 6.2: First safety study adhesion score based on treatment group. ....	52
Figure 6.3: Second safety study Fulton’s condition factor based on treatment group.....	54
Figure 6.4: Second safety study adhesion score based on treatment group.....	55
Figure 6.6: Comparison of hydrogel retention from both safety studies. ....	57
Figure A1: Stress-strain curve of fully wet hydrogel samples.....	70
Figure A2: Stress-strain curve of 60 wt% hydrated hydrogel samples.....	70
Figure A3: Stress-strain curve of 40 wt% hydrated hydrogel samples.....	71
Figure A4: Stress-strain curve of 20 wt% hydrated hydrogel samples.....	71
Figure B1: Short term hydrogel rehydrating percent of initial mass curves.....	72

## LIST OF ABBREVIATIONS

BODIPY - Fluorinated boron-dipyrromethene

CBB - Coomassie Brilliant Blue

CFU - Colony forming units

CMC - Carboxy-methyl cellulose

CNC - Cellulose nano-crystals

CNF - Cellulose nano-fibrils

Dd - Degree day

DI - Deionized

DLS - Dynamic light scattering

DMA - Dynamic mechanical analysis

DNA - Deoxyribonucleic acid

DTAF - 5-(4,6-dichlorotriazinyl) aminofluorescein

ELISA - Enzyme-linked immunoassay

FITC - Fluorescein isothiocyanate

NaOH - Sodium hydroxide

PBS - Phosphate buffer solution

PLGA - Poly(lactic-co-glycolic acid)

Poly I:C - Polyinosinic-polycytidylic acid

RAS - Recirculation aquaculture system

RBITC - Rhodamine B isothiocyanate

RCF - Relative centrifugal force

RNA - Ribonucleic acid

SEM - Scanning electron microscopy

TEMPO - 2,2,6,6-tetramethyl-1-piperdine-1-oxyl

TRITC - Tetramethylrhodamine isothiocyante

Wt%- Weight Percent

# CHAPTER 1

## INTRODUCTION

Aquaculture is a large part of the food production sector which is greatly expanding. One of the largest losses in aquaculture is due to pathogens. Current solutions for protecting farmed finfish from pathogens can be very expensive with variable efficiency. Current disease prevention strategies include vaccination. Types of vaccines include immersion vaccines, feed vaccines, and injectable vaccines. The most popular solution is oil-based injectable vaccines due to its protection. However, the oil-based adjuvant used in most of these formulations causes adverse reactions in the fish including reduced growth. These vaccines require multiple administrations throughout the fish's lifetime causing unwanted handling stress and additional labor costs. Preliminary trials show that cellulose nanomaterials cause minimal adverse reactions when injected into salmon and does not significantly affect their growth. The goal of this research was to create an adjuvant from cellulose nanomaterials which would increase bacterin efficacy while avoiding harmful side effects. A prolonged release formulation was also desirable, obviating the need for multiple vaccinations. Additionally, hydrogels have been used for a wide variety of applications including drug delivery, making them an attractive aquatic vaccine adjuvant. Cellulose nanomaterials were decided as the polymer to make up the hydrogel matrix due to their biocompatibility, sustainability, high tunability, high abundance, low cost. The development of the hydrogel formulation, modifying the hydrogel for easier delivery into the salmon, measuring the diffusive properties of the hydrogel, and *in vivo* testing of the hydrogel for analysis of delivery methods and reactions to the formulation are described in this research.

The proposed aquatic vaccine adjuvant in this research is a cellulose nanomaterial hydrogel. Hydrogels have been used for a wide variety of applications including drug delivery. This makes them an attractive possibility for this application. Cellulose nanomaterials were selected as the hydrogel matrix polymer due to their biocompatibility, sustainability, high tunability, high abundance, and being an inexpensive biomaterial. The cellulose nanomaterial used in this thesis was cellulose nanofibers, more specifically, TEMPO CNF. The development of the hydrogel formulation, modifying the hydrogel for easier delivery into the salmon, measuring the diffusive properties of the hydrogel, and testing the hydrogel *in vivo* using Atlantic salmon for effectiveness of delivery methods and reactions are described in this thesis.

Each chapter within this thesis discusses a specific a hydrogel characteristic that was investigated. Chapters start by introducing the experiments performed and the data collected regarding specific hydrogel properties. Then the methods, experimental design, and/or testing performed are explained. Lastly, the results and discussion of the gathered data are presented. Possible conclusions are expounded from the data in regard to the hydrogel formulation properties or performance as an aquatic vaccine adjuvant. Information in the chapters may intersect such that the chapter(s) containing more details on the subject are listed to direct the reader. The research in this thesis was completed in collaboration with the University of Maine Cooperative Extension and funded by the USDA NIFA's flagship competitive grant program, the AFRI Foundational and Applied Science Program.

## CHAPTER 2

### LITERATURE REVIEW

#### 2.1 Finfish Farming and Salmon

Aquaculture or the farming of aquatic animals is the largest growing food production sector. The global aquaculture market is estimated to be worth \$245.2 billion by 2027 with the US aquaculture market being estimated at 2.7 billion in 2020.<sup>1</sup> Aquaculture is experiencing rapid growth because it is becoming a more sustainable alternative source of seafood for human consumption compared to wild fisheries. Aquaculture was developed to decrease the pressure that fishing caused on native finfish populations by switching from wild caught fish to farmed fish raised in hatcheries. Currently, there are two major kinds of saltwater aquaculture farming, open ocean (offshore) aquaculture and land-based aquaculture.

Coastal and open ocean (offshore) aquaculture is considered an open system where the farmed finfish are kept in large nets (also known as cages or pens) in the ocean. These nets can reside close to the shore or in the middle of the open ocean (the majority are located near shore so that they are more easily accessible for routine maintenance) and provide the only barrier separating the fish from the rest of the ocean.<sup>2</sup> This open design means the waste from the farmed fish enters into the ocean's environment and water quality/chemistry such as salinity and pH is maintained to match the surrounding ocean, leading to little cleaning maintenance.<sup>3</sup> The cost effectiveness of open ocean farming and the availability of space in the ocean to start a farm makes open ocean farming attractive and thus the more common of the two farming practices.<sup>2,4</sup> However, the thin barrier between the fish and the ocean also means that there is a risk of net failure, releasing non-native fish into the surrounding area, potential for negative environmental impacts, and high

rates of pathogen transmission between the wild and cultured populations. When pathogens diffuse into the pen, the high stocking density of fish encourages disease transmission, resulting in high incidence and even mortalities.

Land-based aquaculture can be either partially closed or closed systems that are housed in facilities on land. Partially closed systems will have some connection to the environment such as taking place in pond like enclosures rather than tanks. Closed systems use recirculation aquaculture systems (RAS) which recirculates the water in its system in-house.<sup>4,5</sup> RAS systems are sustainable, can be environmentally friendly, and allow the farming of fish in closer proximity to markets. Land-based systems decrease the risk of releasing invasive species and the introduction of pathogens (but not fully eliminate).<sup>4,5</sup> However, isolating the farmed fish from natural water sources requires all the water quality/chemistry parameters such as waste, pH, and salinity levels to be carefully regulated to keep the fish healthy. The high amount of regulation in closed systems requires the use of more energy, maintenance, and labor which can lead to higher costs of raising finfish.

Salmon farming accounts for 45% of all fish farmed from the ocean.<sup>6</sup> This is due to the fact that salmon, particularly Atlantic salmon, has good meat quality (high Omega-3 content), grows quickly, and they are easy to fillet with high yields of meat compared to other finfish (about 58% yield from a “D trim” fillet).<sup>7</sup> Salmon can be surprisingly easy to farm if you consider their migratory nature and carnivorous diet. Some studies have even found that salmon could even be raised solely in freshwater environments.<sup>5</sup>

Salmon are anadromous creatures which mean that they live in both freshwater and saltwater during their life cycle (Figure 2.1).<sup>3,8</sup> In nature, the Atlantic salmon begins its lifecycle as an egg laid in the gravel of a river. The eggs will hatch into alevins and grow into fry and then

parr in freshwater over the span of 1-3 years until they start smolting.<sup>8,9</sup> During the smolting process, the salmon prepares for the transition to saltwater through significant physiological and biochemical changes such as developing more protective scales, becoming more silvery in color, and swimming with the river's current towards the ocean. Once out in the ocean, Atlantic salmon will take about 1-2 years to mature into adults which is when they will begin the journey back to their river of origin to mate.<sup>8,9</sup> Most of the salmon making the mating journey do not make it back out to the ocean, ending their lifecycle in the river where it began.

Farmed Atlantic salmon mimic the lifecycle of wild salmon such that the cultured salmon will spend the first portion of their life in freshwater hatcheries. They will continue to grow in freshwater tanks for about 10-16 months until they become smolts.<sup>10</sup> Once the salmon smolt, they are transferred out into the net pens in the ocean or saltwater tanks where they will remain until they reach market size (12-22 months).<sup>10</sup>

There are many factors that can limit the potential for successful salmon and other finfish farming including: diseases, parasites, stock quality, handling, predators, natural or environmental disasters, water quality/chemistry, feed quality, and aeration.<sup>11,12</sup> The largest factor leading to production loss of farmed finfish is disease, with estimated global loss of \$1.05-9.58 billion in 2014.<sup>13</sup>

## **2.2 Aquaculture Vaccines**

There are many solutions available to minimize production losses which occur due to disease. One possible prevention strategy is culturing finfish in land-based closed systems (RAS) where the conditions of the water in the finfish tanks are completely controlled.<sup>4,5</sup> Being able to control and regulate the water in a closed system reduces (but not completely eliminates) the risk

of diseases being introduced into the system and infecting the fish. However, running a closed system for aquaculture is more costly than running an offshore aquaculture operation. Although RAS is growing in popularity, most aquaculture producers do not use RAS systems and instead opt for open net farming, which puts aquaculture livestock at high risk of contact with infectious pathogens. Before the 1990's, farmers would combat bacterial diseases by feeding their aquaculture stock antibiotics (chemotherapeutics were and still currently used sometimes to treat diseases).<sup>14,15</sup> The use of antibiotics became controversial due to the potential for negative environmental impacts and ineffectiveness due to the development of antibiotic resistant strains of bacteria. Additionally, antibiotics were ineffective against viral, fungal, and parasitic pathogens. Thus, a movement to replace antibiotics with a new solution that could protect the fish from both

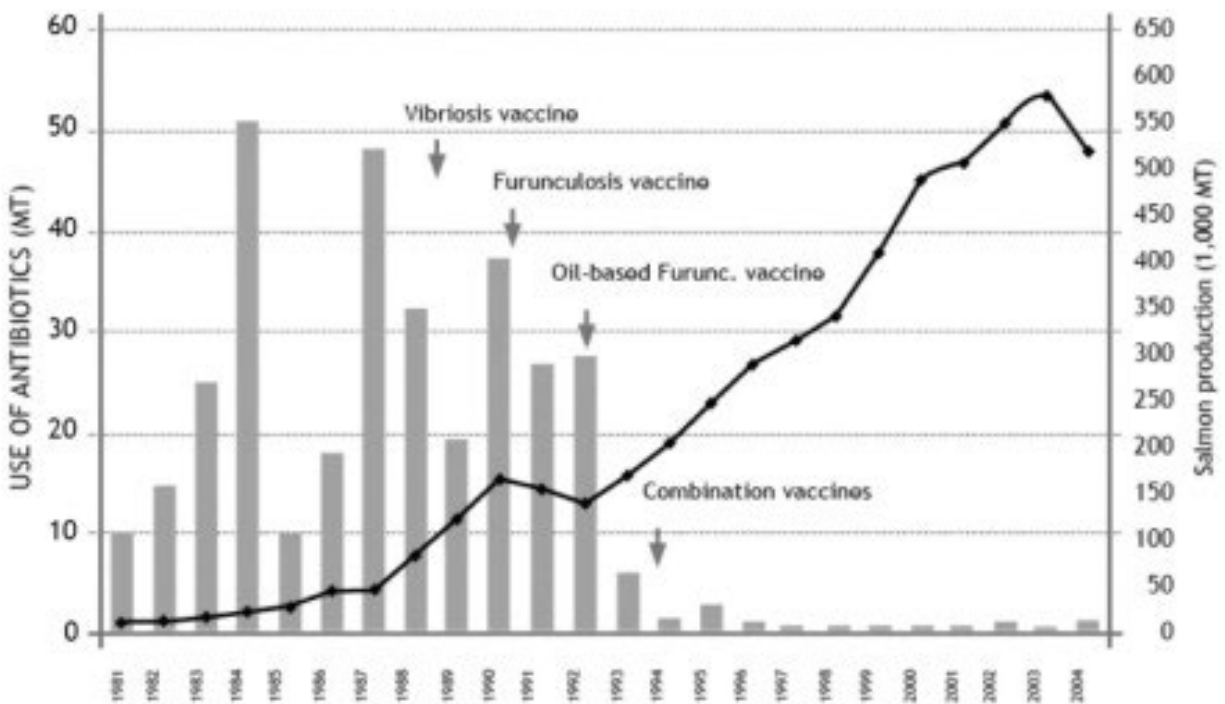


Figure 2.1: Antibiotic use over time (grey bars) related to Norwegian salmon production (black line joining square dots) from 1981-2004. Retrieved from reference (15).

bacterial and viral diseases moved to the forefront of finfish health. This new solution was in the form of vaccines.

Aquaculture vaccines provide protection to the fish by containing a substance which serves as an antigen to stimulate an innate and/or adaptive immune response in the fish against a specific pathogen.<sup>16</sup> Currently there are over 26 licensed vaccines with different kinds of antigens and delivery methods to protect against bacterial and viral diseases.<sup>16</sup> The timing of delivery of these vaccines is critical. These vaccines can be administered at almost any point in the salmon lifecycle using different delivery methods. However, waiting for the fish to develop for as long as possible before administering a vaccine may help decrease the potential for adverse side effects to occur especially with injection vaccines. One study has shown that the earlier a vaccination was given, the more stunted growth, severe lesions, and even vertebral deformations occurred.<sup>17</sup> The most important time to vaccinate Atlantic salmon is before smoltification where they are transitioned to open net pens in the ocean because this is where the fish is vulnerable to physiological stress and will be exposed to possible pathogens. Therefore, the circle in Figure 2.2 shows the time where farmed Atlantic salmon are usually vaccinated which is around the parr to smolt stage.<sup>18</sup> The vaccine takes about four weeks after administration for the fish to develop protection.<sup>17</sup> Salmon can also be vaccinated during their fry stage using immersion and oral delivery methods that work on smaller size fish.<sup>19</sup> The oral and injection method of vaccination can also continue be used later on in the life cycle during the salmon's late smolt to adult stages as a booster.

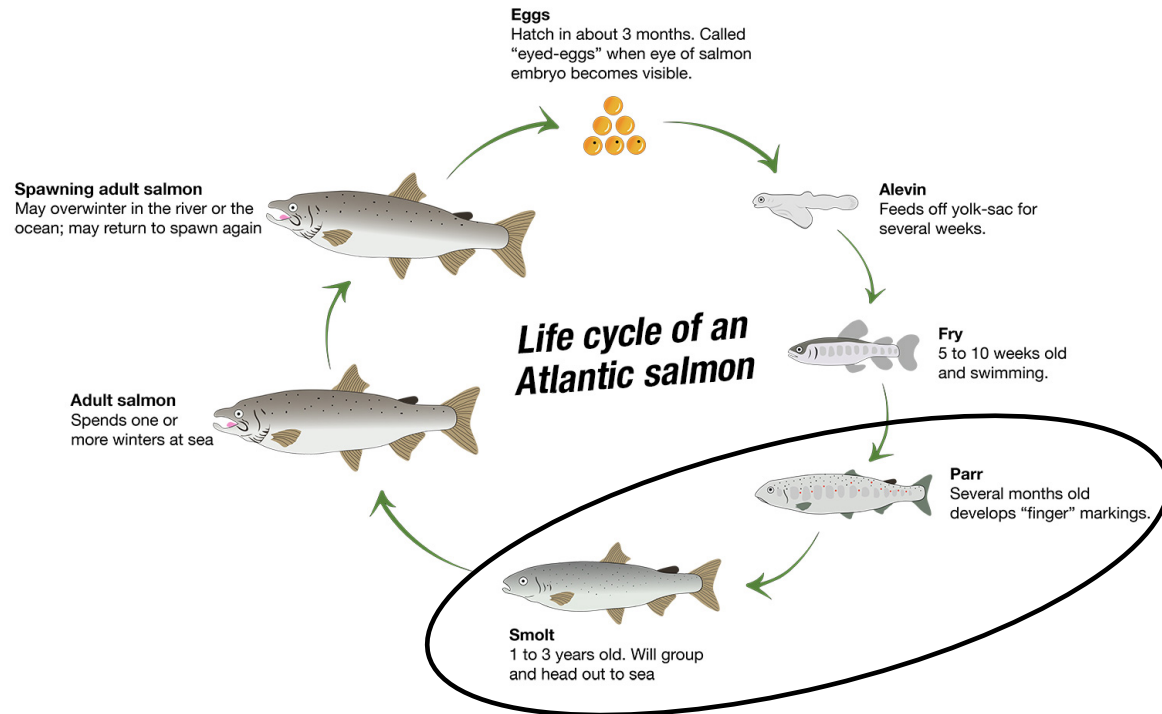


Figure 2.2: Cartoon depiction of the Atlantic salmon life cycle. Atlantic salmon transition to saltwater during the smolt stage. The black circle encompasses the stages where the fish need to be vaccinated before transition to net pens in the ocean. Adapted from reference (18).

The antigens used in aquaculture vaccines to provide protection can be prepared into the following kinds of vaccines: inactivated/killed, live/attenuated, subunit, recombinant vector, DNA, RNA, synthetic/peptide, and anti-idiotypic.<sup>16,19,20</sup> The most common type of antigen used in aquaculture vaccines are inactivated or killed bacteria.<sup>21</sup> There are also autogenous vaccines which are specifically developed for a specific strain of bacteria or virus that is present in a particular aquaculture facility site.<sup>16</sup> Aquaculture vaccines can be delivered to the fish in one of three major ways: oral, immersion, or injection.

Oral vaccination is when antigen is loaded into feed pellets which are fed to the fish to vaccinate them. The vaccine feed can be prepared by mixing the antigen with the feed mixture

before forming it into pellets, bio-encapsulation, or coating (top dressing) the pellets with antigen.<sup>19,21</sup> Extra care must be taken to prepare the antigen in a way that it will be able to survive the fish's gastrointestinal tract until it reaches the second segment of the intestine where it can be absorbed.<sup>21</sup> Successfully developed oral vaccines are beneficial due to their extreme ease of administration which is the least stressful vaccination method, has the least associated labor costs and able to be administered at any point in the lifecycle.<sup>20,21</sup> Additionally, oral vaccinations need a large amount of antigen to be presented to the fish, it is difficult to uniformly dose each fish, only provides short term protection, and the vaccine is prone to poor efficacy or the ability to prevent infection and death in the fish.<sup>21-23</sup> As a result, there are few commercially available vaccines and the oral method of delivery is typically used for booster vaccinations.

Immersion vaccination is when the antigen is dispersed or dissolved in water in an enclosed area that the fish are submerged in, allowing the antigen absorb through the skin, gills, and mouth to vaccinate them. Immersion vaccines can be administered through dip or bath methods.<sup>19</sup> The dip method is when there is a high concentration of antigen in the water that fish are dipped into the mixture for a brief period of time. The bath method is when there is a lower concentration of antigen that the fish are exposed to for a longer period of time. Immersion vaccinations are the most moderate of the three vaccine delivery methods because they require a moderate amount of handling and labor to vaccinate the fish while also being moderately efficacious and delivering mid-range duration of protection to the fish.<sup>22</sup> However, the immersion method of vaccination can only be used on fry or smaller salmon as it becomes impractical for larger fish and difficult for the vaccine to absorb past fish scales. Additionally, there are no viral immersion vaccines which are widely available.<sup>19</sup>

Lastly, injection vaccination is when the antigen is injected directly into the fish either intramuscularly or intraperitoneally (into the fish’s abdominal cavity). The intraperitoneal method of injection is the most common form of vaccination even though mucosal vaccines (oral and immersion) are more practical and affordable. Injection vaccination is used the most in aquaculture because it provides the fish with the best duration of protection (over a year) and is the most efficacious.<sup>19,20,24</sup> However, injection vaccines are the most labor-intensive, stressful to the fish, and causes the most adverse effects.<sup>24</sup> Some adverse side effects include; injection site lesions and granulomas, adhesions between internal organs, granulomatous peritonitis, decreased appetite and growth, malfunction of reproductive organs, and melanin deposits.<sup>17,23,24</sup> These adverse side effects are commonly associated with the adjuvants that are used as antigen carriers due to the strong inflammatory responses they cause.

Vaccine Delivery Method	Reaction to Vaccine	Duration of Protection	Efficiency	Cost
Oral	Green	Yellow	Red	Green
Immersion	Green	Yellow	Yellow	Yellow
Injection	Red	Green	Green	Red

Figure 2.3: Heat map comparing the three different kinds of aquaculture vaccine delivery methods. Cost is based on the cost to the aquaculture farmer. Efficiency takes into account many aspects including efficacy, duration of protection, the dosage needed, and how many times the fish needs to be vaccinated with this method before reaching market size.

Adjuvants are a group of structurally heterogeneous compounds that can change the intrinsic immunogenicity of an antigen or boost the efficacy and protection of an antigen.<sup>20</sup> Adjuvants can boost immune responses to an antigen through two ways; either by presenting the antigen over an extended period of time (signal 1 facilitator) or by producing secondary immune response signals to the adjuvant itself (signal 2 facilitator).<sup>23</sup> One current commercially used adjuvant made of mineral oil (named Montanide™) elicits both of these responses through presenting the antigen in an emulsion while the mineral oil creates an additional innate immune response. Mineral oil adjuvants so far have proven to be the most efficacious and provide the longest duration of protection over multiple studies despite the observed adverse effects.<sup>23-25</sup> Other adjuvants have also been tried and tested for use in injection vaccines such as: aluminum salts (adjuvant used in human vaccines),  $\beta$ -glucan, levamisole, lipopeptides, saponins (oral vaccine adjuvant), PLGA (oral vaccine adjuvant), flagellin, CpG, Poly I:C, and cytokines.<sup>23,25</sup> None of these tested adjuvants were as efficacious at promoting immune response and providing protection against pathogens as compared to mineral oil in the fish.

The current goal of aquatic animal health researchers and this research is to develop an adjuvant which creates an immune response comparable to mineral oil without triggering adverse effects. The injection method of vaccination was chosen for application because it is the most common commercially used vaccination method, allows easy antigen preparation, ease of control over appropriate dosage to each fish, and ability for long durations of protection. It was proposed that a water-based hydrogel vaccine could replace the oil-based emulsion vaccines. It was further hypothesized that a water-based vaccine would not create the adverse effects of an oil-based vaccine while allowing for a controlled and prolonged release of the antigen. As a result, the proposed hydrogel vaccine method would be designed to behave as an adjuvant which presents

the antigen (signal 1 facilitator). The hydrogel formulation allows for modification of the amount of loaded antigen, the rate of antigen diffusion from the hydrogel, the length of diffusion time, and hydrogel breakdown.

The vaccine used for research in this paper was the *Vibrio anguillarum* vaccine because it is one of the most common vaccines given to aquacultured Atlantic salmon. *Vibrio anguillarum* is a bacterial disease which causes lethal vibriosis in over 50 different species of fish along with some mollusks and crustaceans. Vibriosis is hemorrhagic septicemia or bacterial blood poisoning of the fish.<sup>26-30</sup> *Vibrio anguillarum* bacteria are gram-negative, motile, slightly halophilic (requiring salt for growth), curved rod shaped bacteria that are about 1-2  $\mu\text{m}$  in length and 0.5  $\mu\text{m}$  in width with a polar flagellum that is about 4  $\mu\text{m}$  in length.<sup>27-29</sup> *Vibrio anguillarum* can be found in both freshwater and saltwater and are commonly used as formalin inactivated antigens in vaccines.

### **2.3 Hydrogels and Biomaterials**

The desired attributes of drug delivery vehicles are: targetability, control over drug release, capacity of drug entrapment, porosity of material, stability of both the drug and delivery system, sterility, applicability, processability, and cost-effectiveness.<sup>31,32</sup> Hydrogels meet these desired attributes and have other attractive qualities such as biocompatibility. Hydrogels are 3-dimensional crosslinked polymer networks which are water-insoluble while also being mostly made of water.<sup>33</sup>

Hydrogels can be categorized through many different attributes such as: physical structure, ionic charge, synthesis route, size, mechanical and structural characteristics, and the way they are bonded.<sup>34,35</sup> Hydrogels' physical structures can be amorphous, semi-crystalline, supermolecules, hydrocolloid aggregates, or hydrogen bond-gels. The ionic charge of hydrogels can be anionic, cationic, neutral, or ampholytic (capable of ionizing into both anions and cations). Hydrogels can

be synthesized through the crosslinking of homopolymers (only one type of monomer), copolymers (comprised of two types of monomers), or multipolymers (three or more different monomers used). Monomers are the single repeat units that make up polymers. Hydrogels can be classified based on their size as a nanogel, microgel, or macrogel. Crosslinks in hydrogels are either affine (crosslinks are fixed in space at positions defined by the specimen deformation ratio) or phantom (crosslinks have some free motion about their affine deformation positions). There are two types of bonds or crosslinks possible: physical or chemical. Physical crosslinks are reversible bonds that are weaker than chemical crosslinks. This is because physical crosslinks are formed due to polymer entanglement or attraction forces such as ionic bonds, van der Waals, hydrogen bonding, or hydrophobicity properties.<sup>36</sup> Although physical crosslinks are weaker, they are an easier way to form hydrogels than chemical crosslinks which are formed through permanent covalent bonds between the polymers.<sup>34,37</sup>

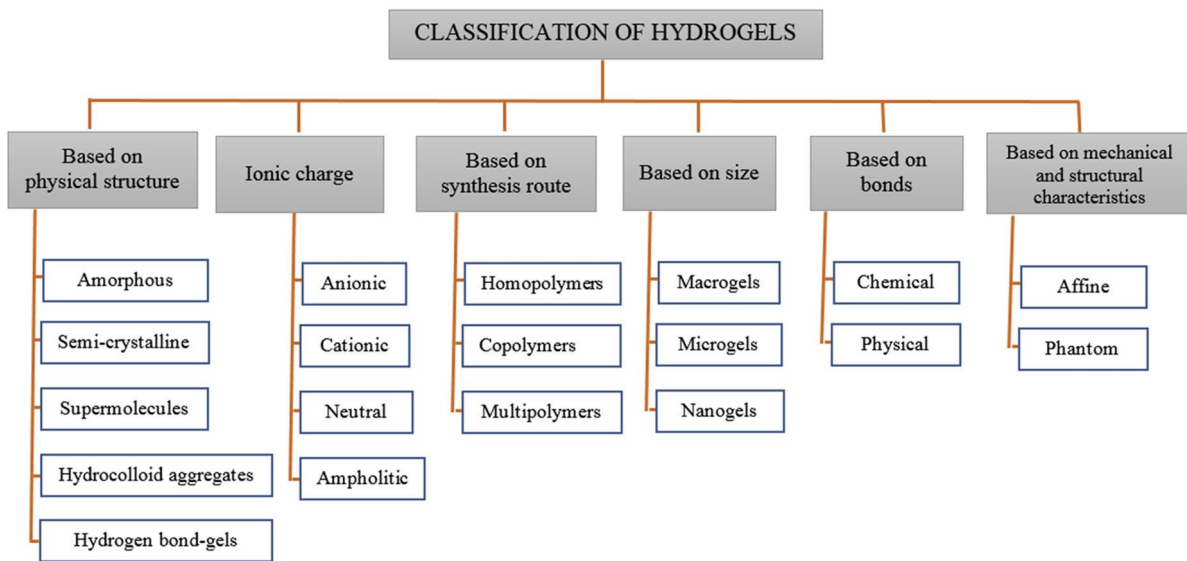


Figure 2.4: Hydrogel classifications and properties. Retrieved from reference (34).

Hydrogels have been explored for use in applications such as: tissue engineering, optics, diagnostics, imaging, agriculture, wound healing, sensors, food industry, hygienic products, biomolecule/cell separation, microelectronics, cosmetics, electrodes, biomedical devices, drug delivery, and more.<sup>34,38</sup> Hydrogels are also used in drug delivery applications due to their biocompatibility, ease of design and control over hydrogel properties, ability to encapsulate water-soluble or water-insoluble molecules, sustained and local release of desired drug, capability of creating local immune-stimulating niches, and being able to suppress adverse effects that are typically associated with the drugs being delivered.<sup>34,39,40</sup> However, hydrogels can also be difficult to deliver if they are not shear-thinning or self-healing.<sup>41</sup> Hydrogels have been found to be used for drug delivery in the following administration routes: oral, ocular, ear, pulmonary, transdermal, central nervous system, cardiovascular, orthopedic, nasal, intestinal, vaginal, parental, injection, and implantable.<sup>31,34,42</sup>

Hydrogels can deliver their drug payloads either through controlled passive diffusion due to swelling and/or erosion of the hydrogel matrix or can encapsulate the drug until a stimulus triggers the hydrogel to swell and release the drug in a burst. Hydrogels that respond to a stimulus or trigger are called smart hydrogels.<sup>31,34,35,39</sup> Some smart hydrogels are responsive to temperature, pH, specific enzymes, mechanical stimuli, magnetic fields, electrical signals, light, ultrasound, specific biomolecules such as glucose, and more. Hydrogels can be one of two delivery systems: reservoir or matrix.<sup>39,43</sup> A reservoir system hydrogel is structured so there is a drug core which is surrounded by a hydrogel membrane (Figure 2.5).<sup>44</sup> The release rate of the drug is controlled by the membrane thickness and properties of the drug encapsulated. The drug is released by water diffusing through the hydrogel membrane, dissolving the drug until saturation solubility, then

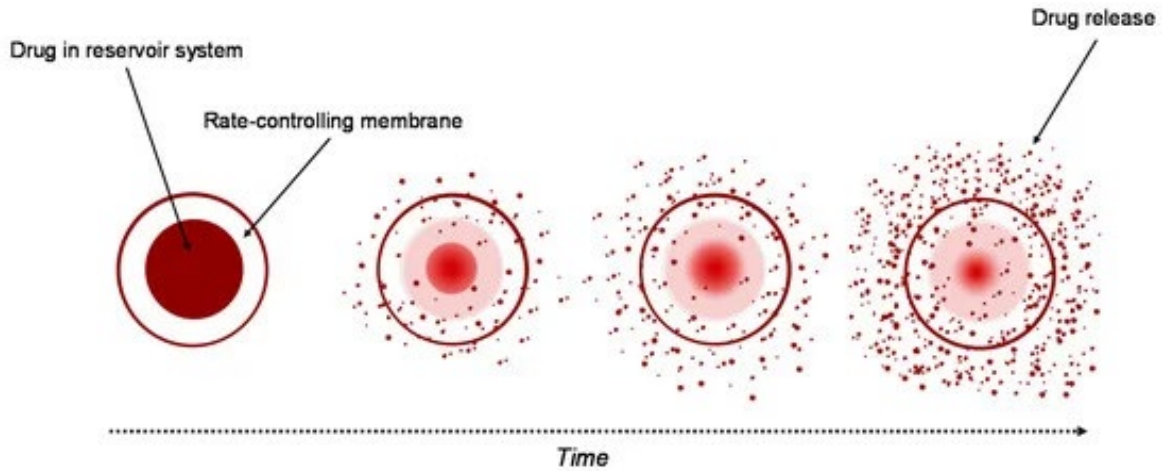


Figure 2.5: Mechanism of delivery from a reservoir system hydrogel. Retrieved from reference (44).

diffusing the drug out of the hydrogel. A matrix system hydrogel is where the drug is uniformly dispersed in a hydrogel matrix (Figure 2.6).<sup>45</sup> The release rate of the drug is based on the properties of the hydrogel matrix and has a time dependent release based on the diffusion of water into the matrix to dissolve the drug and the drug diffusion out of the matrix.

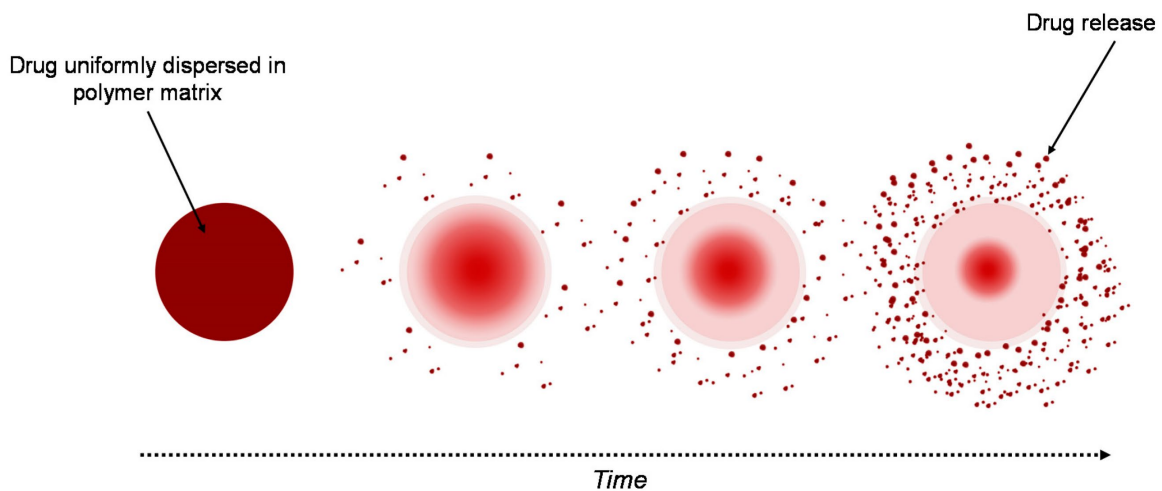


Figure 2.6: Mechanism of delivery from a matrix system hydrogel. Retrieved from reference (44).

The last important part of designing a hydrogel for drug delivery or any application is to decide on the polymer(s) to use. There are two main classifications of polymers which were of interest for this research: natural and synthetic polymers. Synthetic polymers are characteristically hydrophobic, have good mechanical strength for a hydrogel, long service life, absorbability, and good durability.<sup>35</sup> Although the qualities of synthetic polymer hydrogels are desirable, they might not be the best choice for drug delivery because they are typically not biodegradable and can have poor cell recognition/attachment, among other possible cell reactions.<sup>31,46</sup> These negative effects of synthetic polymers are why the USDA does not easily support the use of synthetic polymers without extensive safety testing. Synthetic polymers are currently being replaced by natural polymers to create drug delivery hydrogels because they are biocompatible, non-toxic, hydrophilic (less likely to create a reaction in the body), biodegradable, and have high swelling capacity.<sup>35,38,47</sup> As a result, it made sense to use a natural polymer to form the aquaculture vaccine hydrogel which was designed and explored in the work of this research.

In order to decide which natural polymer to use to form the aquaculture vaccine hydrogel, the following most common natural polymers were researched to compare their benefits and drawbacks: chitosan, alginate, collagen, dextran, hyaluronic acid, DNA, chitin, gelatin, fibrin, and cellulose.<sup>35,38</sup> The desired characteristics of the developed aquaculture vaccine hydrogel is to be biocompatible, biodegradable, hydrophilic, reasonably modified/crosslinked (physical crosslinking desirable), readily available, and inexpensive to scale up the production process. The hydrogel also needs to be pH insensitive in the biological range for fish, well-behaved at low biological fish temperature (no temperature sensitive hydrogels around 5-20°C), and the hydrogel synthesis needs to be compatible with the loaded bacteria (*Vibrio anguillarum*) to deliver. Physical

crosslinking helps to eliminate the possible use of toxic chemicals during the hydrogel synthesis which could affect the loaded bacteria or create an adverse reaction in the fish.

Chitosan is a readily available polymer which is a deacetylation of chitin and a structure in the exoskeleton of crustaceans and insects. It is possible to crosslink chitosan through physical, photo, or chemical methods.<sup>48,49</sup> However, chitosan hydrogels are pH responsive and for this application it is not desirable to use a stimuli responsive hydrogel when we want a long passive diffusion of the drug. Alginate is a readily available polymer extracted from seaweed and is able to be physically crosslinked.<sup>50</sup> However, alginate is also naturally hydrophobic unless ions are added to enable it to dissolve in water which will add difficulties into the hydrogel production process. Collagen is also a readily available polymer which is also a major component of the extracellular matrix in fish making it biocompatible.<sup>51</sup> However, collagen can form crosslinks through chemical, photo, and enzyme means, not through physical crosslinks. Dextran is an easily modified polymer that is derived from bacteria but is easily degraded by dextranase which exists in marine bacteria and some fish tissues that could lead to premature breakdown of the hydrogel.<sup>52</sup> Hyaluronic acid is also easily modified and found in the extracellular matrix of skin, cartilage, and vitreous humors but is expensive and not able to be easily physically crosslinked.<sup>53</sup> DNA is an easily modified polymer that can be obtained from any living organism and can be designed for a wide range of applications with responses to different stimuli, however it is a very expensive polymer to use in this application where low cost is a major factor.<sup>54</sup> Chitin is a readily available polymer (being the second most abundant carbon polymer in nature) extracted from the exoskeletons of crustaceans and insects.<sup>55</sup> However, it is relatively insoluble which would make the hydrogel production more difficult and is also a thermo-sensitive polymer. Gelatin is a readily available polymer which is derived from collagen through hydrolytic degradation but it has poor

Table 2.2: Comparison of Common Natural Polymers used to make Hydrogels.

<b>Type of Polymer</b>	<b>Pros</b>	<b>Cons</b>
Chitosan	Readily available, physical, photo, or chemical crosslinking possible	pH responsive
Alginate	Readily available, physical crosslinking possible	Hydrophobic unless ions are added
Collagen	Readily available, already present in fish (biocompatibility)	Not physically crosslinked into a hydrogel (chemical, photo, and enzyme)
Dextran	Easily modified	Dextranase easily degrades the gel (found in fish and marine bacteria)
Hyaluronic Acid	Easily modified	Not physically cross-linked (chemical, photo, and enzyme), expensive
DNA	Easily modified and designed for a wide range of applications with responses to different stimuli	Expensive
Chitin	Readily available	Thermo-sensitive
Gelatin	Derived from collagen, readily available	Poor thermal stability, weak chemical cross-linking
Fibrin	Naturally forms fibrous matrices	Poor mechanical properties, uncontrolled mechanical integrity loss
Cellulose	Inexpensive, readily available, easily modified, some forms are transparent, physical crosslinking	Challenging to turn cellulose into a hydrogel, needs to be modified

thermal stability and forms hydrogels through weak chemical crosslinks.<sup>56</sup> Fibrin is a polymer that naturally forms fibrous matrices that could entrap and diffuse the bacteria out over a constant, prolonged period but it has poor mechanical properties and can undergo uncontrolled integrity loss leading to premature release of the vaccine.<sup>57</sup>

Lastly, cellulose is a polymer derived from a multitude of sources such as wood and is the most abundant carbon polymer in nature, making it readily available. It is also inexpensive, can be physically crosslinked to form a hydrogel, easily modified, and some modified forms are transparent. However, it is challenging to form pure cellulose into a hydrogel, therefore it does need to be modified before crosslinking. Due to all of the beneficial characteristics of cellulose, and its ability to be made locally, makes it a great research candidate for the development of an aquaculture vaccine hydrogel.

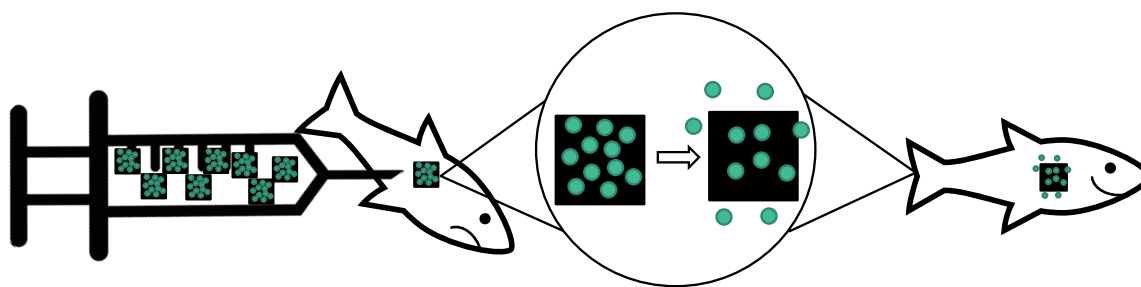


Figure 2.7: Cartoon depiction of the delivery of the aquaculture vaccine hydrogel into the fish and subsequent vaccination. The bacteria (greenish circles) are shown diffusing out of the hydrogel matrix (black square).

## 2.4 Cellulose Nano-Materials

Cellulose nanomaterials can be manufactured from the following sources of cellulose: bast fibers (flax, hemp, jute, ramie), grasses (bagasse, bamboo), seed fibers (cotton, coir), wood (both hardwood and softwood), marine animals (tunicate), algae, fungi, invertebrates, and bacteria.<sup>58</sup> Nanocellulose is created through mechanical and chemical processing of raw cellulose, a polymer made up of  $\beta$ -1,4-anhydro-D-glucopyranose repeat units,<sup>59</sup> to form fibers or crystals of cellulose that are on the micro or nano scale. Nanocellulose has great properties for use in biomedical technologies such as: chemical inertness, stiffness, high strength, low density, easily modifiable

surface chemistry (due to the many hydroxyl groups along the polymer chain), amphiphilic (possessing both hydrophilic and lipophilic properties), biocompatibility, high biodegradability, and biodegradability.<sup>59-62</sup> These properties support its use in applications such as paper, packaging, tissue regeneration and repair, substitute implants, biosensing, drug delivery, separation membranes, antimicrobial products, cosmetics, composites, tissue bioscaffolds, vascular grafts, bone tissue regeneration, and many other biomedical devices.<sup>58-60,63,64</sup>

The manufacturability of nanocellulose is very flexible and tunable based on the desired cellulose derivative and properties. Nanocellulose's easy tunability through surface modification or functionalization makes it easy to label with one of many different fluorophores such as calcofluor white, FITC, RBITC, TRITC, BODIPY, and DTAF for easy visualization during experimentation.<sup>65-71</sup> The general overall process of converting cellulose into nanocellulose is that cellulose is collected and purified through a process such as cooking and bleaching. Then the purified cellulose goes through a mechanical pretreatment, biological/chemical pretreatment, principal mechanical treatment, and then any post treatments such as surface modifications or labeling.<sup>58,59</sup> Modifying any step in this manufacturing process can create different properties in the resulting nanocellulose. The types of cellulose explored in this literature research are pure or "vanilla" cellulose nano-fibrils (CNF), cellulose nano-crystals (CNC), bacterial cellulose, carboxy-methyl cellulose (CMC), and TEMPO CNF.

"Vanilla" CNF is created by breaking down or processing cellulose fibers until they reach a micro or nano size. The typical way to produce CNF is by starting with cellulose pulp such as wood pulp and cooking it and bleaching it to remove it of impurities such as lignin, pectin, and hemicellulose. Then, the pure cellulose undergoes successive refining, enzymatic hydrolysis, more refining, and homogenization to achieve the nano scale fibrils.<sup>58,59</sup> "Vanilla" CNF is about 10 nm

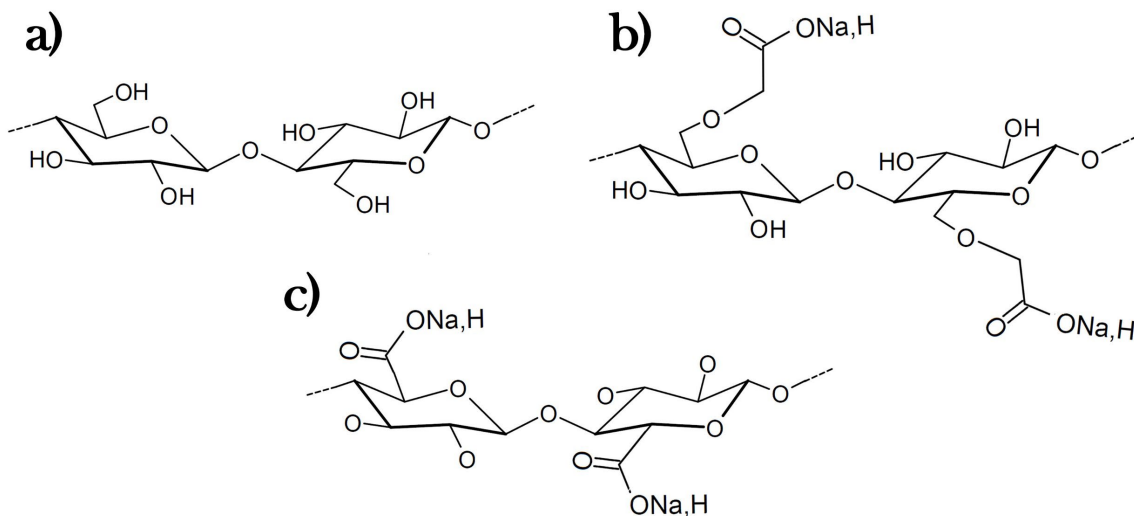


Figure 2.8: Chemical structures of normal and modified cellulose. a) chemical structure of normal cellulose, b) chemical structure of CMC, c) chemical structure of TEMPO CNF.

to 100nm in diameter and can be many microns in length (it is hard to get an accurate length measurement of these fibers because they are usually entangled with each other). These fibers have great mechanical properties due to the fibers' entanglement and hydrogen bonding occurring both intra- and intermolecularly between the cellulose polymer chains. "Vanilla" CNF is typically used more in composites and rarely in hydrogels due to the extent of fiber entanglement and the nature of the fibers to agglomerate instead of staying uniformly dispersed. CNCs are formed from highly organized and crystalline regions of cellulose. Cellulose has two regions: amorphous (disordered) and crystalline (ordered). CNCs are formed by breaking the cellulose down so these two regions are separated, and the crystalline region is collected.<sup>59</sup> CNCs are about 5nm in diameter, 150-200nm long, and needle-like in shape. CNCs are commonly used in chemically crosslinked hydrogel formulations due to their ordered structure and their ability to imbibe strength into the hydrogel.<sup>39,60</sup> Although the hydrogel formulation explored in this thesis doesn't utilize CNCs, it is

a cellulose derivative which could be explored as a different formulation or as an additive in this formulation in future studies.

Bacterial cellulose is a special cellulose derivative because it is made from a bottom-up approach which is different from the usual top-down approach to create nanocellulose. This is because bacterial cellulose is made from certain types of bacteria as a byproduct of when they are given sugar sources. Bacterial cellulose has been explored for use in hydrogels and other biomedical technologies because it enhances cell proliferation and attachment. Bacterial cellulose also has smaller diameters, increased number of fibrils, more purity, better biocompatibility, higher crystallinity, higher elastic modulus, and develops stronger hydrogen-bonds for better mechanical properties than normal nanocellulose.<sup>42,72</sup> However, bacterial cellulose is not commonly used in industry because it is more expensive and time-consuming to produce.

CMC is a functionalized or surface modified cellulose derivative which has been greatly explored in biomedical technology such as hydrogels due to the functionalization making it easier to crosslink.<sup>73</sup> CMC has a modified chemical pretreatment step from CNF which replaces the hydroxyl group with a carboxymethyl group. CMC is generally smaller and more uniform in size than CNF fibers with a 5-15nm diameter and length of up to a micron.<sup>74</sup> CMC has been shown to improve the porous structure and self-healing nature of hydrogel matrices.<sup>39,73</sup> CMC could also be an additional candidate for use in an aquaculture vaccine hydrogel and should be explored for its biocompatibility and possible toxicity in fish.

Lastly, TEMPO CNF is created by TEMPO-oxidizing cellulose as a chemical pretreatment. TEMPO is an acronym for the oxidation mediator which is used, called 2,2,6,6-tetramethyl-1-piperidine-1-oxyl.<sup>75,76</sup> The primary oxidant used to create TEMPO CNF is usually either sodium hypochlorite or sodium chlorite. By TEMPO-oxidizing the CNF, some hydroxyl groups are

replaced with carboxylic acid groups (which is typically deprotonated and replaced with an Na ion for storage to help decrease hydrogen bonding between the fibers). Just like CMC, TEMPO CNF is smaller than “vanilla” CNF with 3-5nm diameter and about a micron in length. TEMPO CNF is also good for forming hydrogels with physical crosslinks due to the carboxylic acid groups on the cellulose chain and its smaller, more uniform size can improve the porous structure of the hydrogel. The addition of the carboxylic acid group also makes it even easier to modify and functionalize than CNF. The functionality and non-toxic nature of TEMPO CNF in addition to its transparency and already gelatinous nature makes TEMPO CNF a great candidate to formulate into an aquaculture vaccine hydrogel. Preliminary safety studies of TEMPO-oxidized cellulose nanofibrils (CNF) in Atlantic salmon resulted in no significant impact on the salmon’s growth along with minimal adverse effects to the fish.

# CHAPTER 3

## DESIGNING CITRIC ACID CROSSLINKED TEMPO CNF HYDROGELS LOADED WITH BACTERIN

### 3.1 Introduction

#### 3.1.1 Crosslinking CNF

Although it might be difficult to crosslink pure CNF to form a hydrogel, modified CNF such as CMC or TEMPO CNF is easier to form a hydrogel with, since there are more chemical and physical crosslinkers available, some of which are listed in Table 3.1.<sup>39</sup> The issue of concern with some chemical crosslinking methods is that they use chemicals that are toxic. Adverse effects can arise if unreacted toxic chemicals are not properly removed from the resulting hydrogel. Therefore, physical crosslinking is beneficial for this aquaculture vaccine application because it is a method that does not require toxic chemicals. Additionally, it is reversible, allowing breakdown of the hydrogel over time or the creation of a stimuli responsive (smart) hydrogel. Physical crosslinks are formed through hydrogen bonding, Van der Waals interactions, ionic crosslinking, hydrophobicity interactions and more. One physical crosslinker, citric acid, lowers pH to create free H<sup>+</sup> ions in the solution which protonates the fiber's COO<sup>-</sup> groups (CMC and TEMPO CNF are usually stored with a Na<sup>+</sup> ion attached to the COO<sup>-</sup> groups).<sup>73,77</sup> When these groups are protonated, stronger hydrogen bonding between fibers along with fiber entanglement occurs to create a hydrogel matrix.

Table 3.1: Common Cellulose Crosslinkers

Type of Crosslinker	Crosslinker
Chemical Crosslinkers	Dialdehydes
	Acetals
	Polycarboxylic Acids
	Epichlorohydrin/Polyepichlorohydrin
Irradiation Crosslinkers	$\gamma$ -Radiation
	Ultraviolet Light
	Visible Light
Physical Crosslinkers	Polyethyleneimine
	Heavy Metals ( $\text{Fe}^{3+}$ and $\text{Ca}^{2+}$ )
	Citric Acid

Citric acid was chosen as the crosslinker for this hydrogel formulation because it was a relatively nontoxic and inexpensive chemical which could be used in a simple and straightforward hydrogel formulation procedure. The only uncertainty that surrounded the use of citric acid in the hydrogel formulation is that it was unknown what kinds of reactions it would cause in living fish. Additionally, since citric acid created a hydrogel with a very acidic pH, the washing steps for the formed hydrogel were crucial to remove excess citric acid in order to increase the pH back to a neutral level.

### 3.1.2 Considerations for Hydrogel Formulation

For the particular application of use in an aquaculture vaccine, there were many factors that needed to be considered throughout the formulation design stage: safety to the fish species, USDA regulations, compatibility with selected antigen, and industry scalability. The final hydrogel formulation needs to be safe to use in salmon which means that no toxic chemicals can

be used in the hydrogel synthesis and that the pH can not fall below 6.0. USDA regulations also prohibit the use of potentially toxic chemicals which could pose a risk to consumers. Additionally, the hydrogel formulation procedure needs to be compatible with antigen to avoid diminished antigen response. As a result, the antigen could not be exposed to temperatures above 80°C or else the proteins in the antigen would be denatured. In order to develop a hydrogel formulation which can feasibly be used in industrial aquaculture farms in the future, the synthesis of the hydrogel needs to be cost effective both in materials and scalability to an industrial level. Lastly, the formulated hydrogel needs to be able to be delivered to the fish in a reasonable manner that is both safe to the fish and able to be quickly administered. Quick administration is important to be able to vaccinate an entire aquaculture salmon population.

Table 3.2: Desired Characteristics of Designed Aquaculture Vaccine Hydrogel

Biocompatible	Biodegradable
Hydrophilic	Reasonably modified/crosslinked
Readily available	Inexpensive at industrial scale
Stable around neutral pH	Stable at low biological salmon temperature (5-20°C)
Reasonably implanted/injected	Hydrogel synthesis compatible with loaded antigen ( <i>Vibrio anguillarum</i> )

Citric acid crosslinked TEMPO CNF hydrogels have the possibility to fulfill all of these conditions. Both TEMPO CNF and citric acid are inexpensive materials, and the crosslinking procedure is extremely simple and scalable. Additionally, both citric acid and TEMPO CNF are labeled as nontoxic materials with preliminary safety studies using TEMPO CNF showing minimal adverse reactions in the fish. Citric acid crosslinking should not affect the antigen response of the inactivated *Vibrio anguillarum* and does not need heat to occur. The effects from the low pH of

citric acid can be suppressed through washing the formed hydrogels until the pH reaches an acceptable range for the salmon.

### **3.2 Materials**

The materials that were used in the synthesis of the TEMPO CNF citric acid crosslinked aquaculture vaccine hydrogels were TEMPO CNF, citric acid, and inactivated *Vibrio anguillarum*. The TEMPO CNF was a 1.1 wt% slurry obtained from the Process Development Center at University of Maine. The TEMPO CNF fibers were estimated to be a little less than a micron long and 20nm in diameter. The citric acid was 99.5% citric acid from Sigma-Aldrich. Lastly the inactivated *Vibrio anguillarum* bacteria used had a concentration of about  $1 \times 10^9$  colony forming units per mL (CFU/mL) mixture which was cultured in a trypticase soy broth with 1.5% NaCl and inactivated with 0.5% formalin (this mixture is commonly referred to as bacterial antigen or bacterin). The inactivated *Vibrio anguillarum* bacteria was prepared by Sarah Turner at the University of Maine Cooperative Extension Diagnostic and Research Laboratory.

### **3.3 Methods of Formulating a TEMPO CNF and *Vibrio anguillarum* Hydrogel**

#### **3.3.1 Crosslinking TEMPO CNF with Citric Acid**

Before attempting to make the vaccine hydrogel, it was decided to first crosslink pure TEMPO CNF with citric acid by adapting previous procedures found in research articles.<sup>73,77</sup> The crosslinking solution used was 10 wt% citric acid (0.5 mol/L). This concentration of crosslinker was chosen because a more loosely bound hydrogel matrix is more desirable for drug diffusion applications than stiff crosslinking which was researched by Wen Jiang Zheng.<sup>73</sup> A stiff hydrogel matrix might not be desirable for drug diffusion applications because a matrix that is too stiff can end up trapping the drug inside the matrix. Looser bound matrices more easily allow swelling of

the matrix and subsequent delivery of drugs out of the matrix. It was also decided to allow the TEMPO CNF gel to crosslink in the citric acid solution for 24 hours since that would help produce a hydrogel with improved mechanical properties compared to crosslinking for a shorter length of time.<sup>73</sup> Additionally, the hydrogel's mechanical properties should be retained after multiple wash steps. The long crosslinking time allows most of the TEMPO CNF fibers to crosslink, which leads to less TEMPO CNF fibers diffusing out of the matrix when exposed to an aqueous environment and therefore maintaining mechanical properties.

The first concentration of TEMPO CNF that was chosen to make hydrogels was the stock 1.1 wt% which was received from the Process Development Center. The first crosslinking tests involved scooping and dropping clumps of TEMPO CNF into the citric acid. The resulting hydrogels were blob-like and spherical in shape. Since the final hydrogel is to be injected or implanted in the fish, a desirable shape for the hydrogel is cylindrical so it can be implanted in an incision or through a needle. To create hydrogels of a cylindrical shape, 5 mL, 3 mL, and 1 mL



Figure 3.1: Size comparison of 5 mL, 3 mL, and 1 mL cut-off syringes used as molds for forming hydrogels. The syringe sizes from top to bottom are: 5 mL, 3 mL, and 1 mL.

syringes were obtained. The ends of the syringes (where the Luer-Lok connection was located) were cut off, leaving a cylindrical tube with a plunger that would be able to act as a hydrogel mold. Each of the syringes was used to form hydrogels by loading the syringe with TEMPO CNF and then pushing the plunger to extrude some TEMPO CNF out of the end of the syringe. When the desired amount of TEMPO CNF was extruded, a spatula was used to slice the TEMPO CNF at the syringe opening, dropping the cylindrical shaped TEMPO CNF into the 10 wt% citric acid solution. The TEMPO CNF was then allowed to crosslink in the citric acid solution for 24 hours, then transferred to fresh DI water once a day to wash away any excess citric acid and uncrosslinked TEMPO CNF fibers.

The 5 mL syringe mold formed hydrogels which were too large in size to be reasonably implanted into the fish. The 3 mL syringe mold also formed hydrogels which were too large in size to use for implantation. However, the 3 mL syringe-formed hydrogels would be a good size for hydrogel mechanical property analysis. The 1 mL syringe was able to form narrow hydrogels with variable lengths which appeared suitable for implantation. As a result, the 1 mL syringe was used as the hydrogel mold going forward (unless otherwise specified). Additionally, a non-modified syringe was tested for forming hydrogels and not only was it more difficult to push the TEMPO CNF out of the syringe, but the formed hydrogels were very small spheres which likely wouldn't be able to contain the proper dosage of vaccine (at least 0.1 mL of bacterin).

After deciding on the 1 mL syringe as the hydrogel mold and seeing that 1.1 wt% TEMPO CNF was able to form a hydrogel that retained its shape even with light handling, other concentrations of TEMPO CNF were tested to see if they could form hydrogels. One higher weight percentage (1.3 wt% TEMPO CNF) was tested to see how the hydrogel properties would change along with 1 wt%, 0.8 wt%, 0.7 wt%, and 0.6 wt% TEMPO CNF to see the lower limit of being

able to form a stable hydrogel. The 1.3 wt% TEMPO CNF hydrogel was able to withstand more handling than the 1.1 wt% TEMPO CNF hydrogel before breaking apart. Both the 0.7 wt% and 0.6 wt% TEMPO CNF hydrogels broke apart after 8 days of being washed in DI water, while the rest of the TEMPO CNF hydrogel concentrations could withstand over two weeks of being washed in DI water. Overall, the higher the TEMPO CNF weight percentage/concentration, the stronger, more durable, and stable the resulting hydrogel became. As a result, it was decided that the aquaculture vaccine hydrogel needed to contain 0.8 wt% TEMPO CNF or greater.

### **3.3.2 Mixing TEMPO CNF and *Vibrio anguillarum***

After confirming that it was possible to crosslink TEMPO CNF using citric acid, bacterin was mixed with TEMPO CNF to see how it affected the TEMPO CNF's crosslinking ability. When first trying to hand mix 1.1 wt% TEMPO CNF and bacterin together in a 1:1 ratio using a spatula, they didn't seem to mix easily or evenly. A 1:1 ratio of TEMPO CNF to bacterin is desirable because the required dosage amount to the salmon is  $1 \times 10^8$  CFU and a 1:1 ratio produces a hydrogel with about  $2.6 \times 10^8$  CFU. A hydrogel with extra bacterin at the start of synthesis will help at least  $1 \times 10^8$  CFU to remain in the hydrogel after crosslinking and any additional necessary wash steps where bacterin has the ability to diffuse out. Extra bacterin is also beneficial when designing a hydrogel providing a slow release of the bacterin because it can provide more protection over a longer duration. The TEMPO CNF and bacterin 1:1 ratio only seemed to homogeneously mix when left on a stir plate overnight or longer (at a stir rate where all the solution was being completely moved by the bar but not enough where air bubbles would become introduced into the mixture). As a result, all TEMPO CNF and bacterin mixtures were left to stir for 24 hours before proceeding onto the next formulation step.

Although a 1:1 ratio of TEMPO CNF and bacterin creates a 0.55 wt% TEMPO CNF solution, this mixture was still tested for crosslinking ability. It was difficult to load the syringes with this mixture since it was much less viscous than the 0.6 wt% pure TEMPO CNF. When samples of the 1:1 ratio mixture was placed in the citric acid, it broke apart and dispersed across the surface of the citric acid (see Figure 3.2). In order to be able to form hydrogels with the desired amount of bacterin, a method of increasing the TEMPO CNF weight percentage while keeping the same volume of the bacterin needed to be developed.

### **3.3.3 Post Drying Addition of Antigen**

The first method of increasing the weight percentage of TEMPO CNF was drying the TEMPO CNF to a higher starting weight percent using a dehydrator. Using this method would be beneficial since it required no modifications to the *Vibrio anguillarum*, lowering the possibility of reducing its antigen response. TEMPO CNF was dried to 2.2 wt% and 11 wt%. The 2.2 wt% TEMPO CNF had an even more difficult time mixing with the bacterin in a 1:1 ratio and appeared to mostly mix but never completely. When samples of this mixture were placed in the citric acid, they also broke apart and dispersed across the surface. The 11 wt% TEMPO CNF would not rehydrate in the bacterin or evenly mix. It remained as TEMPO CNF sheets scattered throughout bacterin solution. This mixture was not placed in citric acid because it was not able to be somewhat evenly mixed.

### **3.3.4 Heating of TEMPO CNF and *Vibrio anguillarum* Mixture**

Since the TEMPO CNF was not rehydrating in the bacterin, the weight percentage of TEMPO CNF would have to be increased after the bacterin was mixed in. A 1:1 ratio of TEMPO CNF and bacterin was stirred for 24 hours and then heated while continually being stirred on a hot

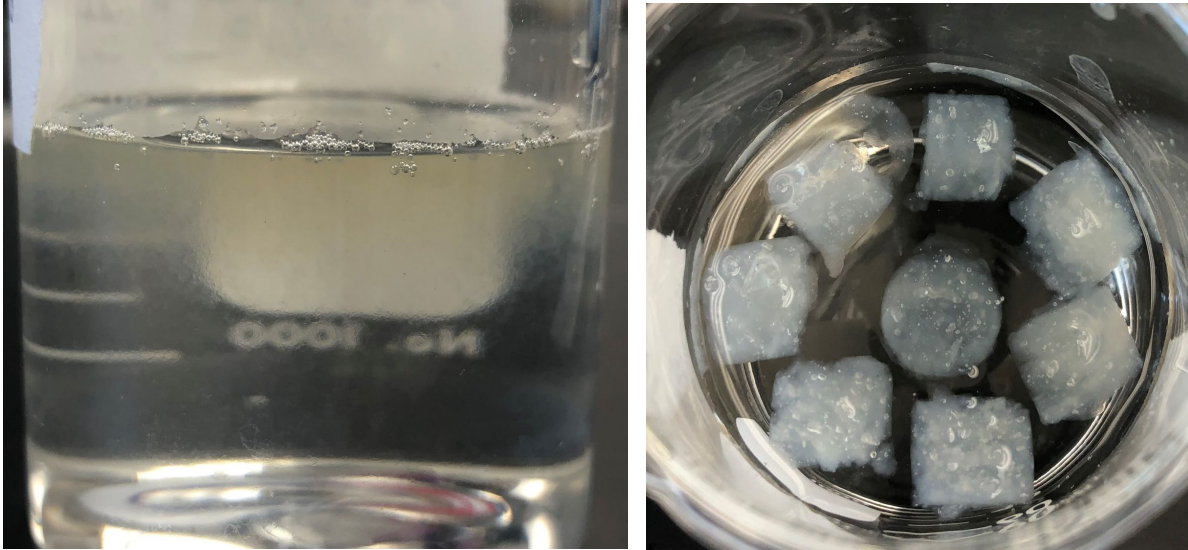


Figure 3.2: Failed attempt at mixing TEMPO CNF and bacterin where it dispersed in citric acid solution (left). Successful attempt at forming hydrogels from TEMPO CNF and bacterin mixture using a 3 mL cutoff syringe (right).

plate until enough water evaporated to make a 1.1 wt% and 1.9 wt% TEMPO CNF solution. The solution was monitored while heating to ensure that the temperature did not exceed 80°C. The 1.1 wt% and 1.9 wt% heated mixtures appeared more homogeneously mixed than previous attempts done with dried TEMPO CNF and were able to be loaded into 3 mL cutoff syringes. The 1.1 wt% TEMPO CNF with bacterin dispersed on the surface when placed in citric acid. The 1.9 wt% TEMPO CNF with bacterin held its shape when placed in the citric acid solution.

The heating experiments concluded that it was possible to form TEMPO CNF hydrogels containing bacterin when the weight percentage of TEMPO CNF was increased to a certain amount. In order to achieve this, the weight percentage needed to increase after the bacterin and TEMPO CNF were mixed. This method required exposing the *Vibrio anguillarum* to relatively high heats (close to the 80°C limit) for an extended period of time. As a result, another method of removing water from the TEMPO CNF and bacterin mixture needed to be found.

### 3.3.5 Filtering TEMPO CNF and *Vibrio anguillarum*

Another way to remove water without the use of heat is through filtration. Two filtration techniques were explored: syringe filtration and vacuum filtration. The filter pore size which was chosen for both filtration methods was 0.45  $\mu\text{m}$  since it was small enough to keep the 1-2  $\mu\text{m}$  in length and 0.5  $\mu\text{m}$  in width *Vibrio anguillarum* from passing through the filter.<sup>27,30</sup>

Being able to squeeze the water out of a syringe filter would make it so the resulting mix was already loaded in a syringe and ready to be placed in citric acid. When the 1:1 ratio TEMPO CNF and bacterial antigen was being pushed through the syringe filter, some water was able to be filtered through. However, the amount of force required to do so was extreme and after too much pressure was applied, the mix squeezed between the sides of the syringe and the plunger and shot into the back of the syringe. As a result, syringe filtration was not a feasible solution for this application.

The next filtration method attempted was vacuum filtration with a vacuum pump, filtering flask, Buchner funnel, and 0.45  $\mu\text{m}$  nylon membrane filter paper from Sterlitech or MilliporeSigma. Nylon membrane filter paper was chosen for this application because it was hydrophobic, which would prevent the TEMPO CNF from forming hydrogen bonds to the filter paper like it possibly could with cellulose filtering paper. The hydrophobicity in addition to the small pore sizes of the nylon filter paper would increase the chances of keeping bacterin endotoxins within the hydrogel formulation.<sup>78</sup> Endotoxins are typically undesirable in most vaccine applications for humans but are shown to promote positive immune responses when incorporated into finfish vaccines.<sup>79</sup>

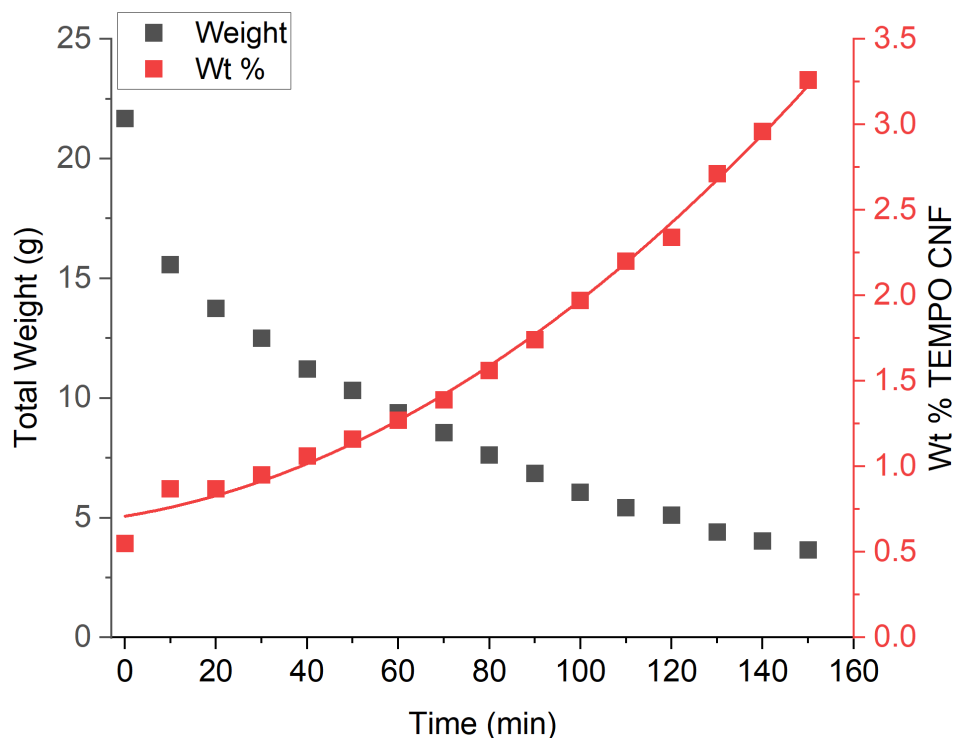


Figure 3.3: Vacuum filtration trends of how the weight and weight percent of TEMPO CNF changes over time. Trendline is shown as a second order polynomial.

Vacuum filtration using 0.45  $\mu\text{m}$  nylon membrane filters were successful in being able to remove water while keeping the TEMPO CNF and bacterin mixed. This allowed ease of removal of the TEMPO CNF and bacterin mixture from the filter paper, and tunability to obtain a range of TEMPO CNF weight percentages. Figure 3.3 illustrated the ability to quickly remove water and increase TEMPO CNF weight percentage following a second order polynomial trend as shown by the red line. Vacuum filtration was used to create 1.3 wt%, 1.1 wt%, 1 wt%, 0.8 wt%, and 0.6 wt% TEMPO CNF with bacterin solutions. When the 0.6 wt% mixture was placed in citric acid, half of the time it dispersed on the surface, while the other half it formed a hydrogel. All the other weight percentages held their shape in citric acid and remained intact over multiple wash days. As a result of being able to form hydrogels even with low weight percentages, ability to control the resulting

TEMPO CNF wt%, decreased probability of modifying the bacterin which would reduce its antigen response, and the ease of being able to scale up vacuum filtration for industrial size applications, it was chosen as the water removal process for hydrogel formulation.

### **3.4 Characterizing *Vibrio anguillarum***

It was decided to characterize the properties of the *Vibrio anguillarum* bacteria to better understand the difficulties that arose when trying to mix TEMPO CNF and bacterin together. Before characterizing the bacteria, it needed to be isolated from the bacterin. This was accomplished by centrifuging the bacterin at 3,500 RCF for 15 minutes to pellet the bacteria. The supernatant was decanted out and the bacteria resuspended in DI water. This solution of isolated *Vibrio anguillarum* was then analyzed for size and surface charge using dynamic light scattering (DLS) and zeta potential using a Malvern Zetasizer Nano-ZS Zen 3600. The bacteria size distributions obtained from the DLS measurements showed the most common particle diameter sizes being: 531 nm, 1280 nm, and 1990 nm (refer to Figure 3.4). These values correspond with the normal size range of 500 nm width and 1000-2000 nm length for *Vibrio anguillarum*. The average measured surface potential of *Vibrio anguillarum* was found to be about -59 mV (refer to Figure 3.5).

The size distribution of *Vibrio anguillarum* was as expected and should not be the cause of reduced interactions between the TEMPO CNF fibers. However, the measured negative zeta potential of the bacteria could cause reduced interactions between the TEMPO CNF fibers. TEMPO CNF at a neutral pH has a zeta potential of about -42 mV.<sup>80</sup> Repulsive forces could be created between the TEMPO CNF and *Vibrio anguillarum* due to their similar and moderate strength of negative zeta potential. These repulsive forces could be why TEMPO CNF does not rehydrate in bacterin. Additionally, the repulsive forces could have caused a larger distance between neighboring TEMPO CNF fibers to occur, leading to weaker Van der Waals interactions

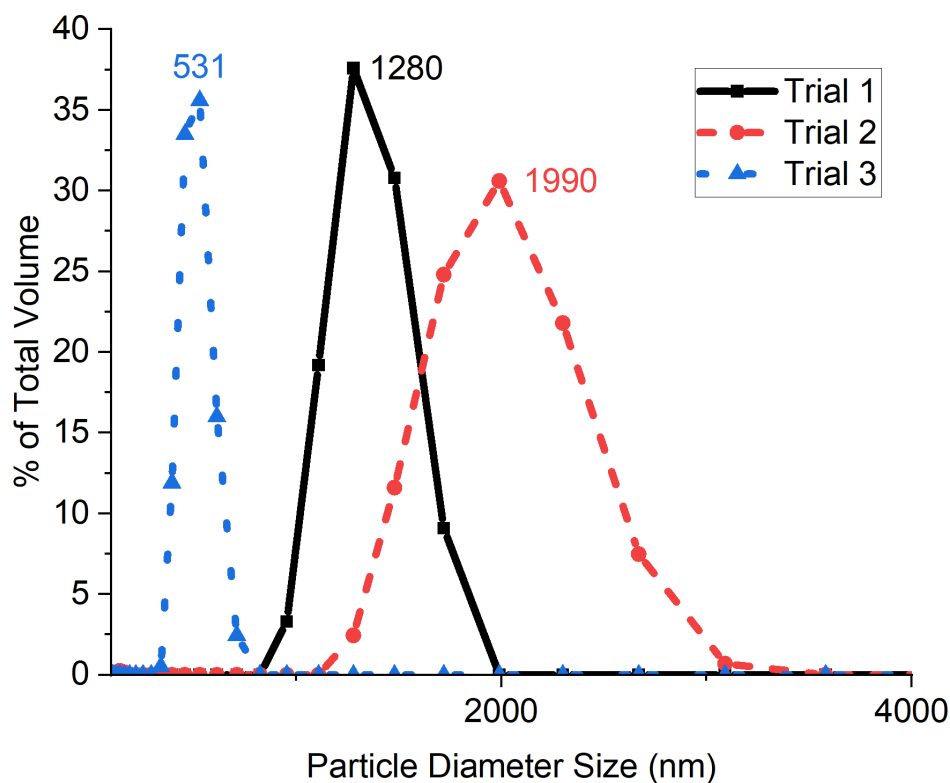


Figure 3.4: Volume distribution of measured bacteria diameter size obtained through DLS.

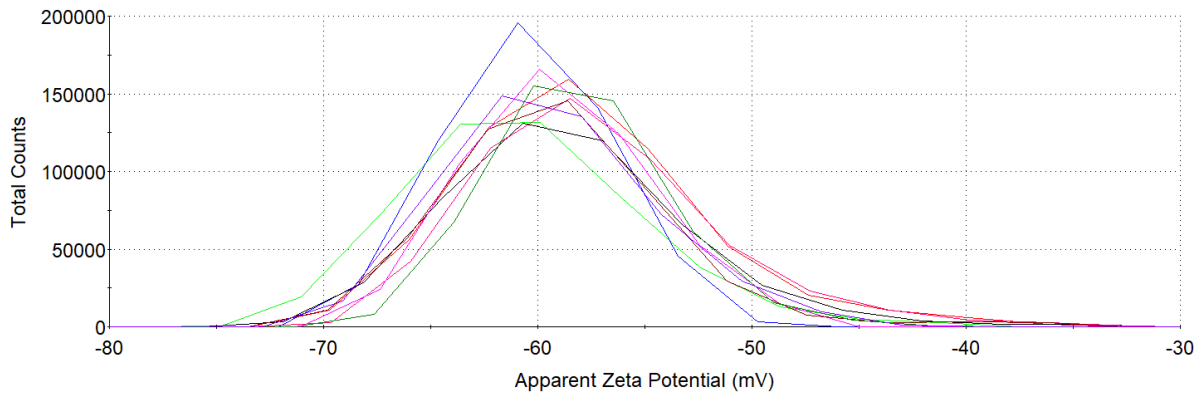


Figure 3.5: Distribution of measured bacteria zeta potential.

and hydrogen bonding which are necessary for TEMPO CNF fibers to crosslink with each other. These repulsive forces could have become more prevalent when TEMPO CNF's zeta potential became more negative in lower pH values, which may explain why most of the low TEMPO CNF weight percentage bacterin mixes dissipated when placed in citric acid.<sup>80</sup>

The higher the TEMPO CNF weight percentages, the closer the fibers should become. The closer the TEMPO CNF fibers are to each other, the stronger the attractive Van der Waals and hydrogen bonding forces are between the fibers. Increasing the attractive forces between the fibers should counteract the repulsive negative zeta potential forces occurring between the bacterin and TEMPO CNF fibers.

### 3.5 Effects of Wash Steps on Cross-Linked Hydrogels

#### 3.5.1 Changes in pH

Since the vaccine hydrogels were formed in citric acid, wash steps were crucial to remove excess citric acid and increase the pH levels back to a safe neutral range for salmon. However, the more wash days the hydrogels underwent, the more likely it was that bacterin prematurely diffused out of the hydrogel. Therefore, it was important to figure out the minimal amount of washing

needed before the hydrogel was deemed safe for implantation. Four batches of hydrogels were made with different TEMPO CNF weight percentages (keeping the initial TEMPO CNF to bacterin ratio at 1:1). Hydrogels with 1.1 wt%, 1.3 wt%, 1.5 wt%, and 1.7 wt% TEMPO CNF were formed in citric acid and then washed with DI water. The pH of the hydrogel DI water wash solution was monitored every 24 hours (represented by the outlined data points on Figure 3.6) and immediately after placing all the hydrogels in new wash solution (represented by the shaded in data points on Figure 3.6).

The pH of the DI water did not appear to significantly change based on the TEMPO CNF wt% of the hydrogel. It was observed that the pH of the hydrogel wash solution remained more acidic than the DI water used for the washes, regardless of the number of wash days conducted. Additionally, the pH of the wash solution for all hydrogels appeared to plateau after 6 days until the gels were washed in PBS on day 11. When the TEMPO CNF 1.7 wt% gels were washed in PBS, the wash solution pH increased and stayed close to the same pH of PBS, which makes sense because it was a buffer solution. The 1.7 wt% hydrogels were chosen to wash in PBS since they appeared to be the strongest of all the hydrogel formulations when they were handled. The plateau of pH after wash day 6 was an indicator that most of the excess citric acid from the hydrogel formation was washed out. Additionally, the ability of PBS to stabilize the pH of the solution surrounding the hydrogel made it a great wash for the day before the hydrogels were implanted into salmon. It can be assumed that the hydrogel's risk of causing adverse reactions in the salmon due to pH should not change from wash day 6 onwards. However, what reactions are caused by different amounts of wash days in the salmon were tested to make a more informative decision on what number of wash days was best (more information in Chapter 6).

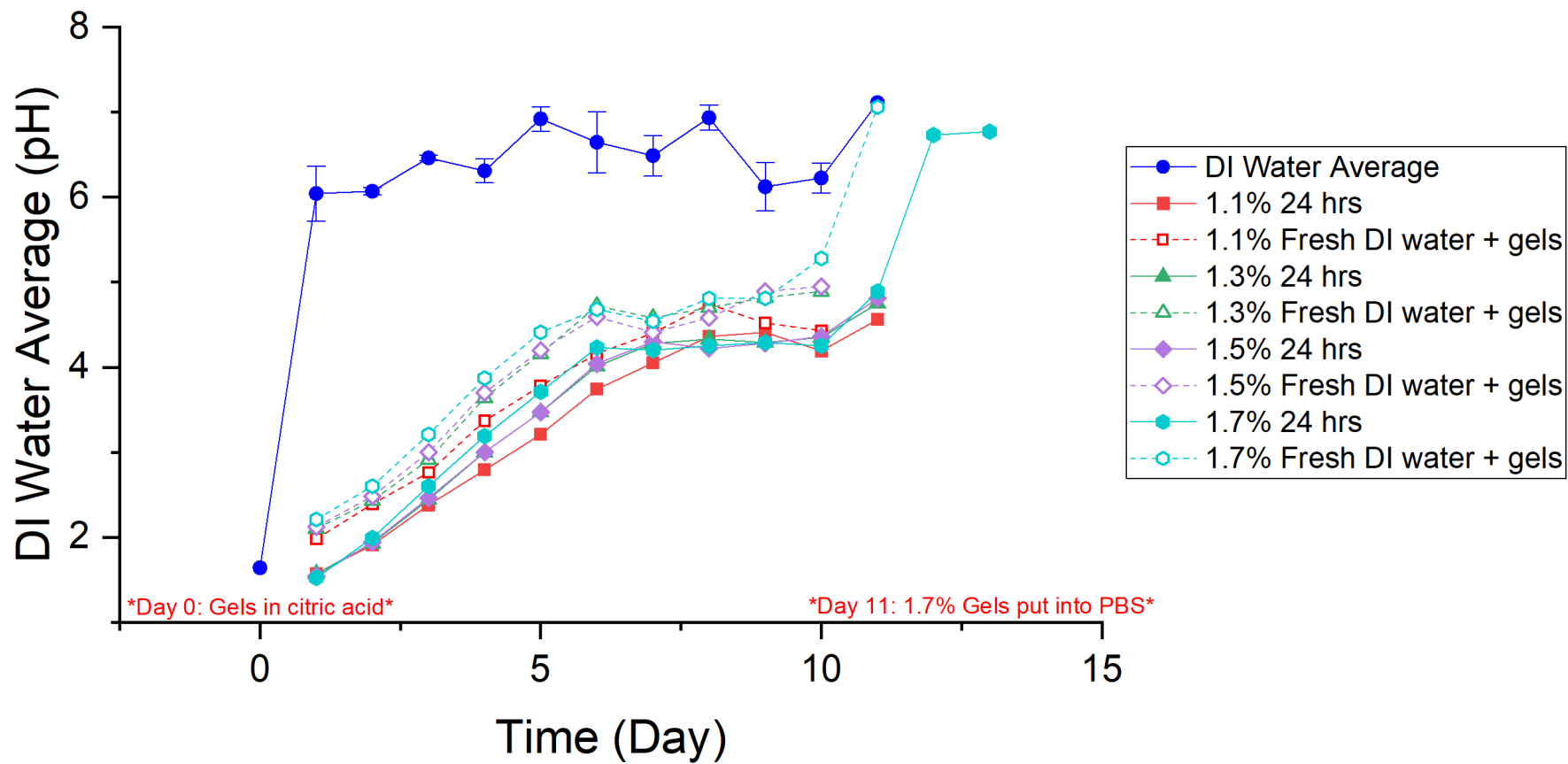


Figure 3.6: Change in hydrogel wash solution pH over time.

### 3.5.2 Diffusion of Dye

To make a fully informed decision on what number of wash days was best for the aquaculture vaccine hydrogels, the diffusion of bacterin out of the hydrogel along with changes in pH needed to be considered. The diffusion of bacterin was modeled using dye to see the effect of wash days on the amount of bacterin that diffused out from the hydrogel. The dye chosen for this experiment was Coomassie Brilliant Blue (CBB) because it was an anionic dye which has the possibility to mimic the negative zeta potential of *Vibrio anguillarum* and its interactions with the TEMPO CNF hydrogel matrix.

The hydrogels were formulated with a 1:1 ratio of 1.1 wt% TEMPO CNF and 1mM CBB dye and then prepared as normal to create a 1.7 wt% TEMPO CNF hydrogel. At each measured time point, five gels were selected at random and sliced in half using a thin wire. Each gel half was imaged under an imaging setup with a fixed camera and fixed white LED lighting for better reproducibility. The camera had a resolution of 2592x1944 pixels and exposure of 0.21~2000ms with an auto exposure feature. Each image taken was analyzed in FIJI (ImageJ) to calculate the average intensity value throughout the gel. The intensity values were obtained by converting the images to greyscale and then measuring the intensity of each pixel in the hydrogel area. The intensity was analyzed on a scale from 0 to 255 where 0 corresponds to black and 255 to white. For this experiment, a higher intensity corresponds to more CBB dye being present within the hydrogel. Then the average intensity values were plotted over the number of wash days (Figure 3.7). The data was also statistically analyzed using Tukey's method for significance between the data points.

There was a significant difference in the intensity and therefore the amount of CBB dye that was present in the hydrogels over multiple wash days. The only two points that were not statistically different from each other were the day 4 and day 6 washes. As a result, the wash days did affect the concentration of dye in the hydrogels where more wash days led to more dye lost due to diffusion. It appeared that the diffusion of dye from the hydrogel had an initial large burst and then plateaued on day 4 where the concentration of dye remained steady to day 6. If CBB dye provided an accurate representation of *Vibrio anguillarum*, with increased wash days, more *Vibrio anguillarum* diffused out of the gel. The data suggested that with more wash days, more bacterin will be lost from the hydrogel. As a result, it was important to find the least number of wash days that wouldn't create adverse reactions in the fish through conducting a safety study. That way as

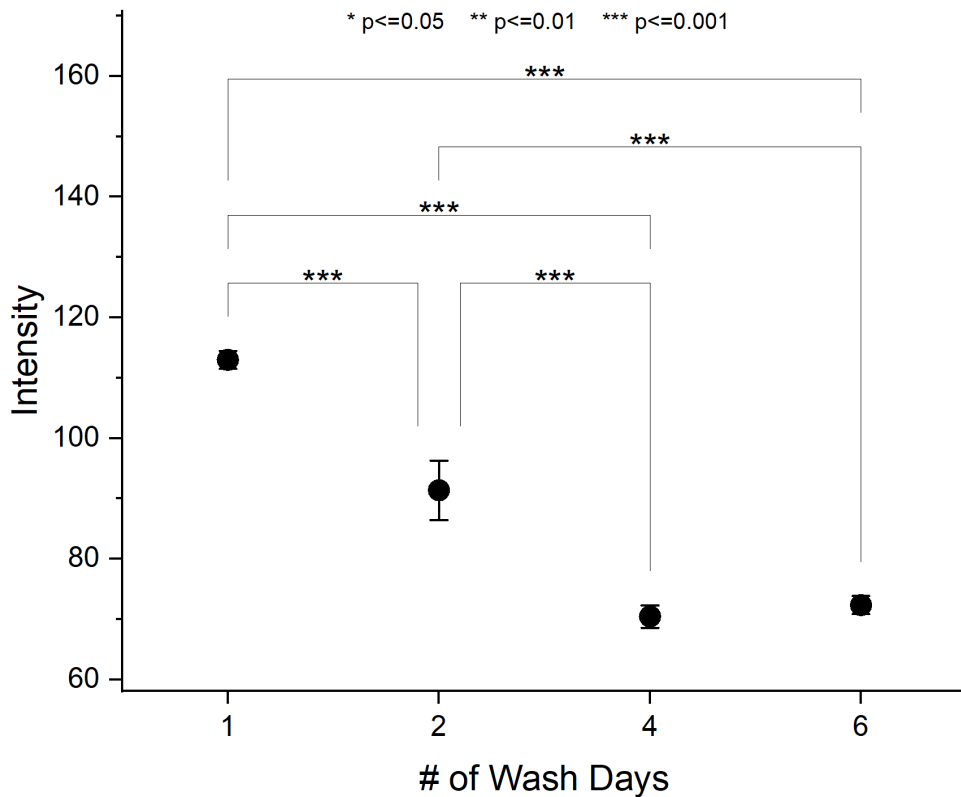


Figure 3.7: Change in intensity of Coomassie Brilliant Blue dye over the number of wash days conducted.

much bacterin as possible is kept in the hydrogel before delivery into salmon. An Atlantic salmon safety trial was conducted where the treatments tested corresponded to different wash day amounts and the resulting reactions from the salmon were recorded and analyzed (refer to Chapter 6).

## CHAPTER 4

### DRYING AND REHYDRATING PROPERTIES OF HYDROGELS

#### 4.1 Introduction

After formulation, it was explored if the hydrogel could withstand the handling necessary to implant the hydrogel into the salmon. To decide what TEMPO CNF wt% hydrogel would be best suited for implantation in the fish, 1.1 wt%, 1.3 wt%, 1.5 wt%, and 1.7 wt% TEMPO CNF and bacterin hydrogels were handled until breakage. Both 1.1 wt% and 1.3 wt% were not able to withstand the handling necessary for implantation before breaking apart. The 1.5 wt% and 1.7 wt% hydrogels appeared to be able to withstand enough handling for implantation with 1.7 wt% being able to withstand more force than 1.5 wt%. The 1.7 wt% TEMPO CNF and bacterin hydrogel was chosen as the hydrogel formulation to use due to the ability of the hydrogel to withstand more force. It is likely that the hydrogel will require moderate handling for implantation since the mucous layer on the fish will make it difficult to get the hydrogel into the incision. Therefore, the hydrogel TEMPO CNF weight percentage which was used for all formulated hydrogels throughout the rest of the thesis was 1.7 wt% unless otherwise noted.

Once the 1.7 wt% TEMPO CNF hydrogel formulation was decided for the aquaculture vaccine hydrogel, it was test implanted into five parr Atlantic salmon. The hydrogels were formed in citric acid, washed for 5 days in DI water, then washed for 1 day in PBS before implantation. An incision was made on the peritoneum of the fish and the hydrogel was pushed through the incision into the peritoneum cavity. Most of the hydrogels broke while trying to implant them into the salmon. However, it appeared that two of the hydrogels ended up being able to be implanted intact into the peritoneum cavity. Two days later, the salmon were euthanized and sampled to see

if the hydrogels remained in the peritoneum cavity. No remnants of the hydrogels were found in any of the salmon. This result could be due to the hydrogel falling out of the incision or because the hydrogel broke apart during the implantation process. Additionally, the incisions did not appear to heal properly over the two days. It was concluded that the hydrogels were not strong enough to be successfully implanted into the fish and that the incision needed to implant the hydrogels was too large. Therefore, a method of strengthening and shrinking the hydrogels needed to be developed.

## **4.2 Methods**

### **4.2.2 Drying Methods**

The drying methods and analysis were performed on 1.7 wt% TEMPO CNF only hydrogels. This was done because TEMPO CNF only hydrogels were easy to formulate and store for long periods of time in large quantities. The bacterin and TEMPO CNF hydrogels sometimes promoted bacterial or fungal growth over time due to the trypticase soy broth still present in the hydrogel. Additionally, it can be assumed that any changes which occurred in TEMPO CNF only hydrogels through experimentation would reflect as the same changes in the bacterin and TEMPO CNF hydrogels. For example, finding a drying method that was able to shrink and strengthen TEMPO CNF only hydrogels would also be able to shrink and strengthen the bacterin and TEMPO CNF hydrogels. The 1.7 wt% TEMPO CNF hydrogels were prepared by diluting the TEMPO CNF by half (to 0.55 wt%) using DI water, then vacuum filtering to 1.7% wt%. The DI water was added in the same proportions as bacterin to the TEMPO CNF to mimic the formulation of the bacterin and TEMPO CNF hydrogels. The 1.7 wt% TEMPO CNF was formed into hydrogels in citric acid and washed as normal.

Three different methods of drying the formed hydrogels were explored in this thesis; air drying, controlled drying with a dehydrator, and freeze drying. The hydrogels were air dried on a raised netted silicone dehydrator sheet placed on a lab benchtop in ambient room conditions. The controlled drying using a dehydrator was performed by putting the hydrogels on a netted silicone dehydrator sheet in a laminar flow dehydrator with adjustable temperature. Since the dehydrator had a laminar flow of heat, the tray of hydrogels was rotated 180° between measurements to promote even drying of all the hydrogels. The hydrogels were freeze dried by placing them in a freeze dryer that slowly decreased the temperature of the chamber until the hydrogels froze. Once the hydrogels were frozen, the pressure in the chamber was increased to sublime the water in the hydrogel. Air drying was combined with freeze drying by partially air drying the hydrogels before freeze drying.

#### **4.2.2 Methods of Analysis**

The air dried and dehydrated hydrogels were measured for changes in weight and volume during the drying process and when they were rehydrated. The hydrogels were rehydrated in PBS solutions. PBS was chosen because the hydrogels would be rehydrated in it before implantation into the salmon to help regulate their pH. The hydrogel weights were obtained by weighing each individual hydrogel on a scale. The volumes of the hydrogels were obtained by dropping a group of hydrogels into a small graduated cylinder filled with silicon oil (volume displacement measurement). The volume of the silicon oil was recorded before and after the hydrogels were fully submerged. The overall volume change was divided by the number of hydrogels in the silicon oil to obtain an average volume measurement of the hydrogel group. The freeze-dried hydrogels were measured for initial weight, weight after air drying, and weight after they were freeze dried.

SEM images were taken of fully wet, freeze dried, and dehydrated hydrogels to compare pore sizes. The SEM images were taken on an AMRAY 1820 scanning electron microscope. All the hydrogels were flash frozen in liquid nitrogen and dried if they were not already freeze dried. Flash freezing and then drying is different from the freeze-drying process because it reduces ice templating and the formation of artifacts.<sup>81</sup> Ice templating and artifacts are formed when hydrogels are frozen slowly which allows the water to expand and modify the hydrogel matrix. When hydrogels are flash frozen, the water doesn't modify the hydrogel matrix to the same extent, creating a dried hydrogel with similar initial morphology. The imaged hydrogels were broken in half in liquid nitrogen and placed upright to image the cylindrical cross-section of the hydrogel. The hydrogels were sputter coated with about 6nm of gold/palladium using a Denton DV-502 Rotary Evaporator and imaged at magnitudes of 25x, 100x, 250x, and 1500x. The pore sizes of the different hydrogels were measured and compared using the SEM images.

The mechanical properties of the hydrogels at different drying points were analyzed by measuring the compression modulus and strength of the hydrogels. The compression modulus and strength were obtained from a compressive stress vs. strain curve that was measured on a Discovery 850 DMA by TA Instruments. The compression modulus was analyzed from the stress-strain curve by finding the slope of the curve from 10% to 40% strain.<sup>61,82</sup> The compression strength was analyzed by finding the max stress value on the curve. The hydrogels were prepared as usual except for being formed using a cut-off 3 mL syringe instead of a cut-off 1 mL syringe to be large enough in size to test their mechanical properties. When the hydrogels formed using a cut-off 1 mL syringe, the compression DMA would crush the hydrogel sample before taking any measurements due to its small size. The 3 mL formed hydrogels were dried using the dehydrator to specific weight percentages (20%, 40%, 60% and 100% hydrated hydrogels) to match certain

points on the drying curve (Figure 4.1). This allowed the analyzed mechanical properties of the 3 mL hydrogels to directly correlate to mechanical properties of the 1 mL hydrogels.

Lastly, the long-term breakdown of the hydrogels was analyzed by staining the 1.7 wt% TEMPO CNF only hydrogels with calcofluor white. Calcofluor white is a fluorescent dye stain which fluoresces a blue color when exposed to UV light. These hydrogels were formed through a 1:1 ratio of TEMPO CNF and 100  $\mu$ M calcofluor white and prepared as normal. The hydrogels were dried in a dehydrator at 46°C for 30 minutes and then left to sit in PBS for eight weeks. After eight weeks, the calcofluor white hydrogels were imaged under a fixed camera setup with UV light (combined wavelengths of 254 nm and 365 nm) along with a calcofluor white hydrogel that was not rehydrated in PBS. The camera had a resolution of 2592x1944 pixels and exposure of 0.21~2000ms with an auto exposure feature. The edges of the hydrogels were outlined in ImageJ by using an edge finder process on separated color channels.

## **4.3 Results and Discussion**

### **4.3.1 Mass and Volume of Dried Hydrogels Using Different Methods**

The weight and volume of the hydrogels were measured as the hydrogels dried. 20°C represents the air-dried hydrogels which were dried on the lab benchtop because it was the average temperature of the room. The 29.5°C, 35°C, 40.5°C, 46°C, 51.7°C, 57°C, and 63°C temperatures represent the temperature that the dehydrator was set to. These temperatures were monitored by putting a thermometer inside of the dehydrator. The data in Figure 4.1 was graphed as the percent of initial hydrogel mass over the amount of time dried. Drying using the dehydrator decreased the percent mass of the hydrogels to a greater extent over shorter drying times than air-drying the hydrogels. Additionally, increasing the temperature in the dehydrator also caused an increase in

drying rate. However, changing the temperature of the dehydrator did not change the drying rate as much as switching from air-drying to using the dehydrator.

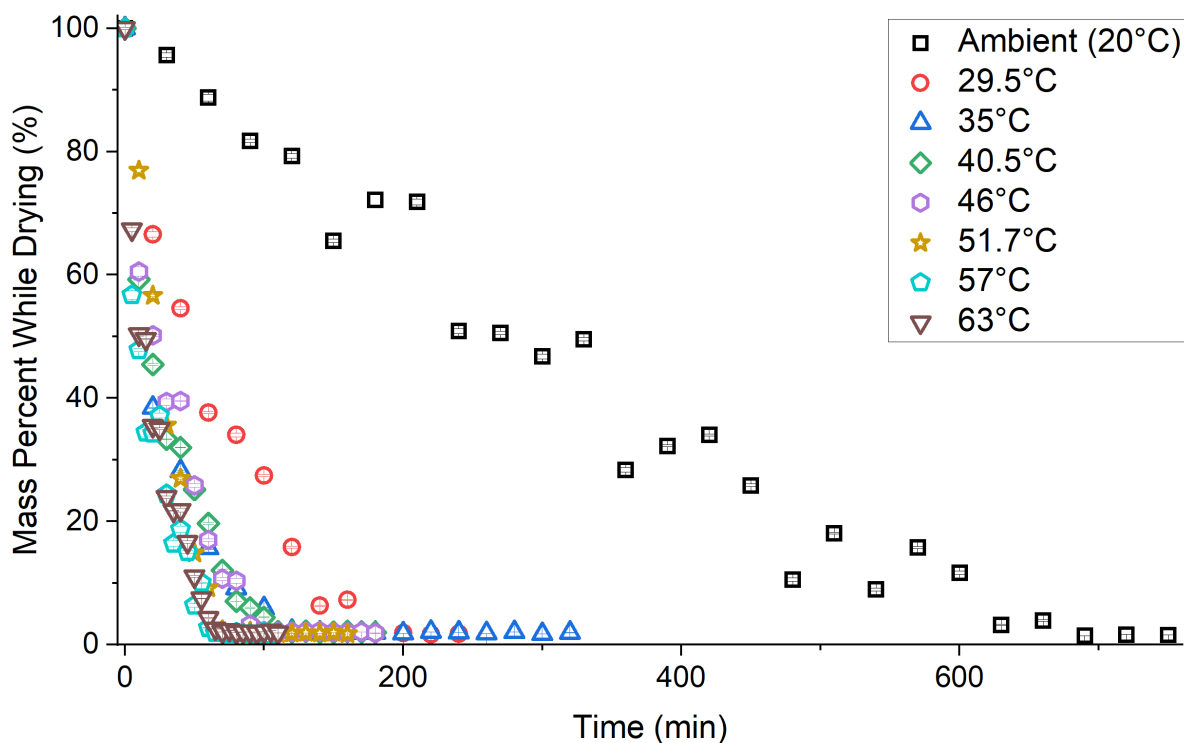


Figure 4.1: Changes in percent of initial hydrogel mass over time dried at different drying temperatures.

The volume of the hydrogels was measured in mL and then converted to  $\text{cm}^3$  using an average volume displacement method. The error bars on the graph were calculated by dividing the smallest amount of volume change that can be measured by the number of samples that were measured. The volume of the hydrogels were omitted from the graph when the volume displacement became too small to be accurately measured. The same trends from Figure 4.1 can be seen in the volume changes recorded in Figure 4.2. The hydrogel volume was only measured for the first four different temperatures because it showed that the volume while drying followed the mass drying curve. Additionally, by recording the volume change over four temperatures, it

provides enough data to be able to reliably relate a hydrogel's mass to its volume. This relation was important when deciding which hydrogels were the optimal size for implantation. The volume measurements could be improved on by measuring more samples at a time for more accurate values, especially when the hydrogels reached smaller sizes. The measurements could also be improved by using a volume displacement container or other volume measuring technique that allows for more precision.

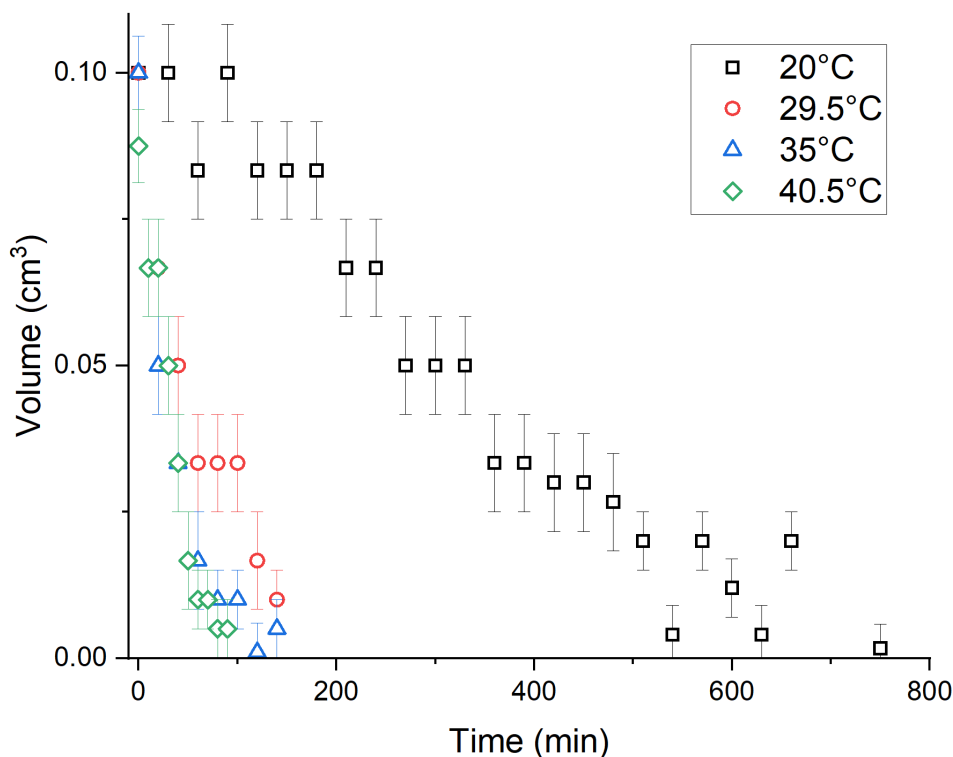


Figure 4.2: Changes in hydrogel volume over time dried at different drying temperatures.

The hydrogel mass drying data was also analyzed for hydrogel drying rates (Figure 4.3). The drying rates were calculated by finding the slope of the linear portion of a mass over time graph. 20°C corresponds to the hydrogels which were air dried. The drying rates were statistically analyzed using Tukey's method for significance between the different temperatures. Increasing the temperature from 20°C to 29.5°C to 35°C showed a highly significant increase in drying rate

of the hydrogels. Changing the temperature from 35°C to 46°C or 51.7°C to 63°C showed no significant increase in the drying rate even though the rate had a slight uptick for 46°C. However, changing the temperature from 46°C to 51.7°C showed a significant increase in drying rate.

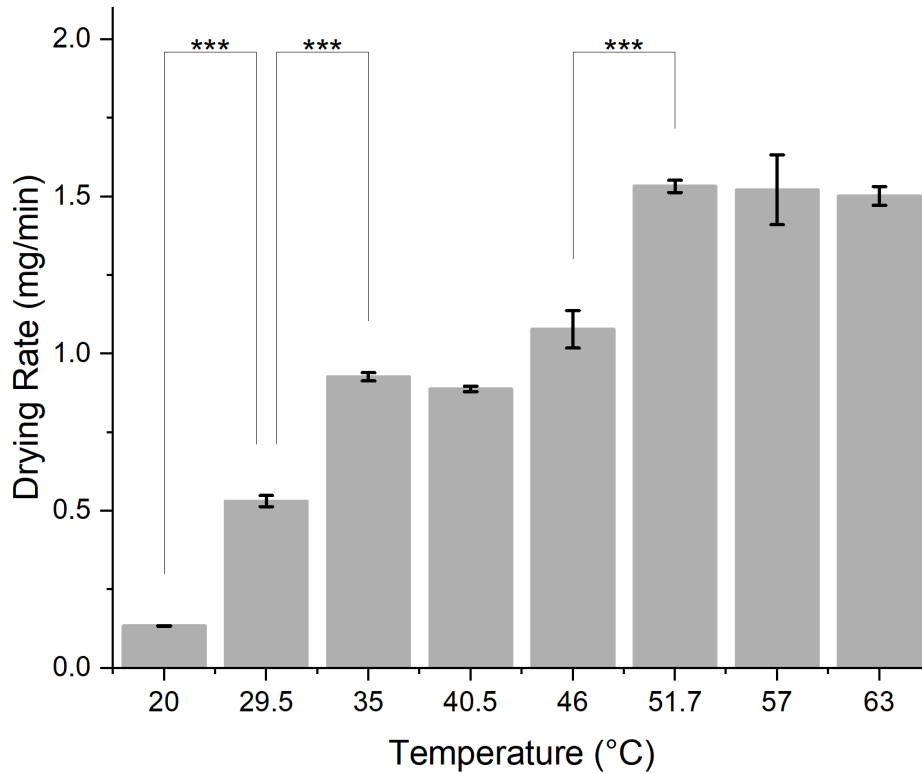


Figure 4.3: Comparison of hydrogel drying rates based on the drying temperature.

The use of a dehydrator to dry hydrogels significantly increases the drying rate. Therefore, the use of a dehydrator will lead to shorter preparation time for the aquaculture vaccine hydrogel. Additionally, the temperature of the dehydrator affects the drying rate of the hydrogel to some extent. To choose which temperature is best for drying the hydrogels, the bacterin needs to be considered. A balance must be found between drying the hydrogels at a fast rate but also not exposing the hydrogels to high temperatures which diminishes the antigen response of the bacterin. Therefore, the highest drying rate possible without diminishing antigen response would be 51.7°C because increasing the temperature beyond that point does not show a significant increase in the

drying rate. Temperatures above 63°C were not explored in this research because they would be too close to the 80°C which is shown to decrease the bacterin's antigen response. To further reduce the possibility of decreasing the bacterin's antigen response while still drying the hydrogels at an increased rate, a temperature of 35°C should be used.

Lastly the hydrogels were dried through freeze drying or a combination of air-drying with freeze drying. The weights of the hydrogels were measured initially, after air-drying, and after being freeze dried (Figure 4.4). Each color corresponds to the amount of time the hydrogel was air-dried before being freeze dried. Regardless of how long the hydrogels were air-dried, they all ended up with the same final mass. This was expected because freeze drying is a process that completely dries the hydrogel. However, the longer the hydrogels were air-dried before freeze drying, the smaller in size and more narrow the resulting hydrogel became. The freeze-dried hydrogels were easily able to be crumpled or crushed by tweezers. Additionally, when the freeze-dried hydrogels were rehydrated, they appeared to become more delicate than before drying. The freeze-dried hydrogels also had spiderweb-like white lines staying present inside the hydrogel as it rehydrated. These spiderweb lines were likely due to the ice templating that occurred during freeze drying. The ice templating appeared to expand the pores of the hydrogel matrix where water was present, pushing neighboring TEMPO CNF fibers close enough to each other to form permanent hydrogen bonding (hornification). As a result, these hornified sections of the hydrogel wouldn't rehydrate or separate with the introduction of water. The resulting properties of the freeze-dried hydrogels made the freeze-drying process a less attractive solution than the dehydrator for producing smaller and stronger hydrogels for implantation.

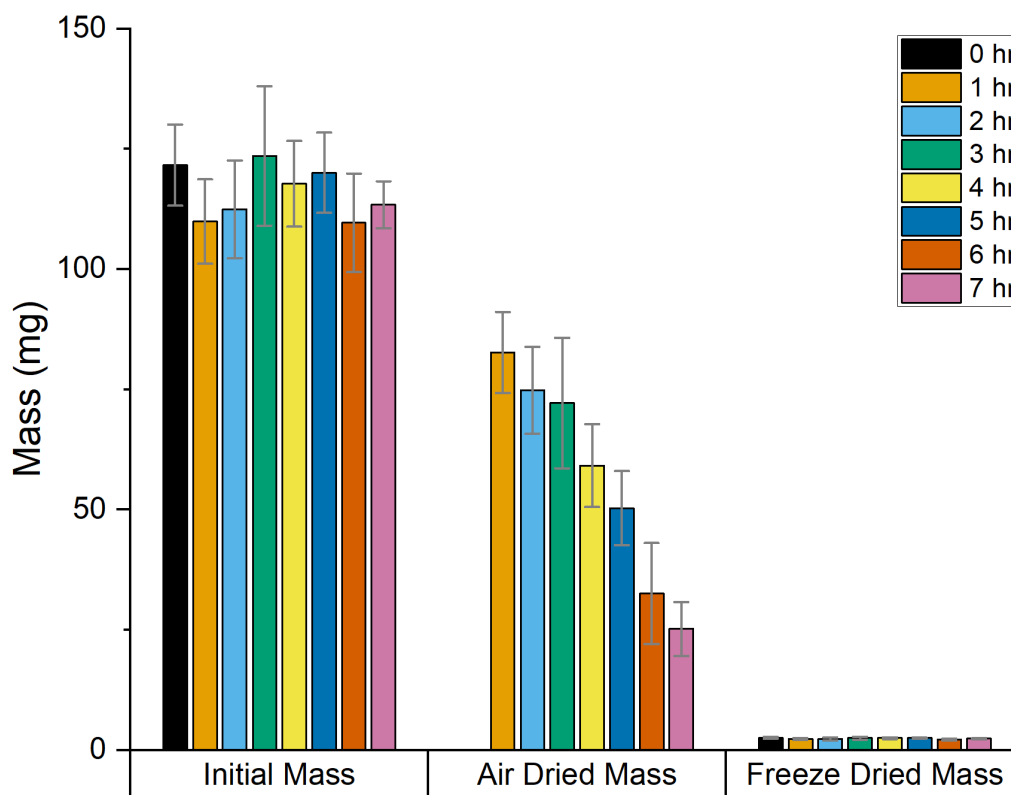


Figure 4.4: Changes in hydrogel mass after being air-dried and then freeze dried.

Drying the hydrogels at 46°C was chosen for SEM imaging, measuring mechanical properties, the second safety trial, monitoring the breakdown of hydrogels over time, and an ELISA test of antigen response from the hydrogel. This temperature was used because it was in the middle of all of the temperatures. Also, it is close to the highest temperature that should be used to dry the hydrogels, to show if temperatures around this range would begin to reduce the antigen response of the bacterin. More information on how temperatures affect the properties of the hydrogel could be obtained by redoing the tests done on the hydrogels dried at 46°C for hydrogels dried at different temperatures. The reasons why freeze-dried hydrogels were not tested in most of the above tests were explained in sections 4.3.3 and 4.4.

### 4.3.2 SEM Imaging of Different Drying Methods

Three types of hydrogels were compared using SEM imaging. The first hydrogel was a fully wet hydrogel that was freeze-dried with a slow freezing process (designated as freeze-dried). The second hydrogel was a fully wet hydrogel that was flash frozen then dried using the freeze dryer (designated as fully wet). The third hydrogel was dried at 46°C for 30 minutes then flash frozen and dried using the freeze dryer (designated as dried). Drying the hydrogels at 46°C for 30 minutes resulted in a hydrogel that had 40% its initial mass, which was roughly halfway dried. This extent of drying was chosen because it was the optimal size for implantation into the salmon (refer to section 4.4 for more details).

The SEM images of the three kinds of hydrogels were drastically different. The hydrogel with the smallest and most uniform pores was the dried hydrogel. This hydrogel also appeared to be the least porous because of the miniscule pore size. The dried hydrogel had pores that were about 12  $\mu\text{m}$  in diameter when measured in ImageJ. Also, the largest hole seen in the dried hydrogel 250x magnification image was caused by over magnification of the microscope leading to some of the TEMPO CNF melting. The hydrogel with the mid-sized pores was the fully wet hydrogel. The 25x image of the fully wet hydrogel shows a large range of pore sizes which makes the hydrogel appear to be very porous. The smallest pores in the 25x magnification image were captured at 250x magnification (Figure 4.5e) and were about 50 $\mu\text{m}$  in diameter. The hydrogel with the largest and least number of pores was the freeze-dried hydrogel. The 25x magnification image of the freeze-dried hydrogel showed four extremely large pores, one or two medium sized pores, and a lot of flat non-porous surface. One of the large pores in the freeze-dried hydrogel was about 300  $\mu\text{m}$  in diameter, such as the pore shown in Figure 4.5f (located to the far left of the hydrogel on Figure 4.5c).

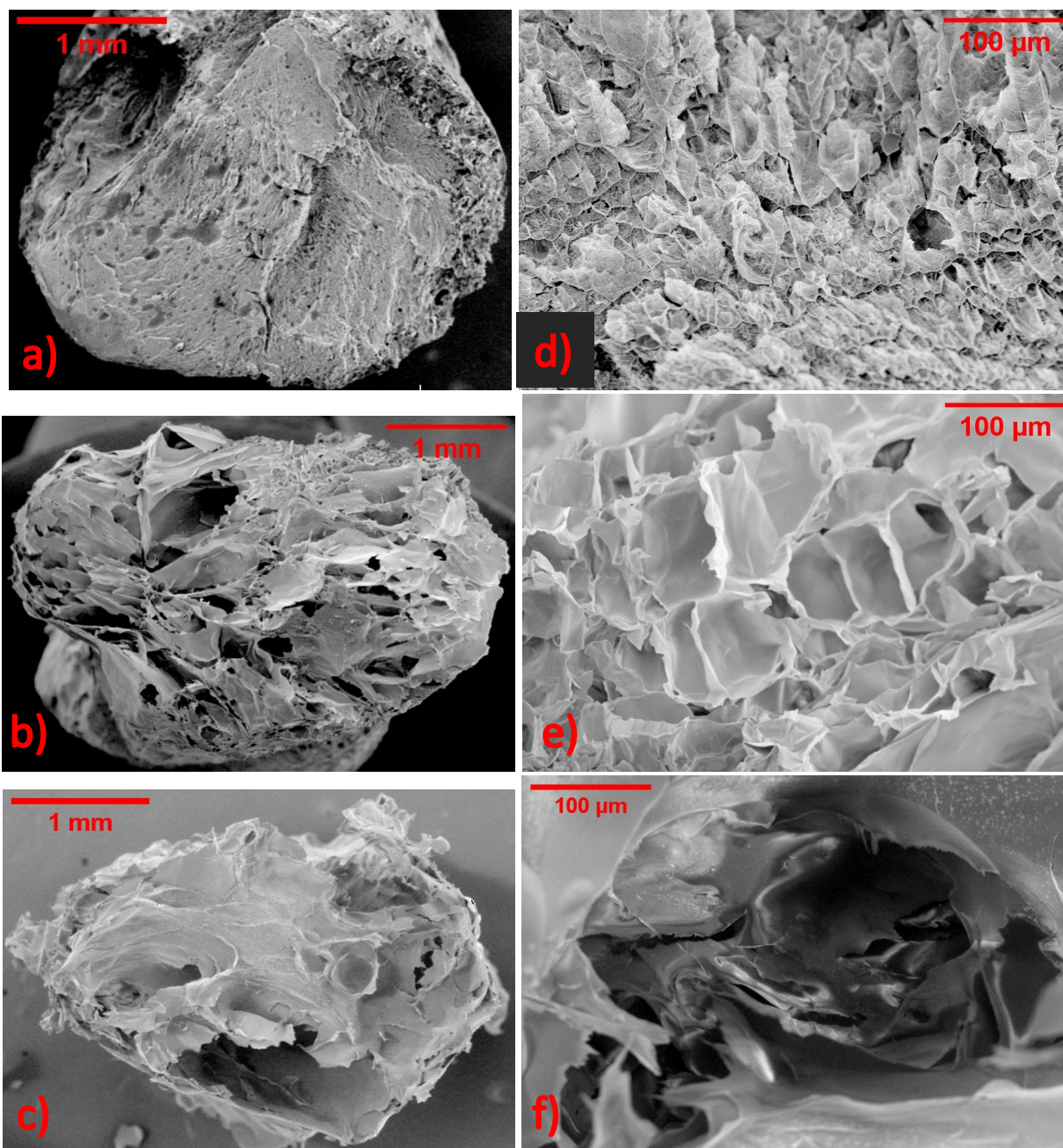


Figure 4.5: SEM images of dried, fully wet, and freeze-dried hydrogels. (a) and (d) is a dried hydrogel at 25x and 250x magnification. (b) and (e) is a fully wet hydrogel at 25x and 250x magnification. (c) and (f) is a freeze-dried hydrogel at 25x and 250x magnification.

The fully wet hydrogel had large pores in comparison to the 1-2  $\mu\text{m}$  in length bacteria which the hydrogel was designed to deliver. The pores on the fully wet hydrogels were not uniform in size which likely would cause an uneven diffusion rate of bacterin. The dried hydrogel had much smaller and more uniform pore sizes. With an average pore size of about 12  $\mu\text{m}$  in diameter, these pores were likely to entrap bacterin more efficiently, promoting a long and slow diffusion rate over the desired period of weeks to months. The increased organization of the pores was evident in the closely packed rows and layers of pores seen in the 250x SEM image (Figure 4.5d). A cartoon depiction of what likely happened to the hydrogel matrix during the drying process is shown in Figure 4.6. Based on the SEM images, it appeared that the TEMPO CNF fibers became more closely packed and formed layers and sheets of closely packed pores.

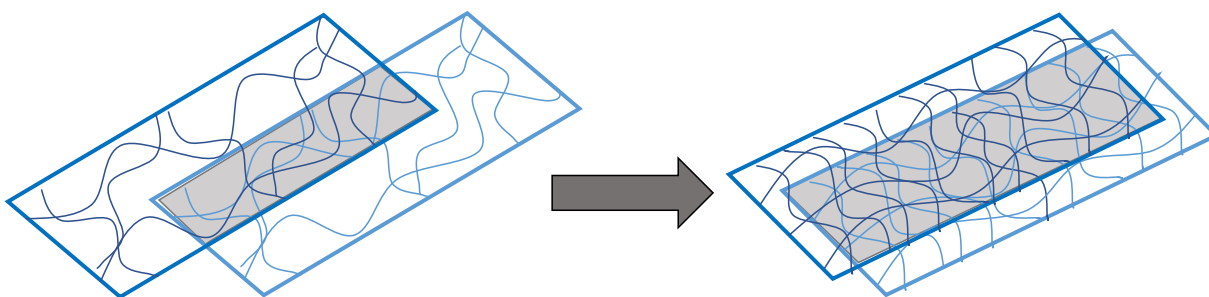


Figure 4.6: Cartoon depiction of changes that occur in hydrogel matrix through drying.

The freeze-dried hydrogel had the largest pores of all three imaged hydrogels. The size of the pores would likely not efficiently entrap the bacterin into the hydrogel matrix. During rehydration, it is likely that the bacterin would mostly diffuse out of the hydrogel in a burst. Additionally, ice templating and artifacts are highly apparent in the freeze-dried hydrogel due to the increase in pore size and the hornified smooth and flat portions. The SEM images of the freeze-dried hydrogel helps confirm the “spiderweb” phenomena which occurred when the freeze-dried

hydrogels were rehydrated. As a result, properties of the freeze-dried hydrogels do not match the desired properties for the aquaculture vaccine hydrogel.

### 4.3.3 Mechanical Properties of Dried Hydrogels

The 1.7 wt% TEMPO CNF only hydrogels for mechanical compression testing were formed using a cut-off 3 mL syringe (refer to Figure 3.1 for syringe sizes). Hydrogels at four different stages of drying were tested to measure their compression strength and modulus. Compression strength is the maximum amount of stress that the hydrogel matrix can withstand overall (note this does not mean maximum amount before deformation). The compression modulus (or compressive Young's modulus ( $E$ )) is a measure of the stiffness of the material or the ability of the material to withstand permanent changes in shape when compressed (Eq. 4.1). A hydrogel with high compression strength has a strong matrix while a hydrogel with a high compression modulus has greater stiffness or is better able to withstand permanent changes in shape when forces or loads are applied to it.

$$E = \frac{\sigma}{\varepsilon} \tag{4.1}$$

$E$  = Compression modulus

$\sigma$  = Compressive stress

$\varepsilon$  = Strain (compressed length/initial length)

The four hydrogel drying stages tested were: fully wet, dried to 60% of the hydrogel's initial mass, dried to 40% of the initial mass, and dried to 20% of the initial mass. Each drying stage had 8 duplicate samples (60% initial mass only obtained 7 data points since the DMA crushed one of the hydrogels without measuring). Each of the sample's stress-strain curves can be seen in the appendix of the thesis. The average compression strength and modulus of each drying stage was calculated and plotted in Figure 4.7. The grey columns represent the compression strength, and the red columns represent the compression modulus. 100% hydrated represents the fully wet hydrogel and 60% hydrated the hydrogel dried to 60% its initial weight and so on. Both the compression strength and modulus values were also statistically analyzed using Tukey's method for significance and are shown in Figure 4.8 and 4.9, respectively.

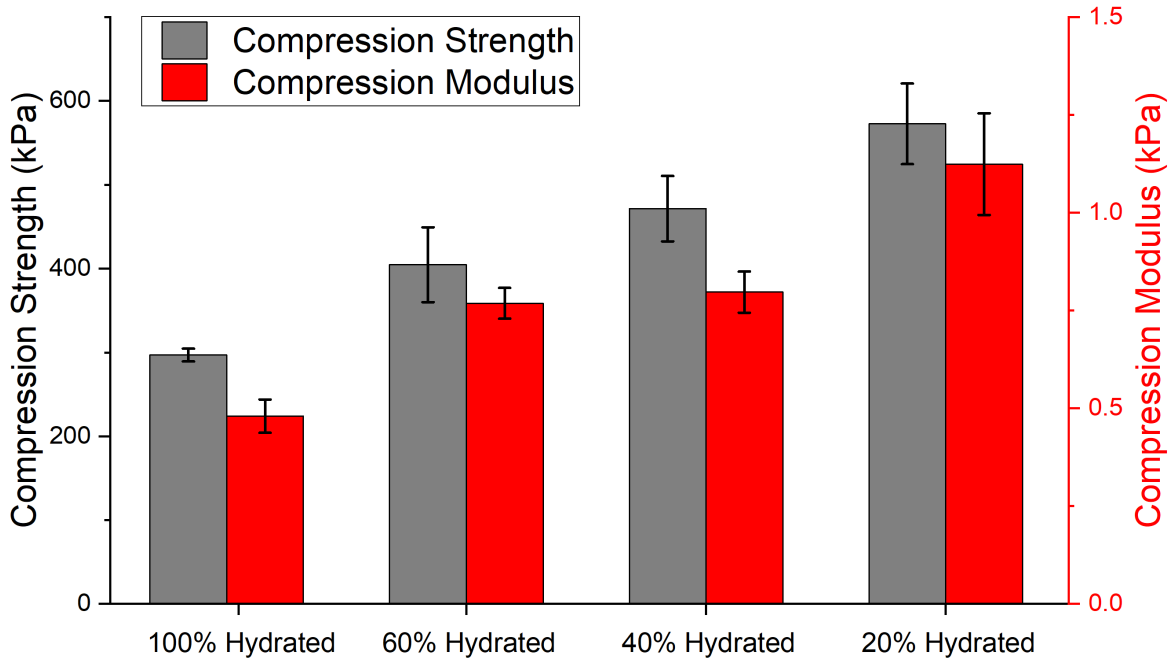


Figure 4.7: Compression strength and modulus of hydrogels at different stages of drying.

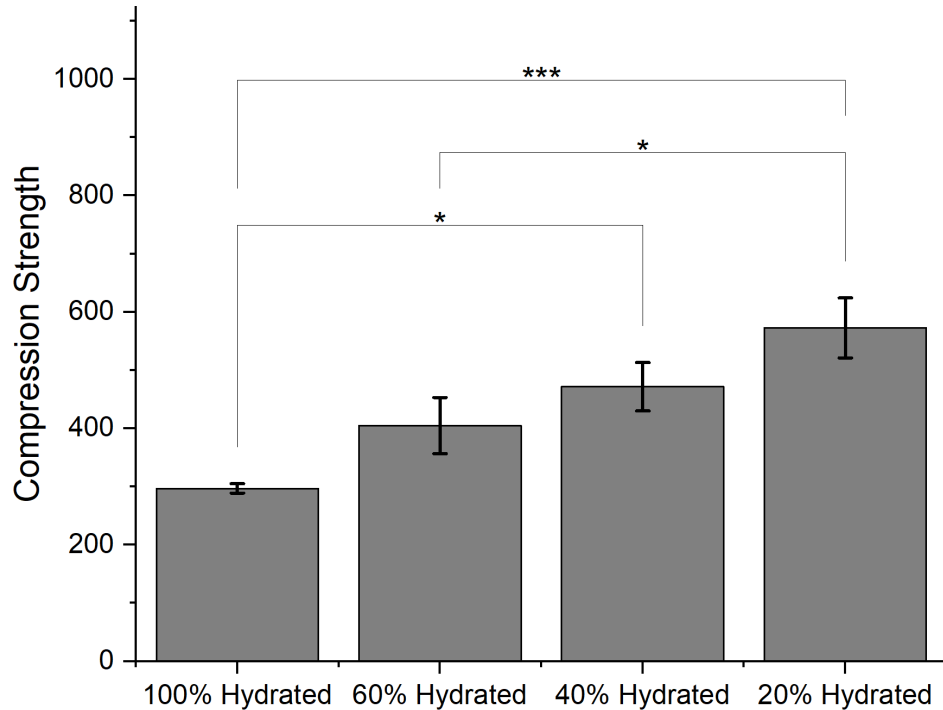


Figure 4.8: Compression strength statistical analysis.

A positive trend can be seen both in the compression strength and modulus where the drier the hydrogel, the higher its compression strength and modulus values. The compression strength of the hydrogel significantly increases from fully wet hydrogels to hydrogels that were dried to 40% their initial mass and from 40% their initial mass to 20% their initial mass. Therefore, drying the hydrogels increases the matrix's overall strength which supports the structure seen in the dried hydrogel SEM images. A less porous and more compact matrix will generally have more strength than a more porous structure. The compression modulus significantly increases from fully wet to 40% initial mass, 60% initial mass to 20% initial mass, and 40% initial mass to 20% initial mass. Therefore, drying the hydrogel increases its compression modulus, creating a stiffer hydrogel. Overall, the mechanical testing data demonstrates the drying the hydrogels using a dehydrator

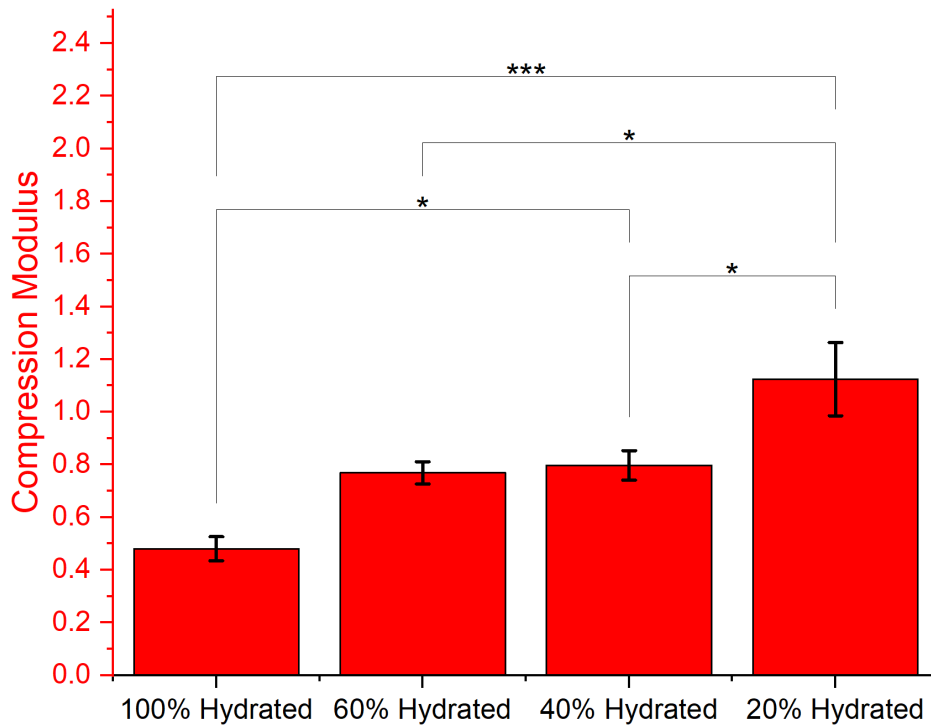


Figure 4.9: Compression modulus statistical analysis.

creates stronger and stiffer hydrogels. Therefore, using a dehydrator is a viable option to create hydrogels that are able to withstand the implantation process.

#### 4.3.4 Mass and Volume of Rehydrated Hydrogels

The rehydration properties of the hydrogels were explored in addition to the drying properties since the hydrogels were rehydrated in PBS before implantation into the salmon. Four temperatures were chosen to dry the hydrogels at (air-dried/20°C, 29.5°C, 46°C, and 63°C). These temperatures were chosen to represent the range of drying temperatures that were used in section 4.3.1. For each temperature, five time points across the range of the drying curve that were roughly equidistant to each other were chosen as the amount of time to dry the hydrogels. It was hypothesized that the hydrogels would significantly increase in size when rehydrating and that the extent of drying affects the rehydration size of the hydrogels, not temperature. The masses of the

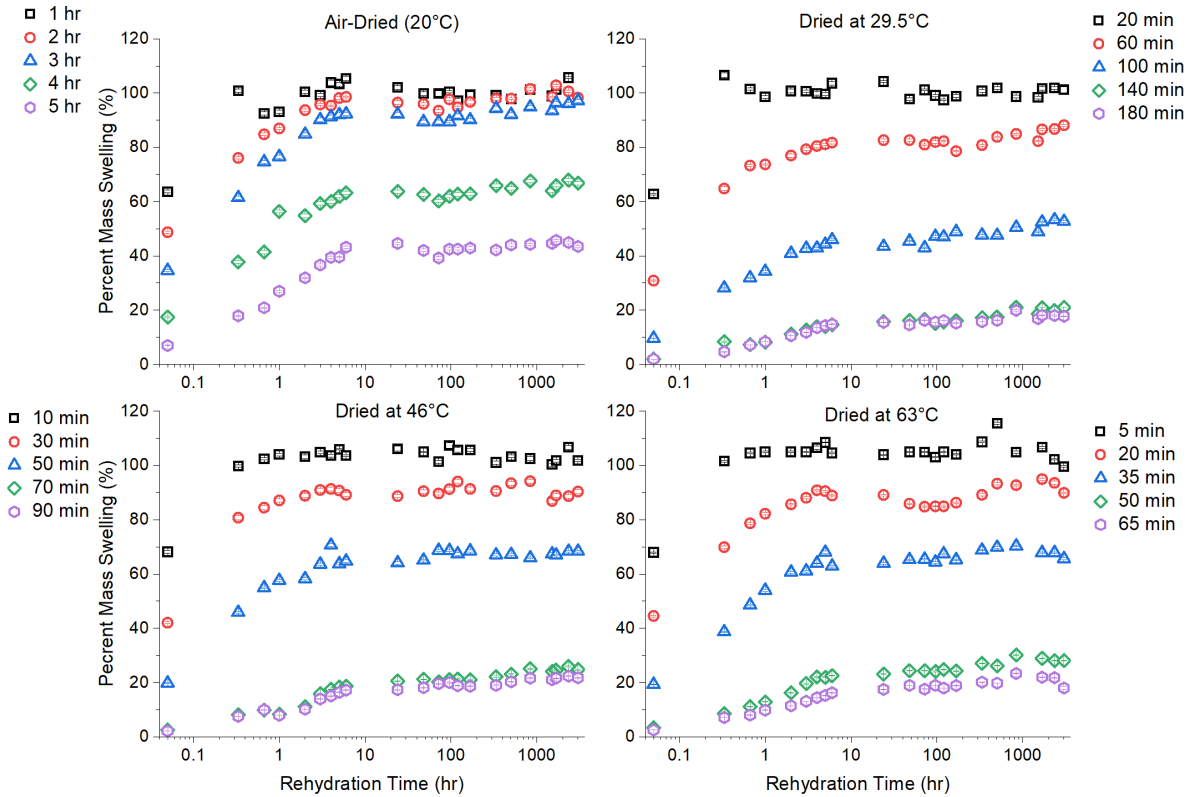


Figure 4.10: Changes in % of initial hydrogel mass over time as the hydrogel rehydrates after being dried at different temperatures for different lengths of time.

hydrogels were measured over time as the hydrogels rehydrated and are plotted as percent of the initial hydrogel mass on Figure 4.10. The volume of the hydrogels was measured after they were left to rehydrate for 24 and 3024 hours and compared to the average volume of a fully wet hydrogel and corresponding dried average volume measured in section 4.3.1 (Table 4.1).

The same rehydration trends can be seen across hydrogels that were dried for different amounts of time or dried at different temperatures. The hydrogels showed a steep initial increase in weight when first put into PBS which gradually increased for six hours and then plateaus. The plateaued rehydration mass stayed steady over a long period of time (over 18 weeks). This plateau suggested that the hydrogels remain stable in the PBS over a long period of time. It also suggested

that the hydrogel was not breaking apart over time or that the crosslinks in the hydrogel matrix were not degrading. Section 4.3.7 further explores how the structure of the hydrogel changes over extended periods of time. The initial increase in mass for the rehydrated hydrogels was further studied in an additional experiment where measurements were taken more frequently. This data can be found in the appendix.

The measured volumes were compared for the air-dried and 29.5°C dried hydrogels which had previously obtained dried hydrogel volume data. The rehydrated hydrogel volume almost always increased from the dried hydrogel volume which suggested that the hydrogels do increase in size when they rehydrate. However, to make any conclusive statements about how the volume of the hydrogel changes from short term rehydration to long term rehydration, a more precise volume measuring method needs to be designed.

Table 4.1: Volume Comparison of Hydrogels

Drying Temperature	Time Dried	Initial volume (cm <sup>3</sup> )	Dried volume (cm <sup>3</sup> )	Volume 24 hrs rehydrating(cm <sup>3</sup> )	Volume 3024 hrs rehydrating (cm <sup>3</sup> )
Air-dried(20°C)	1 hr	0.1	0.0833	0.1333	0.1667
Air-dried(20°C)	2 hr	0.1	0.0833	0.1333	0.13
Air-dried(20°C)	3 hr	0.1	0.0833	0.1125	0.13
Air-dried(20°C)	4 hr	0.1	0.0667	0.0967	0.09
Air-dried(20°C)	5 hr	0.1	0.05	0.04	0.05
29.5°C	20 min	0.1	0.0667	0.1333	0.15
29.5°C	60 min	0.1	0.0333	0.07	0.125
29.5°C	100 min	0.1	0.0333	0.02	0.08
29.5°C	140 min	0.1	0.01	0.016	0.02

To evaluate the hypotheses made about rehydrating hydrogels, the initial dried weight was compared to the last measured weight of the rehydrated hydrogels (3024 hours) and statistically analyzed using Tukey’s method for significance. The data was organized to compare the change in % initial mass before and after rehydration for each temperature to evaluate if the hydrogels

significantly increased in size when they rehydrated (Figure 4.11). Regardless of the temperature or time the hydrogels were dried, they would significantly increase in weight when rehydrated. The positive trend in mass and the general trend of increasing volume suggested that the hydrogels increased from their dried size when rehydrated. Therefore, since the hydrogels were implanted into the salmon after being rehydrated in PBS, the change in hydrogel size due to rehydration had to be considered.

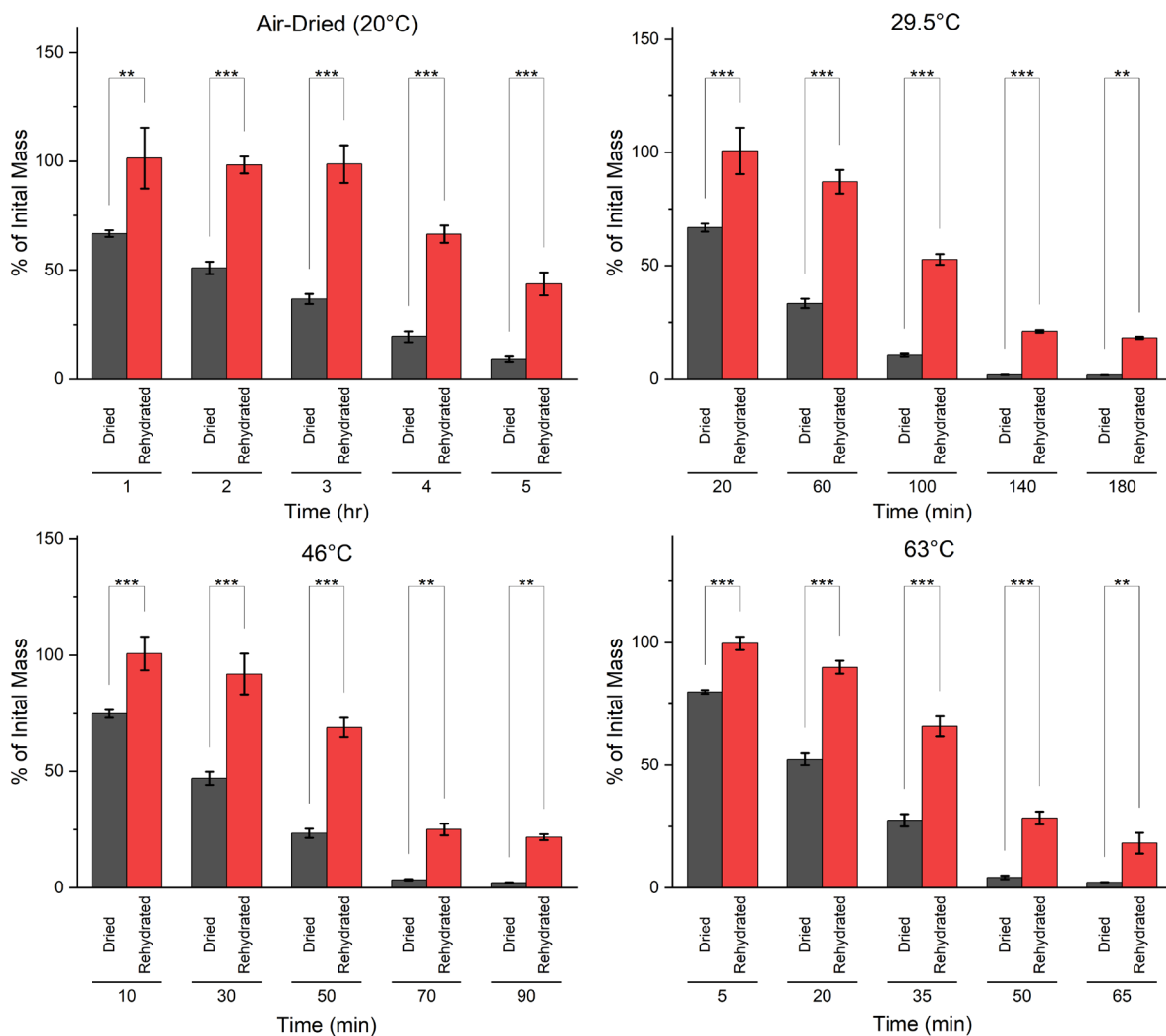


Figure 4.11: Comparison of dried hydrogel mass % to final rehydrated hydrogel mass %.

To test the second hypothesis, the data was organized so the hydrogels dried to a similar extent in different temperatures were compared for possible significance in their dried masses (graphs on the left of Figure 4.12). Then the final rehydration masses of those hydrogels were compared to see if the hydrogels with no significance in their dried masses continued to have no significance in their rehydrated masses (graphs on the right of Figure 4.12). Each graph on the left is directly related to the graph on the right. Overall, the hydrogels that had no significant differences in their dried masses also had no significant differences in their final rehydration mass. This suggests the fact that the amount that the hydrogel changes in size during rehydration is not dependent on temperature, only on the extent dried. In other words, hydrogels that are dried to the same initial mass % will rehydrate to the similar mass %'s regardless of the temperature used for drying. This hypothesis should be further tested by drying hydrogels to the exact same initial mass percent at different temperatures before rehydrating them. Conducting that experiment would produce more accuracy and precision in the measurements instead of comparing timepoints that appeared similar on the drying curve graph (Figure 4.1). If hydrogels rehydrate the same regardless of the temperature used to dry them, then that promotes the decision to use the lowest possible drying temperature that still has the desired drying rate, minimizing the risk of decreased antigen response from the bacterin.

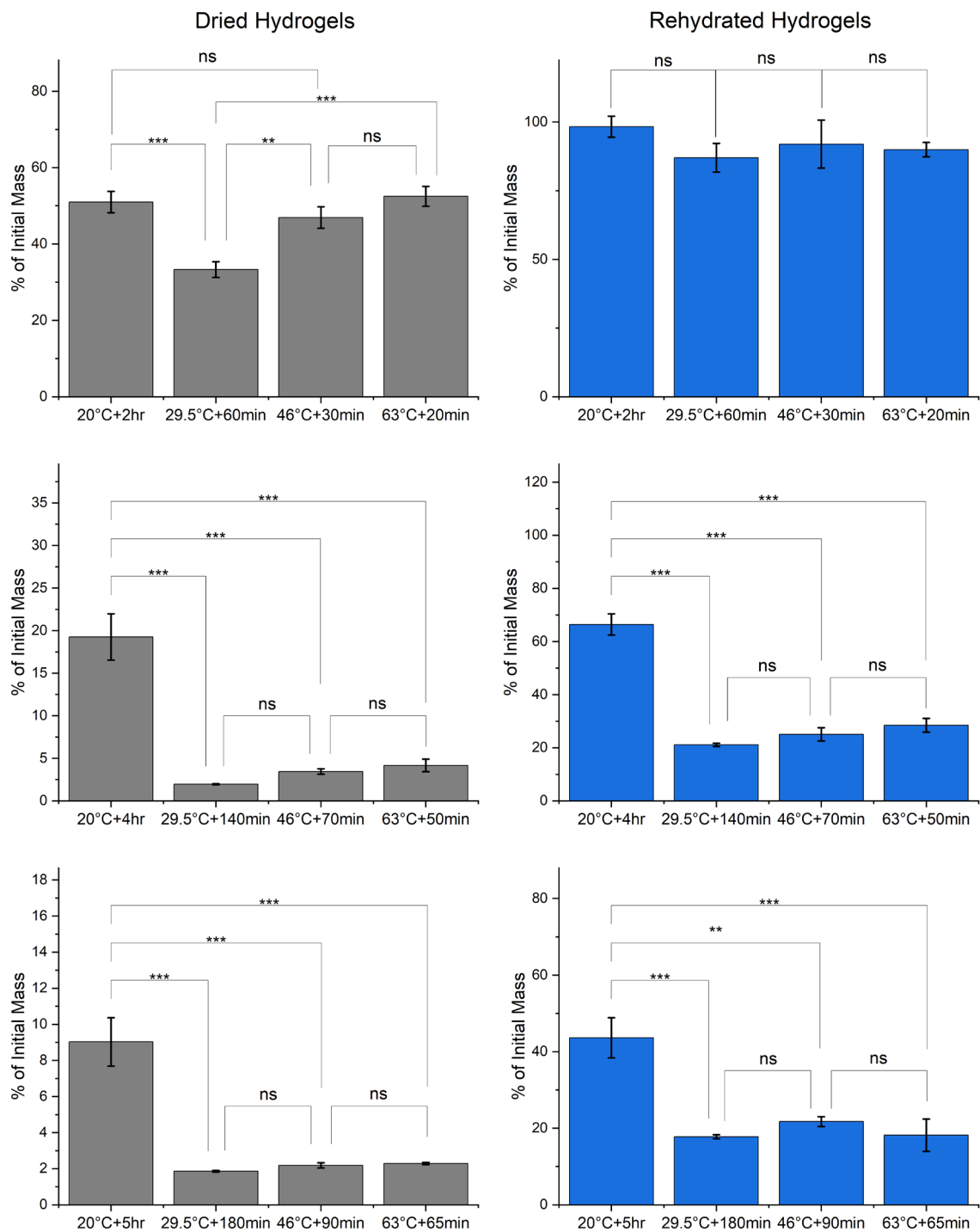


Figure 4.12: Comparison of changes in hydrogel size based on the extent hydrogels are dried to at different temperatures.

#### 4.3.5 Breakdown of Rehydrated Hydrogels over Time

Over long time periods in PBS, the hydrogels appeared to expand and become “cloudy”. In a couple instances, the “cloud” of the hydrogel would connect to the “clouds” of surrounding hydrogels. The rehydration mass data was not able to explain this phenomenon. These “clouds” suggested that the hydrogel was breaking down over time from the surface inwards toward the core of the hydrogel. However, image analysis was not able to be conducted on the rehydrated hydrogels due to their transparency. In order to confirm that the “cloud” was broken down hydrogel matrix, it would have to be proven that the “cloud” was made of TEMPO CNF and not growth of some contaminant. Therefore, a CNF stain needed to be used in order to reliably indicate the presence of TEMPO CNF fibers.

Calcofluor white was chosen as the TEMPO CNF stain due to the bright blue color it produced when placed under UV light and for its simple and easy staining procedure. One batch of hydrogels was placed in PBS for eight weeks while another was left in a sealed vial as a control. After eight weeks the hydrogels from both batches were imaged and analyzed in ImageJ. The cloud

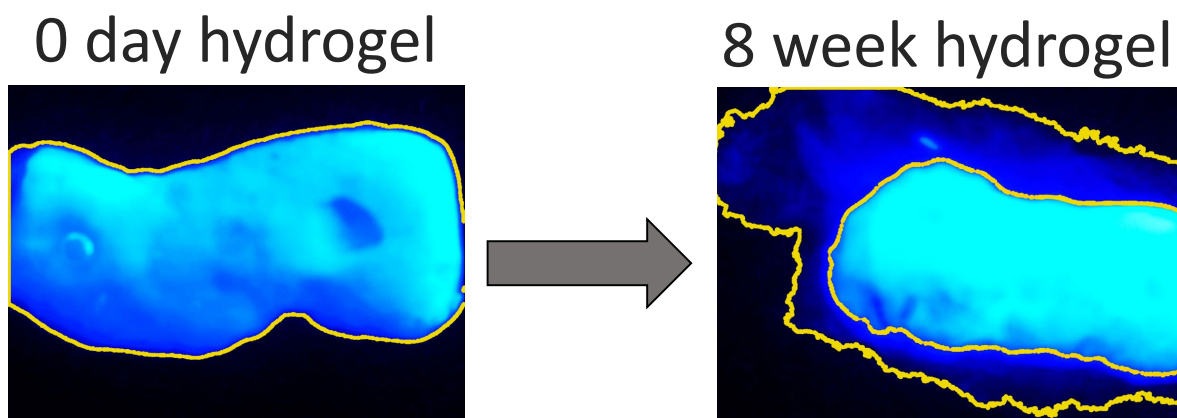


Figure 4.13: Fluorescent images of the hydrogel before and after 8 weeks for breakdown analysis

and hydrogel core were able to be selected separately through different color channels. The image selections obtained highly suggests that the formed “cloud” is TEMPO CNF, thereby supporting that the hydrogel breaks down over long periods of time in PBS.

Although hydrogel breakdown isn't desirable initially because it would signify a premature burst release of bacterin, it is desirable after multiple months for a couple reasons. One reason is that breakdown of the hydrogel enables trapped bacterin at the core of the hydrogel to be released. Another reason is that if the hydrogel breaks down completely before the salmon reaches market size, it removes the risk of being found by a consumer or needing to add an additional step in the filleting process of having to find and remove the hydrogel.

#### **4.4 Most Optimized Delivery Method**

Drying the hydrogels using a dehydrator was the best explored method to use for this application. This method is highly tunable, scalable, and able to dry the hydrogels quicker than air-drying or freeze-drying (which took about 12-24 hours). Lastly, drying the hydrogels using a dehydrator is more inexpensive than freeze-drying at an industrial scale. The collected data proved that drying the hydrogels with a dehydrator created smaller, stronger, and stiffer hydrogels. For data on how drying with a dehydrator affects antigen response refer to section 5.3.1.

After exploring the properties of dried and rehydrated hydrogels, the best way to deliver the hydrogels was explored. There were two salmon safety studies which were conducted for the hydrogel formulation explored in this thesis (refer to Chapter 6 for details). The delivery method of the hydrogels was different for the two safety studies. The delivery method of the hydrogels for the first safety study was pushing the hydrogel into an incision that was slightly larger than the length of the hydrogels. The hydrogels were dried at 35°C for 3.5 hours and rehydrated in PBS

before implantation into the salmon. Although the hydrogels were able to be implanted into the fish, most of them did not appear to remain in the fish (see chapter 6 for more information).

Due to the results from the first safety study, it was determined that the delivery method needed to be improved. Instead of making an incision about the length of the hydrogel, it would be better to make an incision the width of the hydrogel's diameter. Since it would be extremely difficult to implant the hydrogels into an incision of that size by hand, it was decided that the hydrogel would need to be delivered by a needle. Needles up to gauge 6 in size are used for applications such as pit-tagging in aquaculture. The needle had to be large enough to hold a somewhat dried hydrogel but also small enough to be reasonable to use on the parr salmon. The needle size that was agreed upon was an 8-gauge needle because it was able to load dried hydrogels while being small enough for the salmon to easily heal from. An 8-gauge needle was able to fit hydrogels that were about 40% their initial mass ( $\sim 0.05 \text{ cm}^3$ ) or smaller. The device designed for the delivery of hydrogels for the second safety study consisted of a syringe with a plunger that was the same diameter as the 8-gauge needle so the hydrogel could be pushed out of the 8-gauge needle into the salmon's peritoneum cavity. The hydrogel treatments were delivered into the fish by making an incision just big enough to fit the 8-gauge needle and using the needle to implant the gels into the peritoneum cavity. More information on the effectiveness of this delivery method can be found in chapter 6.

## CHAPTER 5

### CHARACTERIZING DIFFUSION OF BACTERIN OUT OF HYDROGELS

#### 5.1 Introduction

In order to fully explore and characterize the aquaculture vaccine hydrogels, the hydrogel formulation needed to be designed (chapter 3), the delivery method of the hydrogel needed to be developed (chapter 4), the diffusion of target drug from the hydrogel needed to be measured, and the salmon's reactions to the developed hydrogel needed to be analyzed (chapter 6). This chapter explores the methods of analyzing the diffusion of bacterin (specifically the inactivated *Vibrio anguillarum*) from the hydrogel matrix.

#### 5.2 Methods

##### 5.2.1 ELISA Method

ELISAs were performed by Sarah Turner at the University of Maine Cooperative Extension Diagnostic and Research Laboratory. ELISAs were performed on isolated bacterin from the hydrogels and bacterin that diffused out of the hydrogel over time. A bacterin positive control and dehydrated TEMPO CNF only hydrogel negative control was compared to fully wet and dehydrated TEMPO CNF and bacterin 1:1 ratio hydrogels. All the hydrogels were prepared as normal. The dehydrated hydrogels were dried at 46°C for 30 minutes. Bacterin in a concentration of  $1 \times 10^8$  CFU was used as the positive control. The bacterin was isolated from the hydrogels by putting a hydrogel with 200  $\mu$ L of PBS. The hydrogels were mashed and vortexed to separate the bacterin from the TEMPO CNF matrix. The isolated bacterin was plated onto a 96 well ELISA plate and analyzed using an indirect ELISA. For the ELISA of diffused bacterin, the hydrogels

were isolated in PBS and after 0-, 100-, 300-, and 600-degree days, the PBS was used in an indirect ELISA to measure antigen response. The antigen response of the hydrogels was compared to a bacterin positive control and dehydrated TEMPO CNF only hydrogel negative control.

### **5.2.2 Coomassie Brilliant Blue Diffusion Method**

To further analyze the diffusion rates of loaded drug from the hydrogel, a diffusion model study was designed. The bacterin was modeled using Coomassie Brilliant Blue (CBB) dye because the anionic dye would mimic the negatively charged inactivated *Vibrio anguillarum*. The hydrogels were prepared by adding a 1:1 ratio of 1.1 wt% TEMPO CNF to 1mM CBB dye. The hydrogels were vacuum filtered to a 1.7 wt% TEMPO CNF, formed, and washed as normal. The hydrogels were dried at the same temperatures and times as the rehydrating experiments. The dried hydrogels (or one group of fully wet hydrogels) would be separated individually into cuvettes with 1.5 mL of PBS. A spectrometer was used to measure the intensity of the PBS just above the hydrogel. The intensity of the hydrogel PBS was taken over time along with the intensity of a non-dyed hydrogel in PBS, and a 0.0125mM CBB dye sample. LabVIEW programs were created to smooth the spectrometer signals and calculate the absorbance based on the non-dyed hydrogel spectra. The absorbance values plotted were calculated as the area under the curve from wavelengths 500 to 750 nm.

### **5.2.3 Fluorescent *in vivo* Study Methods**

The last measurement of diffusion performed was an *in vivo* experiment where TEMPO CNF was fluorescently labeled with FITC and the *Vibrio anguillarum* with BactoView Live Red stain from Biotium. The BactoView Red stains the bacterial cell's DNA so it works to stain both live or dead cells. The inactivated *Vibrio anguillarum* was stained by mixing the stain and bacterin

together in a ratio where the 500x stain stock solution was diluted to 2x (for this exact experiment it was 40 mL of bacterin to 160 $\mu$ L of stain). The stain sat for 30 minutes in the dark and then was centrifuged at 3500 RCF for 15 minutes to isolate the bacteria. The supernatant was pipetted off and the bacterial cells were resuspended in 40 mL of PBS.

The TEMPO CNF was labeled with FITC using an established labeling procedure.<sup>1–3</sup> 50 g of 1.1 wt% TEMPO CNF was mixed with 280  $\mu$ L of epichlorohydrin and 50 mL of 1M NaOH (to make the mixture basic). The mixture was stirred using a stir plate for two hours. After two hours, the mixture was rinsed with acetone and vacuum filtered three times to remove unreacted epichlorohydrin. Then the TEMPO CNF was rehydrated with about 40 mL DI water and mixed with 3.2 mL of ammonium hydroxide and left to stir for two hours. After two hours, the mixture was rinsed with acetone and vacuum filtered three times to remove unreacted ammonium hydroxide. Then about 18 mL of 3.6mM FITC was mixed into the solution and allowed to stir for 24 hours in the dark. After 24 hours, the mixture was rinsed with acetone and vacuum filtered until the filtrate no longer appeared yellowish-green in color to remove unreacted FITC. The FITC labeled TEMPO CNF was then rehydrated in 40 mL of DI water. Some loss of TEMPO CNF was expected to occur during the labeling procedure so it was assumed that adding 40 mL of DI water would create about 1.1 wt% TEMPO CNF.

The fluorescent hydrogels were prepared by mixing the 40 mL of FITC labeled TEMPO CNF to 36.5 mL of stained *Vibrio anguillarum* and stirring the mixture for 24 hours in the dark (3.5 mL of the stained *Vibrio anguillarum* was saved as second testing group). The mixture was vacuum filtered and formed as normal in the dark. All wash steps and storage were done in the dark to prevent the fluorescence from photobleaching. The hydrogels were washed for four days and then implanted into the salmon using the same delivery method as the second safety study (see

section 6.2.2 for more details). In this study, 32 salmon were injected with fluorescent hydrogels and 25 salmon were injected with about 0.1 mL of fluorescently stained *Vibrio anguillarum* in PBS. All preparation and care of the salmon was kept the same as described in section 6.2.2. The salmon were housed in a tank system that contained 500 liters of partial flow-through recirculating freshwater which was shared between four tanks that were 110 liters in size. The salmon were divided into the 4 tanks as evenly as possible with each treatment having a duplicate tank.

The salmon were sampled at 0 hour, 12 hours, 24 hours, 48 hours, 72 hours, 100-degree days, and 300-degree days (the salmon will also be sampled at 600-degree days as an ongoing study). They were euthanized, dissected and imaged under a modifiable light source, fixed camera, and changeable filter setup. The camera had a resolution of 2048x1536 pixels and with an exposure time of 1ms to 0.3s with auto exposure. At least three pictures were taken of each sample: one using white light (white image), one using a filter set to image the BactoView Red stained *Vibrio anguillarum* fluorescence (red image), and one using a filter set to image the FITC labeled TEMPO CNF fluorescence (green image). The filter set to image BactoView Red consisted of a  $550 \pm 40$  nm bandpass excitation filter on a white light lamp source and a 660 nm longpass emission filter before the camera lens. The filter set for imaging FITC consisted of a 473 nm longpass and 500 nm shortpass excitation filters on a white light lamp source and a 500 nm longpass and 500 nm shortpass for the emission filters before the camera lens. Images for the hydrogel treatments were taken of the hydrogel found in the salmon. Images for the *Vibrio anguillarum* only treatments were of locations that red fluorescence was detected on the camera or of the injection site area.

All the images were analyzed in ImageJ to enhance the contrast and decrease the noise of the red and green images. Then the red and green images were overlaid on the white images to show the location of the fluorescence. The locations of fluorescence were marked down for the

hydrogels and for the stained *Vibrio anguillarum*. Additionally, the raw hydrogel red and green images were analyzed for average intensities by finding the area of the smallest hydrogel and using that same area on all of the other hydrogel samples. The intensity of the stained *Vibrio anguillarum* samples were not analyzed because the signals of fluorescence which were found ranged from faint spots of red to streaks of bright red. Additionally, each salmon sample had muscle tissue around the injection site, liver, spleen, and kidney imprints done on glass microscope slides. These slides will be analyzed in a future study for the presence of fluorescent *Vibrio anguillarum*.

### **5.3 Results and Discussion**

#### **5.3.1 ELISA of Bacterin in the Hydrogels**

The antibody response percentage was based off the bacterin positive control being considered having 100% antibody response. The isolated bacterin ELISA data was statistically analyzed using a one-way ANOVA. The antibody response of the bacterin isolated from the hydrogels showed both the fully wet and dehydrated hydrogels having a significantly lower antibody response than the positive bacterin control ( $P=0.02$ ). This significance suggests that the hydrogel does not contain the correct dosage of bacterin for vaccination or that not all of the bacterin was able to be isolated from the hydrogel. The ELISA also showed that the antibody response from the dehydrated hydrogel had no significant difference from the antibody response from the fully wet hydrogel. The lack of significance suggests that the use of the dehydrator at 46°C doesn't reduce the antibody response of the bacterin in the hydrogel. This result helps support the use of a dehydrator as the drying method to strengthen and shrink the hydrogels before implantation.

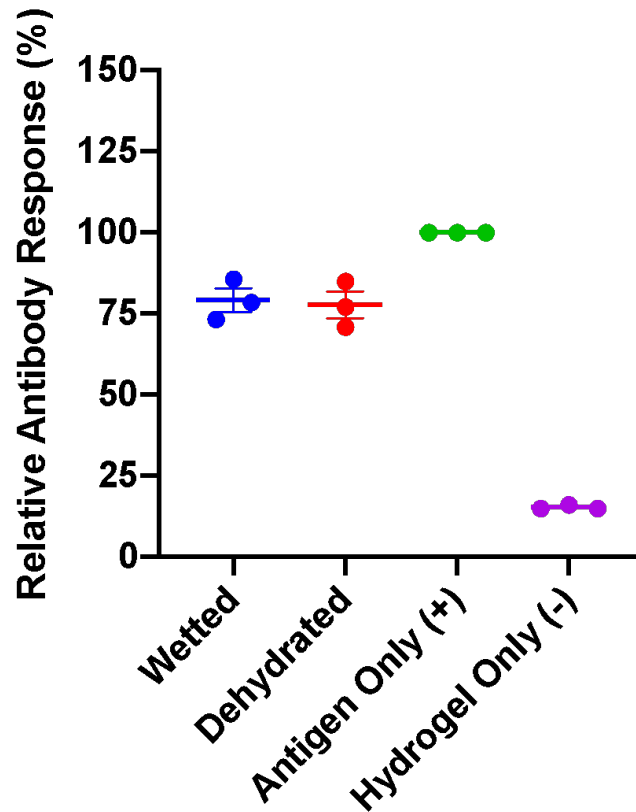


Figure 5.1: Antibody response percentage of the bacterin isolated from the hydrogels.

The antigen response from the dehydrated hydrogels was further analyzed by measuring the antibody response of the PBS surrounding the hydrogel over time. The time elapsed was measured in degree days which is a unit of measurement commonly used in aquaculture. Degree days are a summation of the difference in temperature of the ambient air from the temperature of the water. The antibody response percentage was based off the bacterin positive control being considered having 100% antibody response. The antibody response can be seen increasing from time 0 to 300-degree days. Then the antibody response appeared to plateau from the 300-degree day measurement to the 600-degree day measurement. This trend suggested that the bacterin diffuses out of the hydrogel until sometime between 100-degree days and 300-degree days. The plateau in the antibody response between 300- and 600-degree days showed that no significant

amount of bacterin diffused out of the hydrogel after the 300-degree day timepoint. Figure 5.2 also showed the antibody response of bacterin that diffused out of some of the hydrogels at the 300- and 600-degree day measurements to be greater than the bacterin positive control. This measured antibody response was unexpected since Figure 5.1 showed the hydrogel’s antibody response being lower than the bacterin positive control. However, this data proved that the lower antibody response from the isolated bacterin in the first ELISA was because not all the bacterin was isolated from the hydrogel.

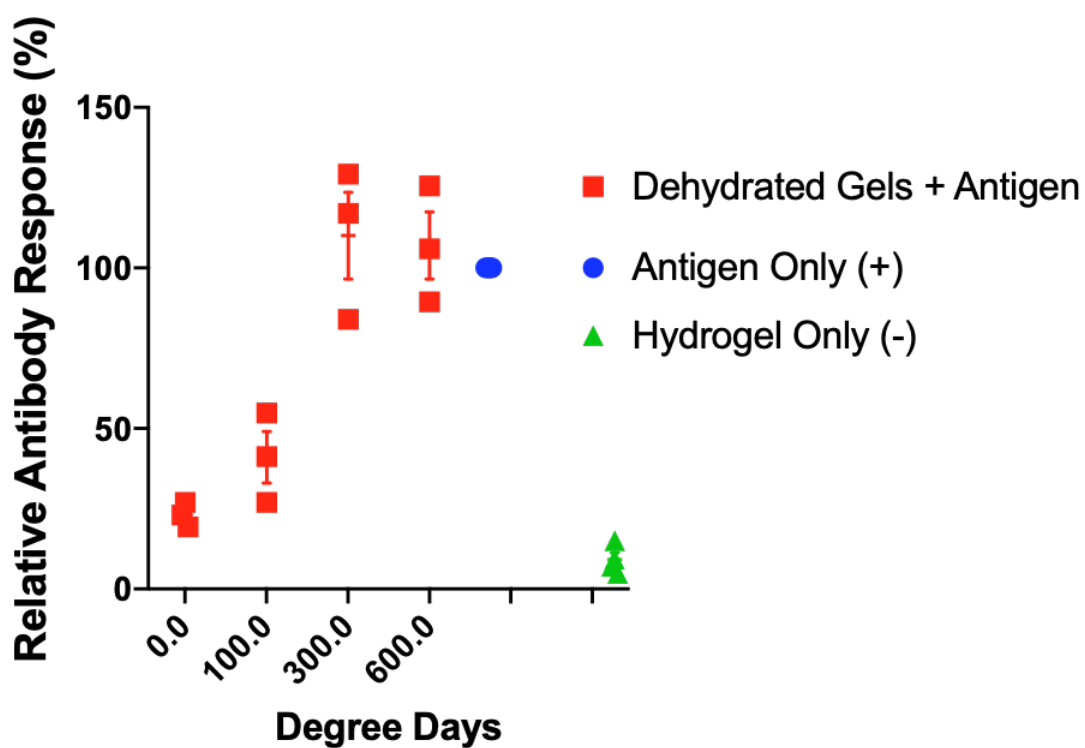


Figure 5.2: Antibody response percentage of the bacterin diffused from the hydrogels.

### 5.3.2 Diffusion of Coomassie Brilliant Blue from Rehydrated Hydrogels

It was hypothesized that taking measurements of dye-loaded hydrogels would create a reliable diffusion model that would be comparable to the obtained ELISA data. This type of model could be measured more frequently and inexpensively than the ELISA tests, allowing for diffusion

rate calculations. The samples were measured hourly, daily, and then weekly for changes in intensity which would correspond to CBB dye diffusing out of the hydrogel. Consideration needed to be taken to understand that CBB dye might not be the best model of the bacterin to use to measure accurate diffusion rate since the dye is much smaller in size than the bacterin and has a different shape.<sup>83-85</sup> Therefore, any calculated diffusion rates of CBB dye cannot be assumed to be the same as the diffusion rate of bacterin. Instead, the changes in diffusion rates of CBB from different dried hydrogels could be compared to note whether drying the hydrogels affects its diffusive properties. It can be assumed that any changes in diffusion rates of CBB that occurred by drying the hydrogels would translate to changes in the diffusion rates of bacterin from similarly dried hydrogels.

The changes in absorbance over time of hydrogels which were dried at different temperatures for different amounts of time was plotted in Figure 5.3. A greater absorbance value corresponded to a greater concentration of CBB dye. Although a general increasing trend in absorbance can be seen in most of the graphs, there is a lot of noise in the measurements leading to there being no significance between the plotted points. Even the measurements taken of the constant known concentration of CBB dye was noisy. Therefore, accurate diffusion rates cannot be calculated from the obtained data. The results only suggest that there appears to be dye diffusing out from the hydrogel over time which agrees with the findings found from the ELISA testing.

Although diffusion rates were unable to be calculated from the gathered data, the presence of general increasing trends supports that this method of measurement could be used to measure diffusion rates with some improvements. The amount of noise seen in the measured absorbances could be improved upon for future testing in a multitude of ways. A more precise spectrometer could be used for testing. Additionally, more hydrogels could be added to the cuvette to increase

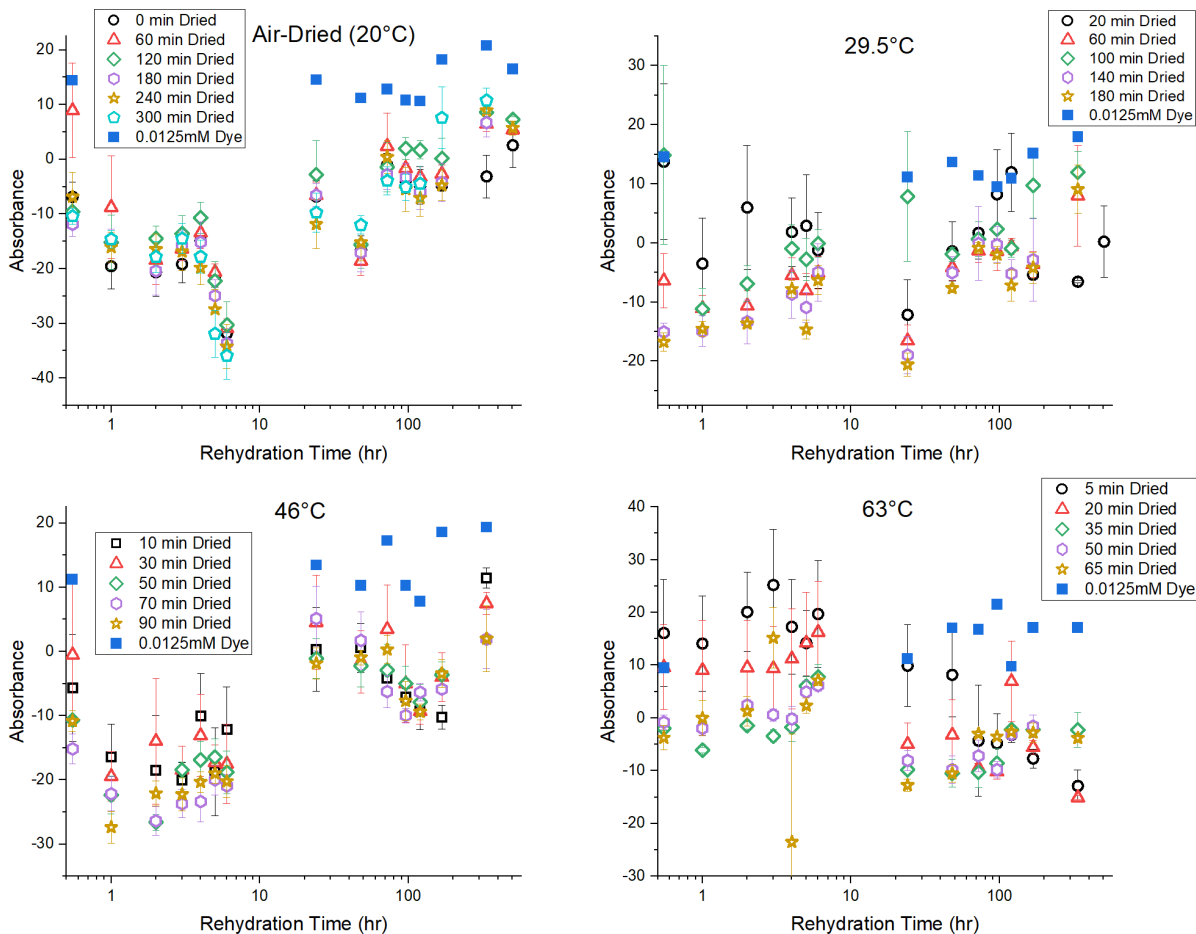


Figure 5.3: Changes in absorbance due to presence of CBB dye over time.

the hydrogel to PBS ratio and therefore provide more available sources of dye to diffuse out into the PBS. The plotted data can also be smoothed by scaling the absorbance based on the CBB dye control (maybe as difference of measured PBS absorbance from CBB dye control absorbance). Smoothing the data in this way will more clearly show if the absorbance of the PBS is getting closer in value to the dye control, regardless of the noise (seen by the dips and bumps of the dye control measurements which should be steady).

Also, it was noticed that some of the hydrogels would float in the cuvette instead of sinking which would cause absorbance values greater than that of the control dye to occur. The samples with floating hydrogels were therefore omitted from the plotted data. In future testing, more

hydrogels could be added with more PBS (for example four hydrogels with 3 mL of PBS) so there would be a gap between the floating and sinking hydrogels that wouldn't have obstructions. This clear gap right in the middle of the cuvette could be the measurement point while still increasing the hydrogel to PBS ratio. Additionally, when measuring the samples at 336 and 504 hours, it was noticed that enough PBS evaporated out of the cuvette (although it was covered in parafilm) to the point that the level was below where the spectrometer measured. This led to more samples being omitted from the plot and increasing the error of the measured samples. In future testing, cuvette caps could be used to close the cuvettes properly and reduce the chance of evaporation over long periods of time. Lastly, some of the cuvettes used ended up leaking and those samples were also omitted from the plot. This could be improved by putting the PBS into the cuvettes and waiting a couple hours to see if the cuvette leaks before adding the hydrogel.

### **5.3.3 Fluorescent *in vivo* Study**

The goal of the fluorescent *in vivo* study was to locate where the bacterin travels after being injected or how it diffuses out of the hydrogel. It was also desired to be able to see if the hydrogel breaks down over time when in the salmon. The fluorescence from the stained *Vibrio anguillarum* was relatively easy to find and image. However, the fluorescence from the FITC labeled TEMPO CNF appeared to mostly disappear after the hydrogel was formed in citric acid, making it difficult to detect on camera. Oddly enough, more fluorescence from the FITC was seen in some of the hydrogels at the longer timepoints. Theories on why the FITC fluorescence produced weak signals which was likely due to the fluorescence labelling process can be found in section 5.3.3.1. As a result of the lack of FITC, the focus of analysis was on the red images and the locations within the fish where red fluorescence was found.

Figure 5.4 shows the intensity of red and green fluorescence of the hydrogels over time. The data was statistically analyzed for significance using Tukey’s method. The graph showed the intensity of green fluorescence as being relatively small and having large error bars. Significance of the green fluorescence intensity over time was only found between the last time point (300-degree days) and the first two timepoints. The red fluorescence intensity of the hydrogels stayed the same for the 0- and 12-hour measurements and then increased at the 24-hour measurement. After 24 hours, the red fluorescence intensity steadily decreased over time, leading to a plateau from 100- to 300-degree days. There was a significant decrease in red fluorescence seen from the 24-hour measurement to the 100- and 300-degree day measurements. The red fluorescence

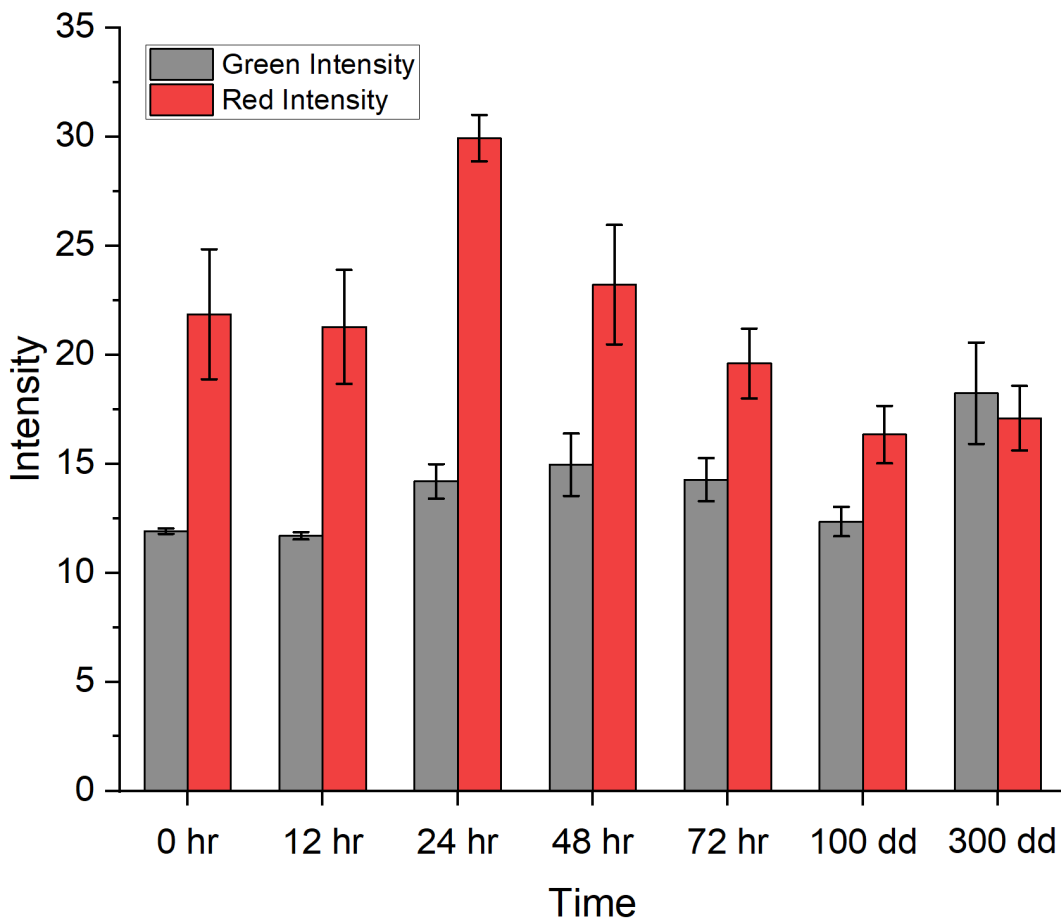


Figure 5.4: Green and red fluorescence intensities of the hydrogels over time in the salmon.

intensity data suggested that the diffusion of bacterin out of the hydrogels would slow down and head towards a plateau over time.

Although there was measured significance, the analysis method to measure the intensity had a degree of bias to it that could be reflected in the data. Since the hydrogels were not the same size, imaged in the exact same position, or the same hydrogel being imaged, each of the images were different from each other and therefore could not be analyzed with the exact same method. The measured intensities were an average of an elliptical area which covered most of the smallest hydrogel. This same sized area was used to measure a portion of all the other hydrogels. Since the location of each hydrogel to measure was chosen by hand, there was bias based on which portion of the hydrogel was chosen. Additionally, the hydrogels were imaged directly in the fish, meaning that some of the hydrogels could have had some bodily fluids or debris that was on the hydrogel, thereby blocking some of the fluorescence signal. The possibility of bodily fluid or debris affecting the measurements was further supported by the fact that the most of the 300-degree day hydrogels needed to be removed from cysts in order to image them. Bodily fluid such as blood coating the hydrogel could be the reason why the 0- and 12-hour measurements had smaller intensities than the 24 hour measurement. When the 0- and 12-hour salmon were dissected, blood was found within the peritoneum cavity where the hydrogel was located. Debris from the internal organs could have gotten onto the hydrogels in the later timepoint measurements as well. The majority of times, the hydrogel was found in between the liver and pyloric caeca and had to be tweezed out for imaging. Tweezing out the hydrogel could also have led to breakdown and loss of some of the hydrogel either left behind in the place it was tweezed from or left on the tweezers used to handle the hydrogel.

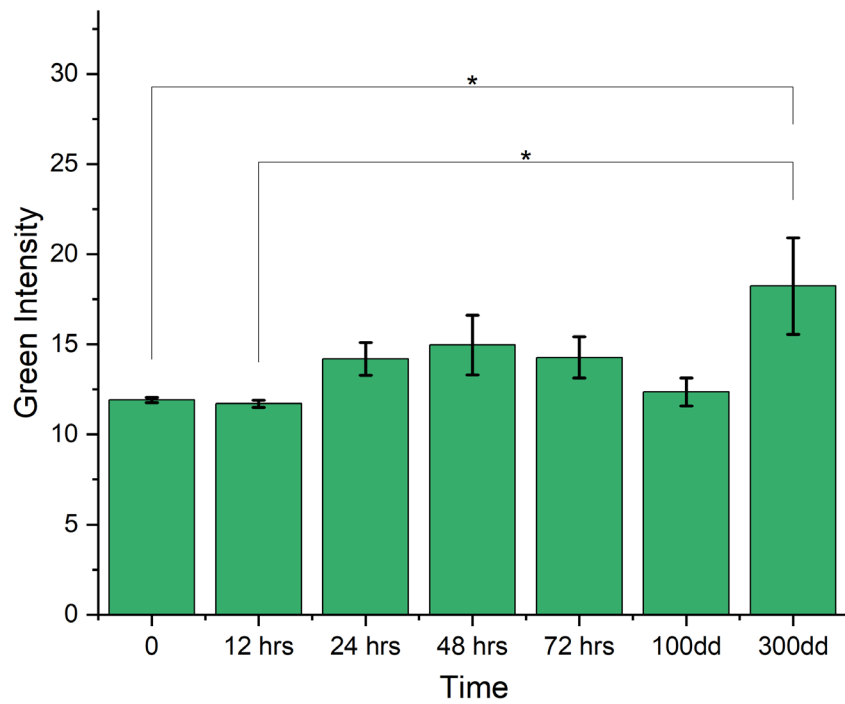
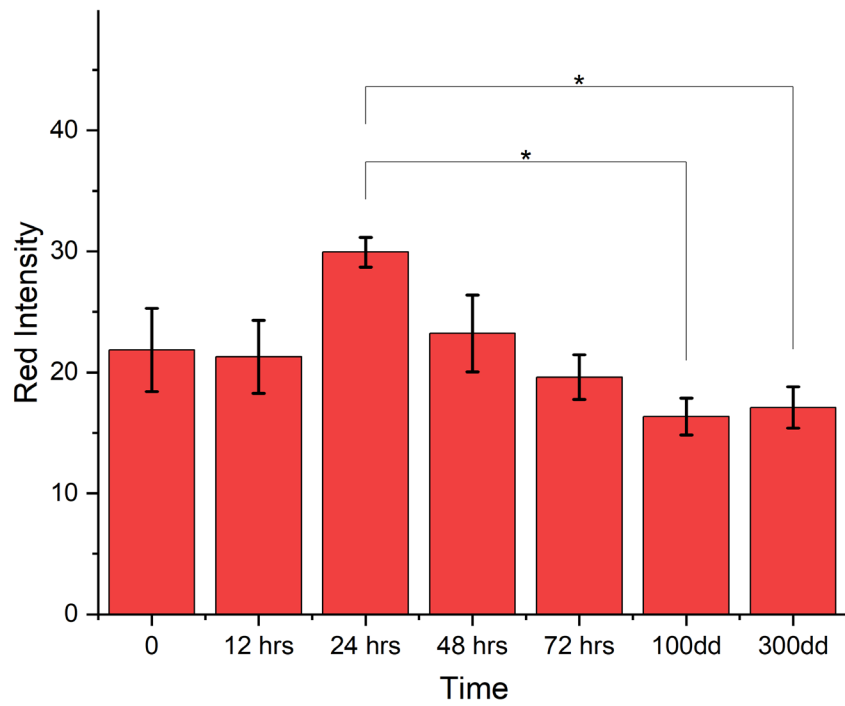


Figure 5.5: Hydrogel red and green fluorescence intensities analyzed for statistical significance.

Figures 5.6 and 5.7 show merged red, green, and white images of the most commonly found locations of hydrogels and injected bacterin over time. The greenish or reddish tints on the whole image are due to the linear noise present in the camera which was used. Overall, the hydrogels were almost always found embedded in between the liver and pyloric caeca of the salmon regardless of the time point. At later timepoints the hydrogels would have to be tweezed out and removed from cysts that started to form between the liver and pyloric caeca and connect to the muscle. One cyst formed on the muscle of the salmon near the incision site which the hydrogel had to be tweezed out from for imaging. The location of the hydrogels was most likely due to their method of delivery. It was likely that when the needle was pushed through the incision,

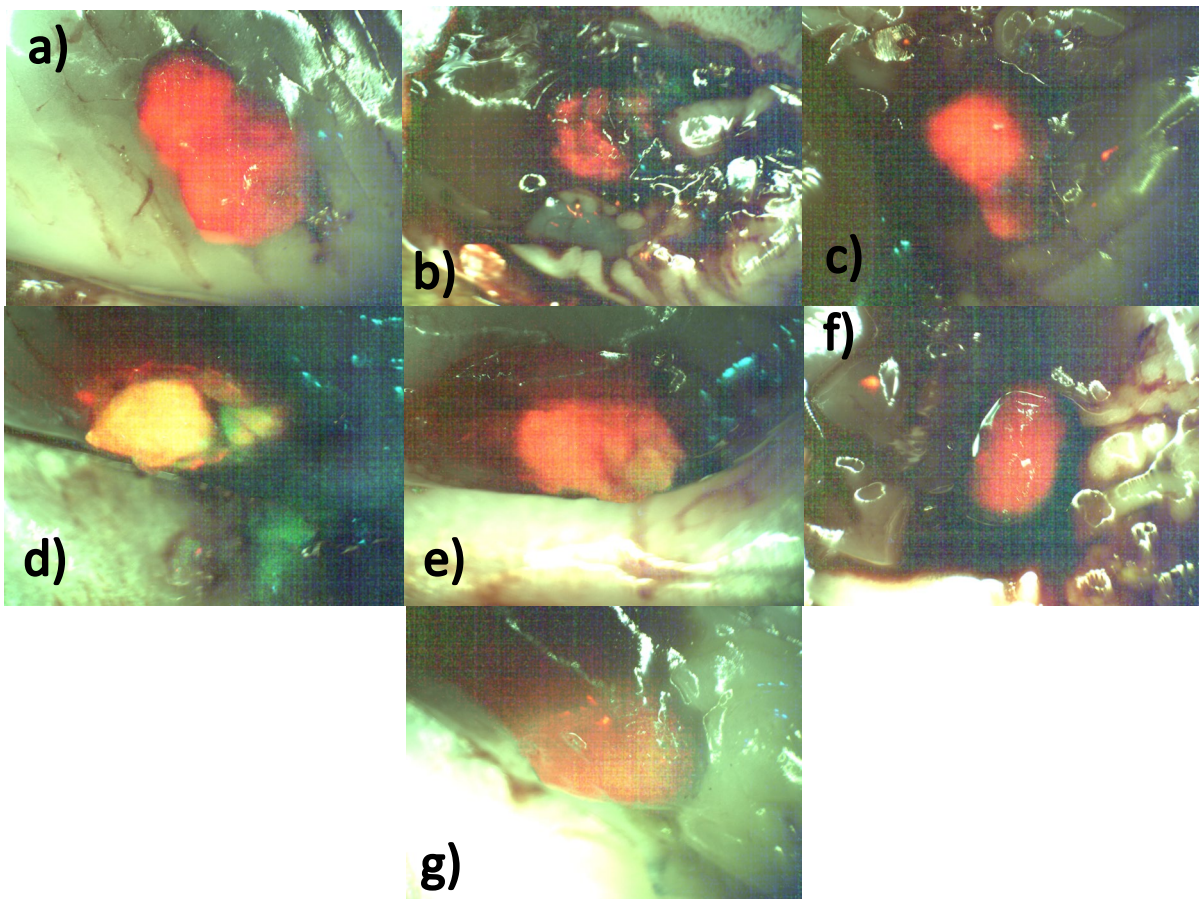


Figure 5.6: Merged red, green, and white images of hydrogels over time. A) 0 hours, B) 12 hours, C) 24 hours, D) 48 hours, E) 72 hours, F) 100-degree day, G) 300-degree day.

the tip of it was located between the liver and pyloric caeca. To reduce chances of embedding the hydrogel into this location in the future, the incision could be placed further back on the salmon's peritoneum to allow more room for the needle.

Unlike the hydrogels, the location of the bacterin changed over time. However, the presence of red fluorescence does not always mean that bacterin was present. While imaging, it was noticed that the salmon feed would appear to also fluoresce red along with the scales of the salmon reflecting light to appear as red fluorescence. These instances were identified and not imaged as much as possible while sampling. In the beginning, the bacterin was found near the

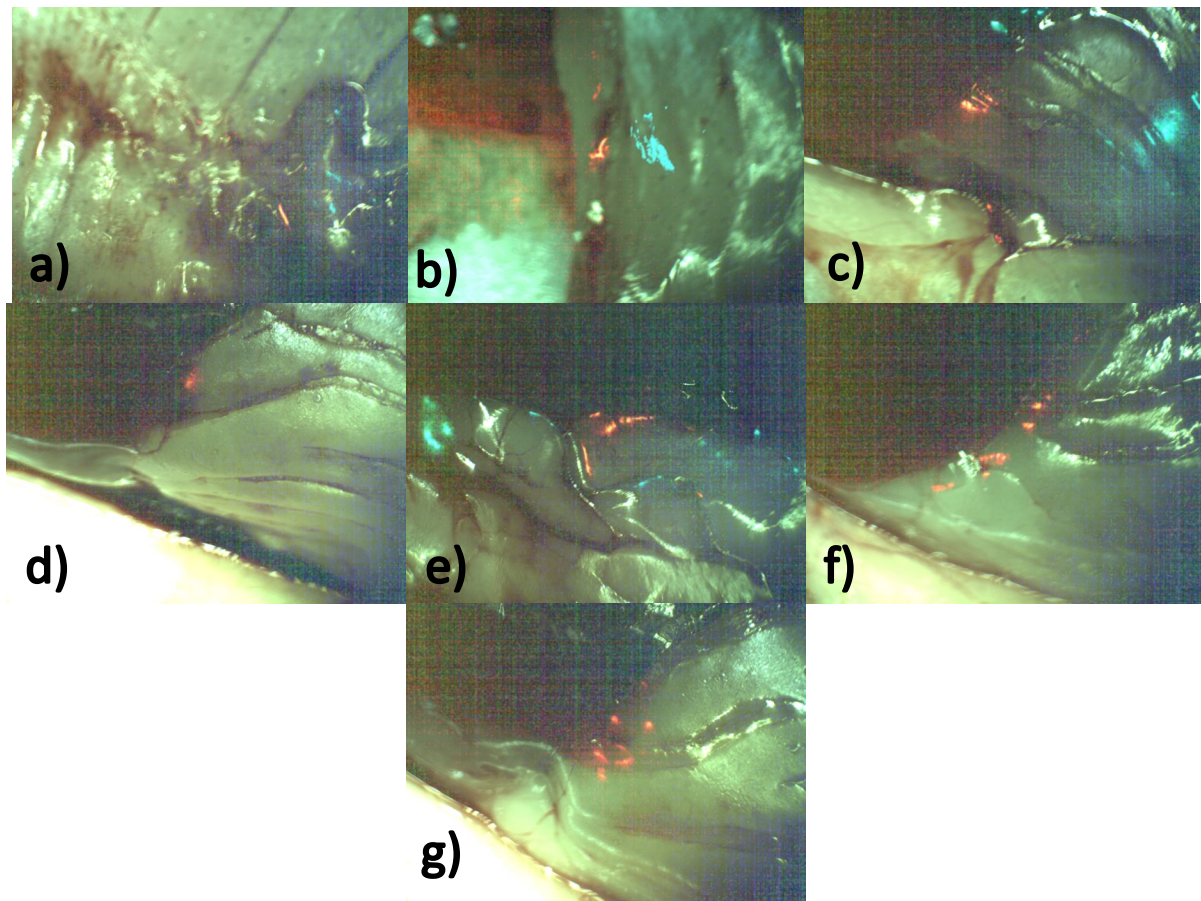


Figure 5.7: Merged red, green, and white images of injected bacterin over time. A) 0 hours, B) 12 hours, C) 24 hours, D) 48 hours, E) 72 hours, F) 100-degree day, G) 300-degree day.

injection site on the muscle (or paper towel the salmon was dissected on, likely due to the bacterin pooling out after the salmon was dissected). Over time, red fluorescence signals would be found mostly on the pyloric caeca or muscle. Additionally, after 12 hours, no fluorescence signal was detected around the injection site. Sometimes red fluorescence signals would be found on the swim bladder or near the intestines. By the 100-degree day measurement, red fluorescent signals were found in less locations in the same salmon (either 1 location or 0). The fact that a lot of red fluorescence signals showed up around the pyloric caeca suggested that this organ had a role in the salmon's immune response or that the bacterin was somehow attracted to this organ. For future *in vivo* fluorescence testing, it would be interesting to image salmon that had no bacterin injected in them. If red fluorescent signals popped up in the salmon without bacterin, then it could help deduce whether the signals found from the injected bacterin samples were likely the presence of bacterin or not.

### 5.3.3.1 Fluorescence Signal Limitations

FITC labels TEMPO CNF and other forms of CNF by forming covalent bonds to the fibers. Figure 5.8 shows the chemistry that occurs during the FITC labeling procedure. Therefore, it was surprising when FITC was not easily detected in the hydrogels. However, there are multiple reasons why the FITC fluorescence signals were weak in the hydrogels. More experimentation

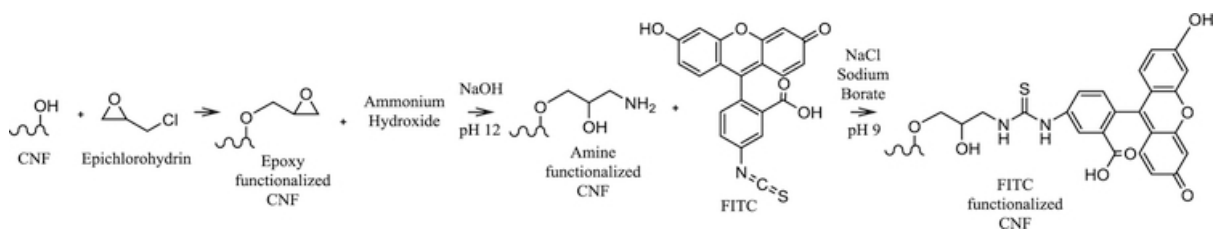


Figure 5.8: Chemistry of the procedure to label CNF with FITC. Retrieved from reference (83).

would have to be conducted to confirm which reasons led to the diminished FITC signals in this experiment and how to avoid weak FITC signals in the future experiments with hydrogels. Research article searches for labeling TEMPO CNF with FITC or labeling CNF hydrogels with FITC came up empty. However, recent work by Emilia Purington suggest that FITC fluorescence signals decrease when the CNF was exposed to lower pHs.<sup>86</sup> The hydrogels were formed in citric acid which created hydrogels with a low pH, possibly explaining the diminished FITC fluorescence. Another possible explanation for the limited signal could be due to steric hinderance. Although some loss of TEMPO CNF due to the FITC was assumed and attempted to be accounted for, the resulting hydrogels seemed less stiff than usual 1.7 wt% TEMPO CNF hydrogels. That could either mean that more TEMPO CNF was lost than was assumed or that steric hinderance from the bound FITC prevented crosslinking from occurring. FITC is a large chemical group that hangs off TEMPO CNF monomers on the fiber when properly covalently bonded. FITC's large size could've made it difficult for neighboring TEMPO CNF fibers to get close enough together to form the hydrogen bonds necessary for crosslinking. As a result, the TEMPO CNF fibers that were FITC labeled weren't able to be crosslinked into the hydrogel matrix. This would've led to less TEMPO CNF making up the hydrogel matrices and the hydrogels losing their fluorescence. Steric hinderance was likely because the citric acid that the hydrogels were formed in glowed green when excited by the FITC excitation filter set.

As a result of the lack of FITC fluorescence in this *in vivo* study, any future studies would have to change the fluorescence staining protocol of TEMPO CNF. Calcofluor white seemed to be a better stain for the cellulose hydrogels in this application than FITC and should probably be used for future TEMPO CNF hydrogel fluorescence staining. The other option is that the FITC labeling procedure should be further analyzed to see how FITC labels TEMPO CNF differently than

“vanilla” plain CNF. It should also be researched if FITC causes steric hinderance that discourages physical crosslinking.

## CHAPTER 6

### EFFECT OF CITRIC ACID CROSSLINKED HYDROGEL VACCINES ON SALMON

#### 6.1 Introduction

All the performed experiments and gathered data in this chapter was done in collaboration with Sarah Turner and Deborah Bouchard at the University of Maine Cooperative Extension Diagnostic and Research Laboratory. After designing the aquaculture vaccine formulation and improving upon its mechanical properties and delivery method, the effectiveness of the developed delivery methods needed to be tested. Additionally, the potential reactions in the salmon caused by the hydrogel formulation also needed to be observed. A preliminary study was done previously by injecting pure TEMPO CNF into the salmon and observing the resulting reactions. Overall, the TEMPO CNF had no significant impact on the salmon's growth, caused no melanization reactions, and minimal adhesions. However, there was no recorded study of how a citric acid crosslinked TEMPO CNF hydrogel behaved in salmon and what reactions it caused. As a result, safety studies were conducted to observe the effects of the formulated hydrogel on the salmon.

#### 6.2 Methods

##### 6.2.1 First Safety Study

The first safety study consisted of 35 salmon and seven treatment groups. Each treatment group consisted of five salmon. The treatment groups tested were 1.7 wt% TEMPO CNF hydrogels that were washed for 4 days, 6 days, or 8 days, 1.7 wt% TEMPO CNF and bacterin 1:1 ratio hydrogels that were washed for 4 days, 6 days, or 8 days, and PBS control. All the hydrogels were rehydrated in PBS for 24 hours before implantation.

The salmon were anesthetized for hydrogel implantation by being netted into 100 mg/L tricaine methanesulfonate (MS-222) buffered with 150 mg/L sodium bicarbonate. The salmon were kept in anesthesia until they no longer reacted to external stimuli such as light or physical touch. Once sedated, an incision about the length of the hydrogel was made and the hydrogel was pushed through the incision into the peritoneum cavity using tweezers. The salmon were then fluorescently tagged along the jaw line sub-dermally to identify treatment group and placed into their housing tank to recover. All the treatment groups for this study were housed in the same 490-liter circular tank. The tank was supplied with 2 L/min of oxygenated water and siphoned daily to remove particulates. The care for all of the salmon throughout the study was the same.

After 300-degree days (about a month's time), the salmon were euthanized with 250 mg/L MS-222 buffered with 200 mg/L sodium bicarbonate and sampled. The salmon were sampled by measuring their weight and fork length (used for calculation of Fulton's condition factor), observing the state of the incision site, then dissected and scored for adhesions, viscera appearance, peritoneum appearance, and residue. Fulton's condition factor is a number that corresponds to the overall condition of the salmon and is calculated from the weight and fork length of the fish. Additionally, it was noted whether the hydrogel was found inside the peritoneum and could be retrieved from the salmon. The scoring sheet which was used for adhesions, viscera appearance, peritoneum appearance, and residue can be found in the appendix. Overall, the scores are graded from 0 to 6 (for adhesions) or 0 to 3 (for viscera, peritoneum, and residue) where a greater score corresponds to a more adverse reaction. The focus of analysis for the first safety study was on the effectiveness of the hydrogel delivery method and the reactions that the hydrogel caused in the salmon. The two pieces of data that were focused on to determine the extent of adverse reactions were Fulton's condition factor and the adhesion score.

### 6.2.2 Second Safety Study

The second safety study consisted of 80 salmon and five treatment groups. Each treatment group consisted of 16 salmon. The treatment groups tested were 1.7 wt% TEMPO CNF bacterin 1:1 ratio hydrogels that were washed for 2 days, 4 days, or 6 days and rehydrated in PBS for 12 hours, 1.7 wt% TEMPO CNF bacterin 1:1 ratio hydrogels washed for 4 days and not rehydrated in PBS prior to implantation, and bacterin mixed with PBS control. The rehydrated hydrogels were dried at 46°C for 60 minutes while the dehydrated hydrogels were dried at 46°C for 30 minutes. The resulting hydrogels were all roughly 40% their initial mass at the time of implantation.

The salmon were anesthetized for hydrogel implantation by being netted into 100 mg/L tricaine methanesulfonate (MS-222) buffered with 150 mg/L sodium bicarbonate. The salmon were kept in anesthesia until they no longer reacted to external stimuli. Once sedated, an incision about the diameter of the 8-gauge needle was made and the hydrogel was implanted into the peritoneum cavity by inserting the needle into the cavity and then pushing the hydrogel out of the syringe. The salmon were then placed into their respective housing tanks to recover. Each treatment group was housed in separate tanks in duplicates of two on separate recirculating systems for sampling replication. Each tank system contained 500 liters of partial flow-through recirculating freshwater that was shared between six tanks that were 76 liters in size. The salmon were housed in ten tanks with 8 fish in each tank. The care for all of the salmon throughout the study was the same.

After 300- and 600-degree days, the salmon were euthanized with 250 mg/L MS-222 buffered with 200 mg/L sodium bicarbonate and sampled. Half of the salmon were sampled at each time point. The salmon were sampled by measuring their weight and fork length, observing the state of the incision site, then dissected and scored for adhesions, viscera appearance,

peritoneum appearance, and residue (residue was only scored for the 300-degree day samples). Additionally, it was noted whether the hydrogel was found inside the peritoneum and could be retrieved from the salmon for the 300-degree day samples. In addition to measuring weight, fork length, adhesions, viscera appearance, and peritoneum appearance for the 600-degree day samples, the incision site and surrounding muscle and viscera were sampled and stored in formalin for histology analysis. The focus of analysis for the second safety study was on the effectiveness of the hydrogel delivery method and the reactions that the hydrogel caused in the salmon. The two pieces of data that were focused on to determine the extent of adverse reactions was Fulton's condition factor and the adhesion score.

## **6.3 Results and Discussion**

### **6.3.1 First Safety Study**

Although the hydrogels were able to be implanted into the fish, they didn't necessarily stay in the fish once they were returned to water. Additionally, the implantation process for the first study trial was relatively time consuming, so even if the hydrogels were successfully delivered, the delivery method would need to be improved for industrial scale vaccinations.

When the salmon were sampled after 300-degree days, data was collected on whether the hydrogel was still present in the salmon. Table 6.1 shows the percentage of hydrogels found in the salmon based on treatment. The PBS control treatment group was excluded from this table because hydrogels were not expected to be found in this group. The number of hydrogels that stayed in the salmon after implantation was extremely low with only two treatments having hydrogels present. The absence of the hydrogels could be because the hydrogels are breaking down when inside the salmon or that the hydrogels fell out of the incision after they were put back into the tank. It is

more likely that the hydrogels fell out of the salmon than got broken down since the TEMPO CNF that was injected into salmon in a preliminary cellulose nanomaterial study remained in the fish after 300-degree days. As a result, differences in Fulton’s condition factor and adhesion score cannot be used to make conclusive results since most of the hydrogels did not remain in the fish for length of the study.

Table 6.1: First Safety Study Hydrogel Retention Rate in 30 Salmon after 300-Degree Days

Treatment	% of Fish with Hydrogel still Present
TEMPO CNF Hydrogel 4 Day Wash	0%
TEMPO CNF Hydrogel 6 Day Wash	0%
TEMPO CNF Hydrogel 8 Day Wash	0%
TEMPO CNF + Bacterin Hydrogel 4 Day Wash	40%
TEMPO CNF + Bacterin Hydrogel 6 Day Wash	60%
TEMPO CNF + Bacterin Hydrogel 8 Day Wash	0%

Even though the measured Fulton’s condition factor and adhesions scores measured can’t be directly related to the hydrogel treatment, it still can be used as an indicator for how the hydrogel delivery method/incision size affected the development of the salmon. Both the Fulton’s condition factor and adhesion score data was analyzed for significance using Tukey’s method. Based on the Fulton’s condition factor, the delivery method did not appear to affect the growth of the salmon since all condition factors were above 1.0. Additionally, no significance was found between the Fulton’s condition factor of different treatments. The adhesion scores gathered from the first safety study did show that the delivery method of the hydrogel did cause significant adhesions in the salmon that were graded about 1-1.5 in severity versus the PBS control with caused no adhesions.

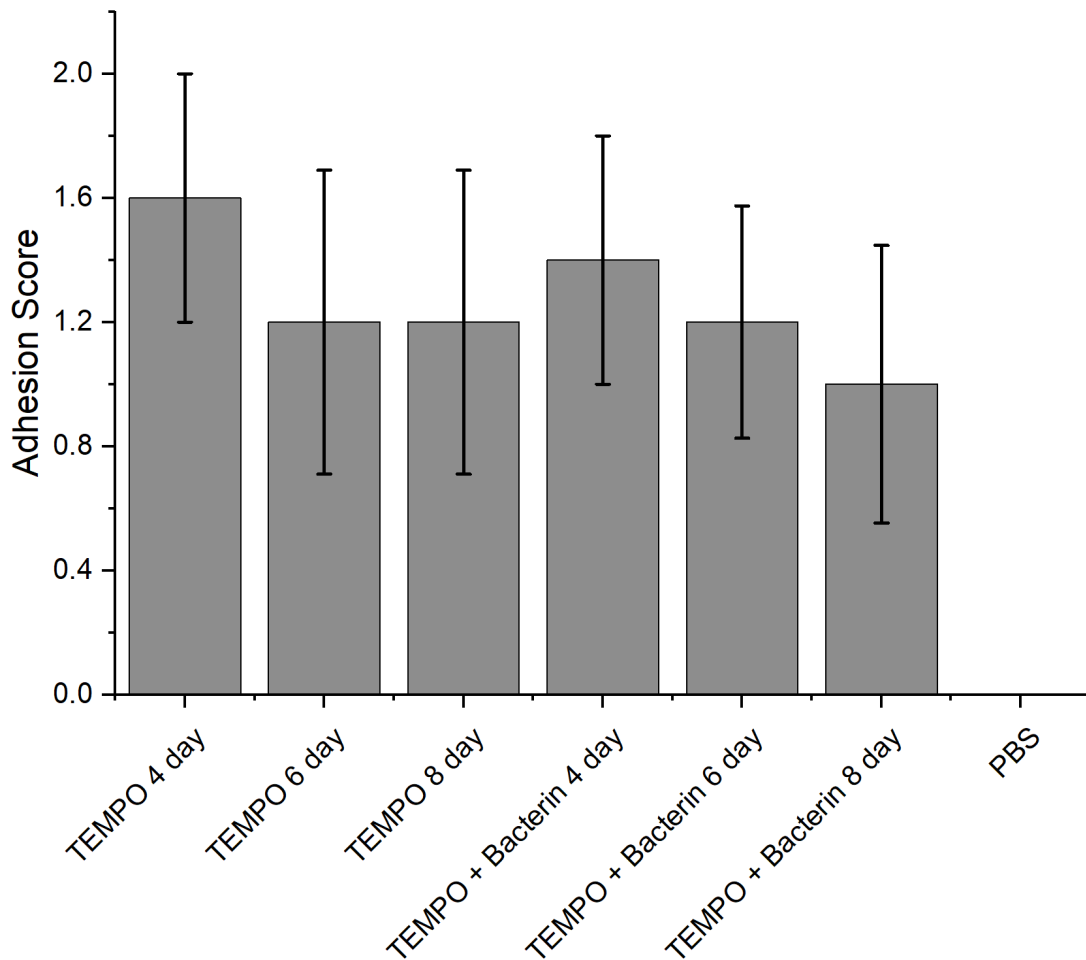


Figure 6.2: First safety study adhesion score based on treatment group.

No significance was found in the adhesion score between different hydrogel treatments. Additionally, the incisions on the PBS control had healed or mostly healed with no visible lesions while the incisions on the hydrogel treatments ranged from mostly healed to large lesions forming on the incisions. This showed that the delivery of the hydrogel created adverse reactions in the salmon. The main conclusion from the first safety study is that the delivery of the hydrogels needed to be improved upon further.

### 6.3.2 Second Safety Study

Compared to the first safety study, the implantation process of the hydrogels in the second safety study went a lot faster and easier. With some slight modifications, this type of delivery method had the ability to be industrially scaled. However, just because the hydrogels were easily delivered into the salmon, doesn't mean that they stayed for the duration of the study. Due to the 600-degree day salmon being sampled for histology analysis, hydrogel retention data was only collected from the 300-degree day sampling.

Table 6.2 showed the percent of hydrogel retention in the fish at the 300-degree day sampling based on hydrogel treatment. The bacterin mixed in PBS control treatment group was excluded from this table because hydrogels were not expected to be found in this group. The number of hydrogels that stayed in the salmon after implantation was much improved from the first safety study. Only a couple hydrogels fell out before the 300-degree day measurement in the second safety study. Some hydrogel losses were to be expected even with an improved delivery method because a similar implantation process with pit tagging fish also experiences losses. The higher hydrogel retention rates in the second safety study supported the earlier hypothesis that hydrogels were lost after implantation by falling back out of the incision instead of breaking down inside the salmon. It is difficult to determine if hydrogel retention depends on hydrogel treatment based on the obtained data. To be able to support or disprove this relationship, this hydrogel delivery method would have to be repeated again in another study with the same treatment groups. Since the majority of hydrogels remained in the salmon in the second safety study, conclusions can be drawn from how the Fulton's condition factor and adhesion scores changes across different treatment groups.

Table 6.2: Second Safety Study Hydrogel Retention Rate in 32 Salmon after 300 Degree Days

Treatment	% of Fish with Hydrogel still Present
TEMPO CNF + Bacterin Hydrogel 2 Day Wash	50%
TEMPO CNF + Bacterin Hydrogel 4 Day Wash	75%
TEMPO CNF + Bacterin Hydrogel 6 Day Wash	87.5%
TEMPO CNF + Bacterin Hydrogel 4 Day Wash Dried	87.5%

Both the Fulton’s condition factor and adhesion scores were statistically analyzed using Tukey’s method for significance. Based on the Fulton’s condition factor, the growth of the salmon was not affected in this safety study since all condition factors were above 1.0. Additionally, no

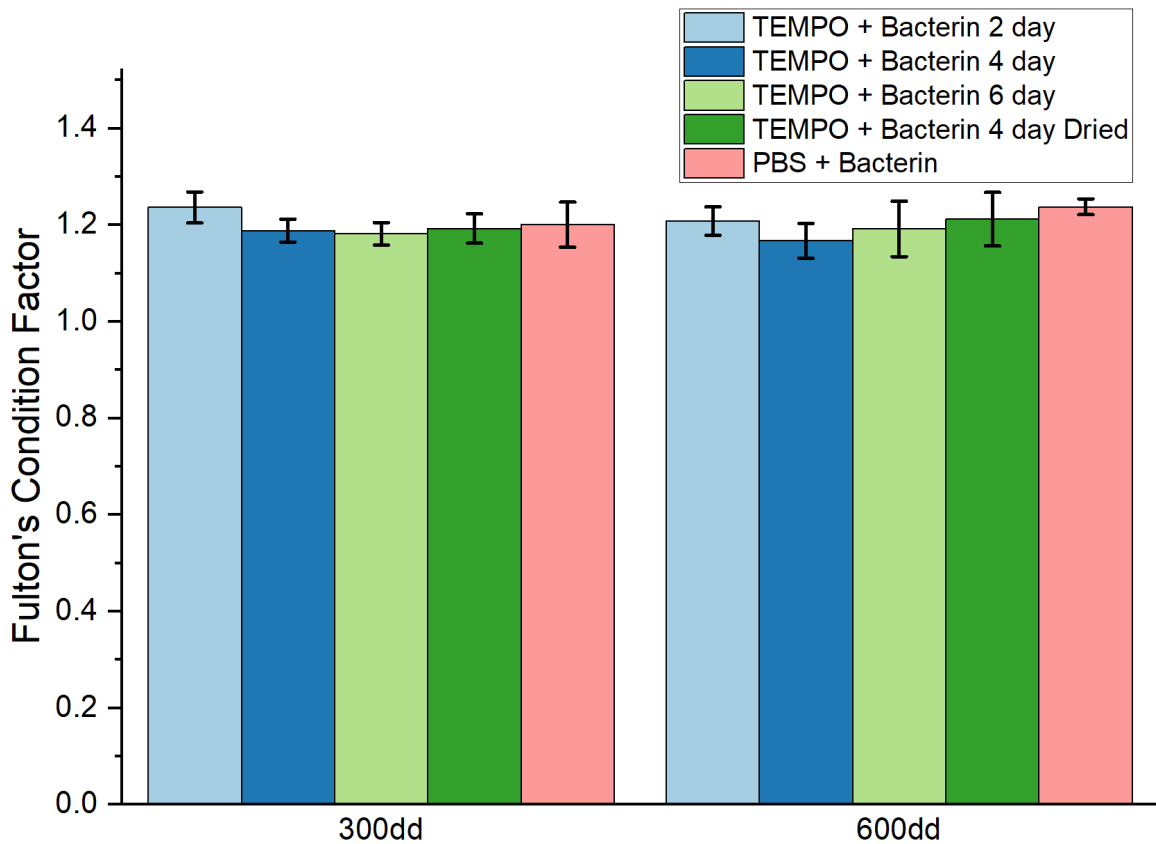


Figure 6.3: Second safety study Fulton’s condition factor based on treatment group.

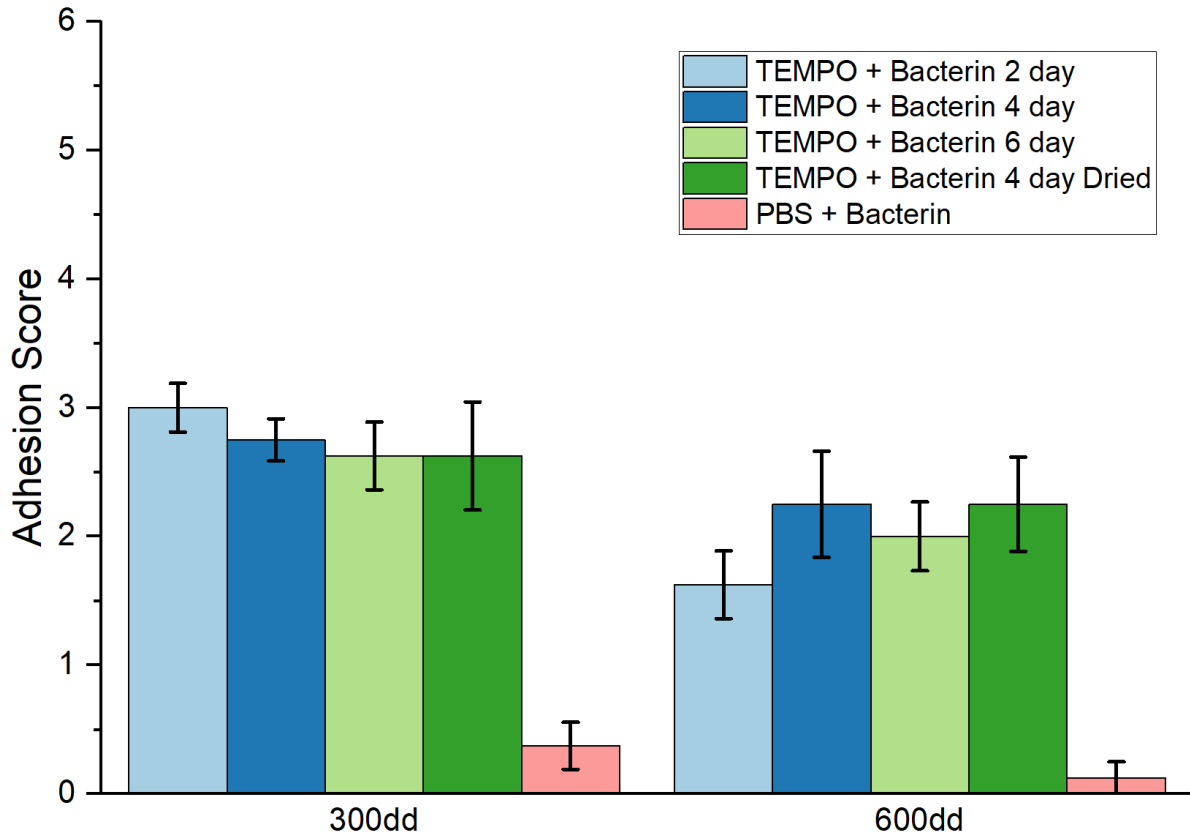


Figure 6.4: Second safety study adhesion score based on treatment group.

significance was found between the Fulton’s condition factor of different treatments. Therefore, neither the hydrogel delivery method or any of the hydrogel treatments significantly affected the growth and development of the salmon. The adhesion scores gathered from the second safety study showed that the delivery method of the hydrogel did cause significant adhesions in the salmon that were graded about a 2-3 in severity versus the bacterin mixed with PBS control which caused minimal adhesions with scores being either a 0 or 1. No significance was found in the adhesion score between different hydrogel treatments. Although no significance was found, the trend seen in the 300-degree data showed that an increase in wash days of the hydrogel caused a slight decrease in average adhesion score. This trend was not seen in the 600-degree day data.

Additionally, the bacterin mixed with PBS control had mostly or completely healed incisions (with one exception where the salmon had a protruding lesion on the incision). The incisions on the hydrogel treatments ranged from completely healed to having large lesions or cysts form near but not on the incision. The most interesting reaction to the hydrogels were when cysts formed around the hydrogel and appeared to be pushing the hydrogel out of the peritoneum cavity and into the muscle. These cysts formed more often in the TEMPO CNF + bacterin 2 day wash and TEMPO CNF + bacterin 4 day wash dehydrated hydrogels than in the other two hydrogel treatments. These more severe reactions suggested that the hydrogels should be washed for at least 4 days before implantation since the change in pH appeared to affect the salmon. Additionally, a stiffer dried hydrogel appeared to create more severe reactions than a rehydrated softer and more liquid filled hydrogel. This reaction could be due to the salmon rejecting a foreign, rigid object in its body or that the dried hydrogel invoked a greater inflammatory response because it was trying to rehydrate using the salmon's bodily fluids. Further experimentation needs to be performed to determine the cause of the increased severity of adhesions in the dehydrated hydrogels versus the rehydrated hydrogels.

### 6.3.3 Comparison of Hydrogel Delivery Methods

Overall, the second safety study hydrogel delivery method was better compared to the first safety trial. Figure 6.5 compares the overall hydrogel retention rate across all treatments for both the first and second safety study. The hydrogel retention percentages were statistically analyzed using the Mann-Whitney Test for significance. The second safety study had significantly more hydrogels remain inside the salmon. Not only did the hydrogels remain in the salmon's peritoneum, the implantation process was much quicker, and the incisions on the fish generally healed better and quicker in the second safety trial. As a result, the hydrogel delivery method used for the second safety study should be used instead of the first safety study delivery method for this hydrogel formulation in future studies. Even though the second safety study hydrogel delivery method was mostly successful in delivering the hydrogels, it can continue to be improved upon if this hydrogel formulation is chosen as a possible adjuvant to make at an industrial scale.

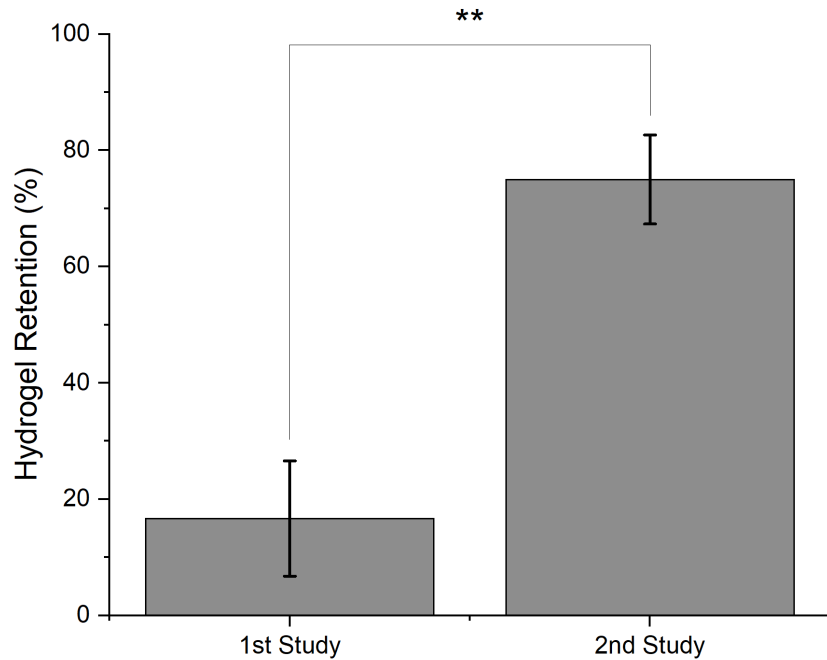


Figure 6.6: Comparison of hydrogel retention from both safety studies.

## CHAPTER 7

### CONCLUSION

#### 7.1 Summary

The field of aquaculture is a rapidly growing field for both research and industry. Many ways of advancing the field are being explored to produce more sustainable and efficient finfish for market. One of the largest areas of concern for aquaculture is the loss of finfish due to diseases. The use of aquatic vaccines are able to help decrease disease loss but can still be improved upon. There is a lot of exploration into different adjuvants for aquatic vaccines that protect the fish without producing additional adverse reactions. Cellulose nanomaterials are nontoxic and sustainable biomaterials which are being explored for many applications including drug delivery. As a result, this makes cellulose nanomaterials a great adjuvant candidate for aquatic vaccines.

In chapter 2 of this thesis, current issues in aquaculture and aquatic vaccines were explored. Current commercial aquatic vaccines use an oil-based adjuvant called Montanide which provides long-lasting protection in fish while also causing adverse effects such as lesions. The possibility of an alternate adjuvant in the form of a hydrogel was investigated by researching hydrogel properties, applications, and potential materials. The material of cellulose nanofibers (specifically TEMPO CNF) was also explored for its biocompatible, tunable, and sustainable properties. Current applications of cellulose nanomaterial hydrogels and their formulations were explored as well. This chapter supported the possibility of using a TEMPO CNF hydrogel as an aquatic vaccine adjuvant.

The development of the aquatic vaccine TEMPO CNF hydrogel adjuvant formulation was described in chapter 3. The hydrogel design process started with a modified procedure taken from

previous research of physically crosslinking CMC with citric acid. Difficulties in crosslinking the TEMPO CNF arose after mixing in bacterin. It was discovered that both TEMPO CNF and the bacterin have negative charges which likely makes the two materials repel each other. Strategies of dewatering the TEMPO CNF and bacterin mixture to promote hydrogel formation were explored through mixing higher weight percentages of TEMPO CNF with the bacterin, heating the bacterin and TEMPO CNF mixture, and filtering the bacterin and TEMPO CNF mixture. Vacuum filtration was found to form TEMPO CNF and bacterin hydrogels with the most desired properties and could be easily tuned to create hydrogels of different weight percentages. The effect of wash steps on the formed hydrogel's pH and diffusion of loaded dye or bacterin were also explored. Over time the wash steps increased the hydrogel's solution back to neutral but caused significant diffusion of the bacterin dye model out of the hydrogel.

Chapter 4 explored methods of developing and improving the delivery method of the hydrogels into the salmon. The fully wet hydrogels were found to be too soft and big to be reasonably implanted into the salmon. Air drying, controlled drying with a dehydrator, and freeze drying were explored to create smaller and stronger hydrogels that could be more easily delivered. Drying with a dehydrator was discovered to be the best method of improving the hydrogels for this application because it was able to create smaller and stronger hydrogels while being a quick, cheap, and easily scalable method. The properties of the dried hydrogel were analyzed in addition to their rehydration properties. The hydrogels would significantly increase in weight and size after being dried while remaining relatively stable in aqueous solution before starting to break down over long periods of time (months). Two delivery methods were developed based on the drying and rehydrating properties of the hydrogels and were further explored in chapter 6.

Chapter 5 explored the diffusive properties of the formulated and dried hydrogels. ELISAs performed on the hydrogels showed that drying the hydrogels with a dehydrator did not significantly affect the antibody response of the loaded bacterin. Additionally, the ELISAs showed diffusion of bacterin out of the hydrogels over 300 degree days before plateauing until 600 degree days. A diffusion model experiment was designed where the bacterin was modeled using an anionic dye called Coomassie Brilliant Blue. The data collected from the experiment provided proof of concept for the diffusion testing design but was too noisy to calculate diffusion rates from. With some improvements, this diffusion testing design could collect significant diffusion data. Additionally, an *in vivo* fluorescence study was performed that showed signs of bacterin diffusing out from the hydrogels in the salmon over time and that the delivery method led the hydrogels to become embedded between the liver and pyloric caeca of the salmon. The fluorescence study also suggested that the pyloric caeca played some role in the salmon's immune response or created some attractive forces to the bacterin since red fluorescence signals were found consistently on the pyloric caeca from the injected bacterin samples.

Lastly, chapter 6 described the two salmon safety studies conducted to analyze the hydrogel delivery method along with the salmon's reactions to the hydrogels. The first safety study explored a delivery method where an incision the size of the hydrogel's length was made, and the hydrogel was pushed into the peritoneum cavity using tweezers. It was found that most of the hydrogels fell out of the salmon in the first safety study before sampling, making the delivery method inefficient. The second safety study explored a delivery method where an incision about the diameter of the hydrogel was made, and the hydrogel was implanted into the salmon using an 8-gauge needle. Most of the hydrogels remained in the salmon after 300 degree days making this delivery method more efficient than the one used in the first safety study. Additionally, the hydrogel did not appear

to affect the growth and development of the salmon but did cause significantly more adverse effects such as lesions and cysts than the PBS and bacterin control.

## 7.2 Recommendations and Future Work

Overall, the TEMPO CNF citric acid crosslinked hydrogel could be a possible adjuvant for aquatic vaccines. The formulation and delivery method of the hydrogels could continue to be explored and improved upon. Research could be conducted to see how different weight percentages of TEMPO CNF affect the hydrogel's mechanical, structural, and diffusive properties. Additionally, different concentrations of citric acid crosslinker could be explored to see how it affects the properties of the hydrogel. Delivery methods of the hydrogel could be improved upon by creating a hydrogel mold that makes even skinnier and longer hydrogels that could fit inside a smaller size needle for easier delivery and to reduce the likelihood of the hydrogel falling back out of the salmon.

The diffusion model experiment explored in this thesis should also be repeated with the suggested changes made to improve the reliability, accuracy, and precision of the obtained measurements. The diffusion experiment could also be conducted to measure the intensity of stained *Vibrio anguillarum* instead of Coomassie Brilliant Blue dye to provide a more accurate diffusive model. Diffusive studies could also be conducted in a medium that more closely mimics the properties of the salmon's peritoneum cavity than PBS. Additionally, the next *in vivo* fluorescence study to analyze diffusion should stain the TEMPO CNF with calcofluor white instead of FITC for a more reliable fluorescent tag. The fluorescence imaging setup could also be improved upon by increasing the intensity of the light source and using a camera with less linear noise to improve the captured images and increase the ability to detect fluorescent signals. Salmon

controls without any fluorescent bacterin or CNF should also be imaged to see if red fluorescence signals are detected in salmon other than the presence of bacterin.

Another cellulose nanomaterial adjuvant should also be developed as a shear-thinning hydrogel since the most difficulties with this hydrogel formulation arose in how to effectively deliver it into the salmon. A shear-thinning hydrogel formulation could easily be injected into the salmon without the need for incisions. Shear-thinning hydrogels also typically have self-healing properties that would allow the hydrogel to form into the least invasive shape within the salmon's peritoneum cavity which would help reduce adverse reactions. A shear-thinning hydrogel could reduce adverse effects in the salmon while also increasing the efficiency and effectiveness of the vaccine's delivery method from the current formulation.

Lastly, further *in vivo* testing of the TEMPO CNF and bacterin citric acid crosslinked hydrogel formulation should be conducted. A study should be performed that compares the adverse effects caused by the hydrogel to the adverse effects caused by the commercial oil-based adjuvant. Another *in vivo* study that should be performed is an antibody response study comparing the hydrogel formulation in this thesis to the commercial aquatic vaccines and any other developed cellulose nanomaterial aquatic vaccines (such as the shear-thinning hydrogel). The last type of study that should be performed is a disease challenge study using the TEMPO CNF and bacterin citric acid hydrogel formulation to test how well the hydrogel protects the salmon from diseases.

## REFERENCES

1. Globe Newswire. Global Aquaculture Market to Reach \$245.2 Billion by 2027. Published 2021. Accessed May 10, 2022. <https://www.globenewswire.com/news-release/2021/07/12/2261055/0/en/Global-Aquaculture-Market-to-Reach-245-2-Billion-by-2027.html>
2. *Open Ocean Aquaculture.*; 2010. <https://www.everycrsreport.com/reports/RL32694.html#:~:text=Open ocean aquaculture employs less,in enclosures%2C such as ponds.>
3. Longo SB, Clausen R, Clark B. *The Tragedy of the Commodity : Oceans, Fisheries, and Aquaculture.* University Press; 2015.
4. Tal Y, Schreier HJ, Sowers KR, Stubblefield JD, Place AR, Zohar Y. Environmentally sustainable land-based marine aquaculture. *Aquaculture.* 2009;286(1-2):28-35. doi:10.1016/J.AQUACULTURE.2008.08.043
5. Crouse C, Davidson J, May T, Summerfelt S, Good C. Production of market-size European strain Atlantic salmon (*Salmo salar*) in land-based freshwater closed containment aquaculture systems. *Aquac Eng.* 2021;92. doi:10.1016/J.AQUAENG.2020.102138
6. Food and Agriculture Organization of the United Nations. Fisheries and Aquaculture - All Information Collections - Global Production. Published 2021. Accessed May 10, 2022. [https://www.fao.org/fishery/en/collection/global\\_production?lang=en](https://www.fao.org/fishery/en/collection/global_production?lang=en)
7. Forster J. What Can U.S. Open Ocean Aquaculture Learn From Salmon Farming? *Mar Technol Soc J.* 2010;44(3):68-79. doi:<https://doi-org.wv-o-ursus-proxy02.ursus.maine.edu/10.4031/MTSJ.44.3.4>
8. NOAA Fisheries. Atlantic Salmon (Protected). Published 2022. Accessed May 13, 2022. <https://www.fisheries.noaa.gov/species/atlantic-salmon-protected>
9. Marine Institute. Salmon Life Cycle. Published 2020. <https://www.marine.ie/Home/site-area/areas-activity/fisheries-ecosystems/salmon-life-cycle>
10. Norwegian Seafood Council. SALMON LIFECYCLE & FARMING. Accessed May 12, 2022. <https://salmon.fromnorway.com/sustainable-aquaculture/the-salmon-lifecycle/>
11. IMUA Loss Control & Claims Committee. Aquaculture: An Overview of Exposures, Loss Prevention and Underwriting Concerns. Published online 2008. Accessed May 14, 2022. [https://www.imua.org/Files/reports/Aquaculture\\_An Overview of Exposures, Loss Prevention and Underwriting Concerns.html#potex](https://www.imua.org/Files/reports/Aquaculture_An Overview of Exposures, Loss Prevention and Underwriting Concerns.html#potex)
12. Pincinato RBM, Asche F, Bleie H, Skrudland A, Stormoen M. Factors influencing production loss in salmonid farming. *Aquaculture.* 2021;532:736034. doi:10.1016/J.AQUACULTURE.2020.736034
13. Tavares-Dias M, Martins ML. An overall estimation of losses caused by diseases in the Brazilian fish farms. *J Parasit Dis Off Organ Indian Soc Parasitol.* 2017;41(4):913-918.

doi:10.1007/S12639-017-0938-Y

14. Barnes AC, Silayeva O, Landos M, et al. Autogenous vaccination in aquaculture: A locally enabled solution towards reduction of the global antimicrobial resistance problem. *Rev Aquac.* 2022;14(2):907-918. doi:10.1111/RAQ.12633
15. Kibenge FSB, Godoy MG, Fast M, Workenhe S, Kibenge MJT. Countermeasures against viral diseases of farmed fish. *Antiviral Res.* 2012;95(3):257-281. doi:10.1016/J.ANTIVIRAL.2012.06.003
16. Ma J, Bruce TJ, Jones EM, Cain KD. A Review of Fish Vaccine Development Strategies: Conventional Methods and Modern Biotechnological Approaches. *Microorganisms.* 2019;7(11):569. doi:10.3390/MICROORGANISMS7110569
17. Berg A, Rødseth OM, Tangerås A, Hansen T. Time of vaccination influences development of adhesions, growth and spinal deformities in Atlantic salmon *Salmo salar*. *Dis Aquat Organ.* 2006;69:239-248. doi:https://doi.org/10.3354/dao069239
18. Parks Canada. Restoring Atlantic salmon in the Clyburn Brook - Cape Breton Highlands National Park. Published 2022. Accessed June 7, 2022. <https://www.pc.gc.ca/en/pn-np/ns/cbreton/decouvrir-discover/conservation/saumon-salmon>
19. Komar C, Enright WJ, Grisez L, Tan Z. Understanding Fish Vaccination. *Intervet.* Published 2006. Accessed June 24, 2021. <https://thefishsite.com/articles/understanding-fish-vaccination>
20. Adams A. Progress, challenges and opportunities in fish vaccine development. *Fish Shellfish Immunol.* 2019;90:210-214. doi:https://doi.org/10.1016/j.fsi.2019.04.066
21. Mutoloki S, Munang'andu HM, Evensen Ø. Oral vaccination of fish - antigen preparations, uptake, and immune induction. *Front Immunol.* 2015;6(OCT):519. doi:10.3389/FIMMU.2015.00519/BIBTEX
22. Villumsen KR, Raida MK. Long-lasting protection induced by bath vaccination against *Aeromonas salmonicida* subsp. *salmonicida* in rainbow trout. *Fish Shellfish Immunol.* 2013;35(5):1649-1653. doi:10.1016/J.FSI.2013.09.013
23. Tafalla C, Bøgwald J, Dalmo RA. Adjuvants and immunostimulants in fish vaccines: Current knowledge and future perspectives. *Fish Shellfish Immunol.* 2013;35(6):1740-1750. doi:10.1016/J.FSI.2013.02.029
24. Midtlyng PJ, Reitan LJ, Lillehaug A, Ramstad A. Protection, immune responses and side effects in Atlantic salmon (*Salmo salar*L.) vaccinated against furunculosis by different procedures. *Fish Shellfish Immunol.* 1996;6(8):599-613. doi:10.1006/FSIM.1996.0055
25. Midtlyng PJ, Reitan LJ, Speilberg L. Experimental studies on the efficacy and side-effects of intraperitoneal vaccination of Atlantic salmon (*Salmo salar*L.) against furunculosis. *Fish Shellfish Immunol.* 1996;6(5):335-350. doi:https://doi.org/10.1006/fsim.1996.0034
26. Erkinharju T, Dalmo RA, Hansen M, Seternes T. Cleaner fish in aquaculture: review on diseases and vaccination. *Rev Aquac.* 2021;13:189-237. doi:10.1111/raq.12470

27. Holm KO, Nilsson K, Hjerde E, Willassen NP, Milton DL. Complete genome sequence of *Vibrio anguillarum* strain NB10, a virulent isolate from the Gulf of Bothnia. *Stand Genomic Sci.* 2015;10(1):1-12. doi:10.1186/s40793-015-0060-7
28. Haastein T, Holt G. The occurrence of vibrio disease in wild Norwegian fish. *J Fish Biol.* 1972;4(1). doi:10.1111/j.1095-8649.1972.tb05650.x
29. Frans I, Michiels CW, Bossier P, Willems KA, Lievens B, Rediers H. *Vibrio anguillarum* as a fish pathogen: Virulence factors, diagnosis and prevention. *J Fish Dis.* 2011;34(9). doi:10.1111/j.1365-2761.2011.01279.x
30. Myhr E, Larsen JL, Lillehaug A, Gudding R, Heum M, Hastein T. Characterization of *Vibrio anguillarum* and closely related species isolated from farmed fish in Norway. *Appl Environ Microbiol.* 1991;57(9). doi:10.1128/aem.57.9.2750-2757.1991
31. Mehtani D, Seth A, Sharma P, et al. *Biomaterials for Sustained and Controlled Delivery of Small Drug Molecules.* Elsevier Inc.; 2019. doi:10.1016/B978-0-12-814427-5.00004-4
32. Liu J, Liu J, Xu H, et al. Novel tumor-targeting, self-assembling peptide nanofiber as a carrier for effective curcumin delivery. *Int J Nanomedicine.* 2014;9(1):197. doi:10.2147/IJN.S55875
33. Metters AT, Lin C-C. Biodegradable Hydrogels: Tailoring Properties and Function through Chemistry and Structure. In: *Biomaterials.* CRC Press; 2007. doi:10.1201/9780849378898-5
34. Mahinroosta M, Jomeh Farsangi Z, Allahverdi A, Shakoory Z. Hydrogels as intelligent materials: A brief review of synthesis, properties and applications. *Mater Today Chem.* 2018;8:42-55. doi:10.1016/J.MTCHEM.2018.02.004
35. Gyles DA, Castro LD, Silva JOC, Ribeiro-Costa RM. A review of the designs and prominent biomedical advances of natural and synthetic hydrogel formulations. *Eur Polym J.* 2017;88:373-392. doi:10.1016/J.EURPOLYMJ.2017.01.027
36. Hennink WE, Van Nostrum CF. Novel crosslinking methods to design hydrogels. *Adv Drug Deliv Rev.* 2002;54(1):13-36. doi:10.1016/S0169-409X(01)00240-X
37. Feng L, Jia Y, Chen X, Li X, An L. A multiphasic model for the volume change of polyelectrolyte hydrogels. *J Chem Phys.* 2010;133(11):114904. doi:10.1063/1.3484236
38. Shi Z, Gao X, Ullah MW, Li S, Wang Q, Yang G. Electroconductive natural polymer-based hydrogels. *Biomaterials.* 2016;111:40-54. Accessed December 6, 2021. <https://www-sciencedirect-com.wv-o-ursus-proxy02.ursus.maine.edu/science/article/pii/S0142961216305221>
39. Ciolacu DE, Nicu R, Ciolacu F. Cellulose-based hydrogels as sustained drug-delivery systems. *Materials (Basel).* 2020;13(22):1-37. doi:10.3390/ma13225270
40. Gale EC, Powell AE, Roth GA, et al. Hydrogel-Based Slow Release of a Receptor-Binding Domain Subunit Vaccine Elicits Neutralizing Antibody Responses Against SARS-CoV-2. *Adv Mater.* 2021;33(51):1-35. doi:10.1002/adma.202104362

41. Roth GA, Gale EC, Alcantara-Hernandez M, et al. Injectable hydrogels for sustained codelivery of subunit vaccines enhance humoral immunity. *ACS Cent Sci.* 2020;6(10):1800-1812. doi:10.1021/acscentsci.0c00732
42. Patchan M, Graham JL, Xia Z, et al. Synthesis and properties of regenerated cellulose-based hydrogels with high strength and transparency for potential use as an ocular bandage. *Mater Sci Eng C.* 2013;33(5):3069-3076. doi:10.1016/J.MSEC.2013.03.037
43. Pal K, Banthia AK, Majumdar DK. Polymeric Hydrogels: Characterization and Biomedical Applications. *Des Monomers Polym.* 2009;12(3):197-220. doi:10.1163/156855509X436030
44. Yang WW, Pierstorff E. Reservoir-Based Polymer Drug Delivery Systems. *SLAS Technol.* 2012;17(1):50-58. doi:10.1177/2211068211428189
45. Caccavo D, Cascone S, Lamberti G, Barba A., Larsson A. Swellable hydrogel-based systems for controlled drug delivery. In: Sezer A., ed. *Smart Drug Delivery System.* IntechOpen Limited; 2015:2454–2712.
46. Sankar D, Shalumon KT, Chennazhi KP, Menon D, Jayakumar R. Surface Plasma Treatment of Poly(caprolactone) Micro, Nano, and Multiscale Fibrous Scaffolds for Enhanced Osteoconductivity. *Tissue Eng.* 2014;20(11-12):1689-1702. doi:10.1089/TEN.TEA.2013.0569
47. Farhat W, Venditti R, Mignard N, Taha M, Becquart F, Ayoub A. Polysaccharides and lignin based hydrogels with potential pharmaceutical use as a drug delivery system produced by a reactive extrusion process. *Int J Biol Macromol.* 2017;104:564-575. doi:10.1016/J.IJBIOMAC.2017.06.037
48. Jos Moura M, Faneca H, Pedroso Lima M, Helena Gil M, Margarida Figueiredo M. In Situ Forming Chitosan Hydrogels Prepared via Ionic/Covalent Co-Cross-Linking. *Biomacromolecules.* 2011;12:3275-3284. doi:10.1021/bm200731x
49. Bhattarai N, Gunn J, Zhang M. Chitosan-based hydrogels for controlled, localized drug delivery. *Adv Drug Deliv Rev.* 2010;62(1):83-99. doi:10.1016/J.ADDR.2009.07.019
50. Rowley JA, Madlambayan G, Mooney DJ. Alginate hydrogels as synthetic extracellular matrix materials. *Biomaterials.* 1999;20(1):45-53. doi:10.1016/S0142-9612(98)00107-0
51. Charulatha V, Rajaram A. Influence of different crosslinking treatments on the physical properties of collagen membranes. *Biomaterials.* 2003;24(5):759-767. doi:10.1016/S0142-9612(02)00412-X
52. Sun G, Mao JJ. Engineering dextran-based scaffolds for drug delivery and tissue repair. *Nanomedicine (Lond).* 2012;7(11):1771. doi:10.2217/NNM.12.149
53. Nusgens B V. Hyaluronic acid and extracellular matrix: a primitive molecule? *Ann Dermatol Venereol.* 2010;137(SUPPL. 1):S3-S8. doi:10.1016/S0151-9638(10)70002-8
54. Morán MC, Miguel MG, Lindman B. DNA gel particles. *Soft Matter.* 2010;6(14):3143-3156. doi:10.1039/B923873E

55. Hu X, Tang Y, Wang Q, et al. Rheological behaviour of chitin in NaOH/urea aqueous solution. *Carbohydr Polym.* 2011;83(3):1128-1133. Accessed December 6, 2021. <https://www.sciencedirect.com/wv-o-ursus-proxy02.ursus.maine.edu/science/article/pii/S0144861710007435>
56. Gasperini L, Mano JF, Reis RL. Natural polymers for the microencapsulation of cells. *J R Soc Interface.* 2014;11(100). doi:10.1098/RSIF.2014.0817
57. Voge CM, Kariolis M, MacDonald RA, Stegemann JP. Directional conductivity in SWNT-collagen-fibrin composite biomaterials through strain-induced matrix alignment. *J Biomed Mater Res Part A.* 2008;86A(1):269-277. doi:10.1002/JBM.A.32029
58. Nechyporchuk O, Belgacem MN, Bras J. Production of cellulose nanofibrils: A review of recent advances. *Ind Crops Prod.* 2016;93:2-25. doi:10.1016/J.INDCROP.2016.02.016
59. Lin N, Dufresne A. Nanocellulose in biomedicine: Current status and future prospect. *Eur Polym J.* 2014;59:302-325. doi:10.1016/J.EURPOLYMJ.2014.07.025
60. Trache D, Tarchoun AF, Derradji M, et al. *Nanocellulose: From Fundamentals to Advanced Applications.* Vol 8.; 2020. doi:10.3389/fchem.2020.00392
61. Hossen MR, Dadoo N, Holomakoff DG, Co A, Gramlich WM, Mason MD. Wet stable and mechanically robust cellulose nanofibrils (CNF) based hydrogel. *Polymer (Guildf).* 2018;151:231-241. doi:10.1016/j.polymer.2018.07.016
62. Liu H, Liu K, Han X, et al. Cellulose Nanofibrils-based Hydrogels for Biomedical Applications: Progresses and Challenges. *Curr Med Chem.* 2020;27(28):4622-4646. doi:10.2174/0929867327666200303102859
63. Jorfi M, Foster EJ. Recent advances in nanocellulose for biomedical applications. *J Appl Polym Sci.* Published online 2015. doi:10.1002/app.41719
64. Moon RJ, Schueneman GT, Simonsen J. Overview of Cellulose Nanomaterials, Their Capabilities and Applications. *Miner Met Mater Soc.* 2016;68(9):2383-2394. doi:10.1007/s11837-016-2018-7
65. Purington E, Bousfield D, Gramlich WM. Fluorescent Dye Adsorption in Aqueous Suspension to Produce Tagged Cellulose Nanofibers for Visualization on Paper. *Cellul (London, England).* 2019;26(8):5117. doi:10.1007/S10570-019-02439-4
66. Navarro JRG, Bergström L. Labelling of N-hydroxysuccinimide-modified rhodamine B on cellulose nanofibrils by the amidation reaction. *RSC Adv.* 2014;4(105):60757-60761. doi:10.1039/C4RA06559J
67. Dong S, Roman M. Fluorescently Labeled Cellulose Nanocrystals for Bioimaging Applications. *J Am Chem Soc.* 2007;129(45):13810-13811. doi:10.1021/JA076196L
68. Patel I, Woodcock J, Beams R, et al. Fluorescently labeled cellulose nanofibers for environmental health and safety studies. *Nanomaterials.* 2021;11(4). doi:10.3390/nano11041015
69. Reid MS, Karlsson M, Abitbol T. Fluorescently labeled cellulose nanofibrils for detection

- and loss analysis. *Carbohydr Polym.* 2020;250:116943. doi:10.1016/J.CARBPOL.2020.116943
70. Ding Q, Zeng J, Wang B, et al. Effect of retention rate of fluorescent cellulose nanofibrils on paper properties and structure. *Carbohydr Polym.* 2018;186(November 2017):73-81. doi:10.1016/j.carbpol.2018.01.040
  71. Peretz R, Mamane H, Sterenzon E, Gerchman Y. Rapid quantification of cellulose nanocrystals by Calcofluor White fluorescence staining. *Cellulose.* 2019;26(2):971-977. doi:10.1007/S10570-018-2162-Z
  72. Abeer MM, Mohd Amin MCI, Martin C. A review of bacterial cellulose-based drug delivery systems: their biochemistry, current approaches and future prospects. *J Pharm Pharmacol.* 2014;66(8):1047-1061. doi:10.1111/jphp.12234
  73. Zheng WJ, Gao J, Wei Z, Zhou J, Chen YM. Facile fabrication of self-healing carboxymethyl cellulose hydrogels. *Eur Polym J.* 2015;72:514-522. doi:10.1016/j.eurpolymj.2015.06.013
  74. Aulin C, Ahola S, Josefsson P, et al. Nanoscale Cellulose Films with Different Crystallinities and Mesosstructures—Their Surface Properties and Interaction with Water. *Langmuir.* 2009;25(13):7675-7685. doi:10.1021/la900323n
  75. Patiño-Masó J, Serra-Parareda F, Tarrés Q, Mutjé P, Espinach FX, Delgado-Aguilar M. TEMPO-Oxidized Cellulose Nanofibers: A Potential Bio-Based Superabsorbent for Diaper Production. *Nanomaterials.* 2019;9(9). doi:10.3390/NANO9091271
  76. Saito T, Kimura S, Nishiyama Y, Isogai A. Cellulose Nanofibers Prepared by TEMPO-Mediated Oxidation of Native Cellulose. *Biomacromolecules.* 2007;8(8):2485-2491. doi:10.1021/bm0703970
  77. Raucci MG, Alvarez-Perez MA, Demitri C, et al. Effect of citric acid crosslinking cellulose-based hydrogels on osteogenic differentiation. *J Biomed Mater Res Part A.* 2015;103(6):2045-2056. doi:10.1002/JBM.A.35343
  78. EMD Millipore. *Endotoxin Removal: The Solution With Membrane Separation Technology.*; 2012.
  79. Subbotkin MF, Subbotkina TA. Effect of Infection and Injections of Substances of Different Origin on Lysozyme in Cyprinids (Family Cyprinidae) (Review). *Inl Water Biol.* 2020;13(2):297-307. doi:10.1134/S1995082920020133/TABLES/1
  80. Park JY, Park CW, Han SY, Kwon GJ, Kim NH, Lee SH. Effects of pH on Nanofibrillation of TEMPO-Oxidized Paper Mulberry Bast Fibers. *Polymers (Basel).* 2019;11(3). doi:10.3390/POLYM11030414
  81. Kaberova Z, Karpushkin E, Nevoralová M, Vetrík M, Šlouf M, Dušková-Smrcková M. Microscopic structure of swollen hydrogels by scanning electron and light microscopies: Artifacts and reality. *Polymers (Basel).* 2020;12(3). doi:10.3390/polym12030578
  82. Dadoo N, Zeitler S, McGovern AD, Gramlich WM. Waterborne functionalization of cellulose nanofibrils with norbornenes and subsequent thiol-norbornene gelation to create

- robust hydrogels. *Cellulose*. 2021;28(3):1339-1353. doi:10.1007/s10570-020-03582-z
83. Licata NA, Mohari B, Fuqua C, Setayeshgar S. Diffusion of Bacterial Cells in Porous Media. *Biophys J*. 2016;110(1):247-257. doi:10.1016/j.bpj.2015.09.035
  84. Lee KL, Hubbard LC, Hern S, Yildiz I, Gratzl M, Steinmetz NF. Shape matters: the diffusion rates of TMV rods and CPMV icosahedrons in a spheroid model of extracellular matrix are distinct. *Biomater Sci*. 2013;1(6):581-588. doi:10.1039/C3BM00191A
  85. Nørstebø SF, Paulshus E, Bjelland AM, Sørum H. A unique role of flagellar function in *Aliivibrio salmonicida* pathogenicity not related to bacterial motility in aquatic environments. *Microb Pathog*. 2017;109:263-273. doi:10.1016/J.MICPATH.2017.06.008
  86. Purington E, Bousfield D, Gramlich WM. Fluorescent Dye Adsorption in Aqueous Suspension to Produce Tagged Cellulose Nanofibers for Visualization on Paper. *Cellul (London, England)*. 2019;26(8):5117. doi:10.1007/S10570-019-02439-4

# APPENDICES

## Appendix A: Stress Strain Curves from Mechanical Testing

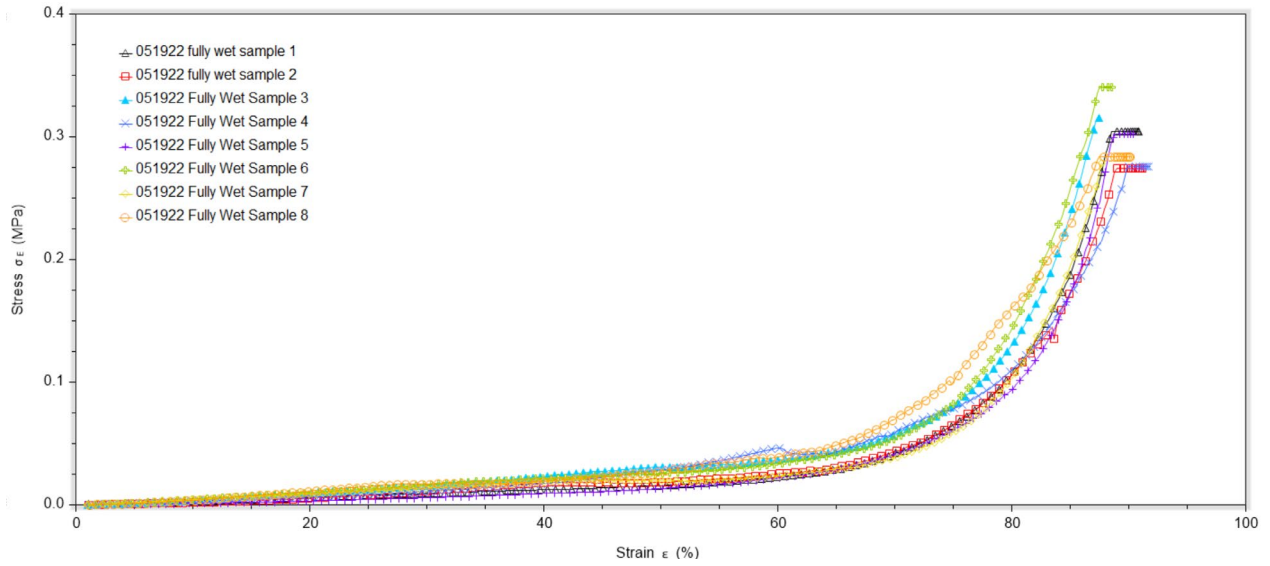


Figure A1: Stress-strain curve of fully wet hydrogel samples.

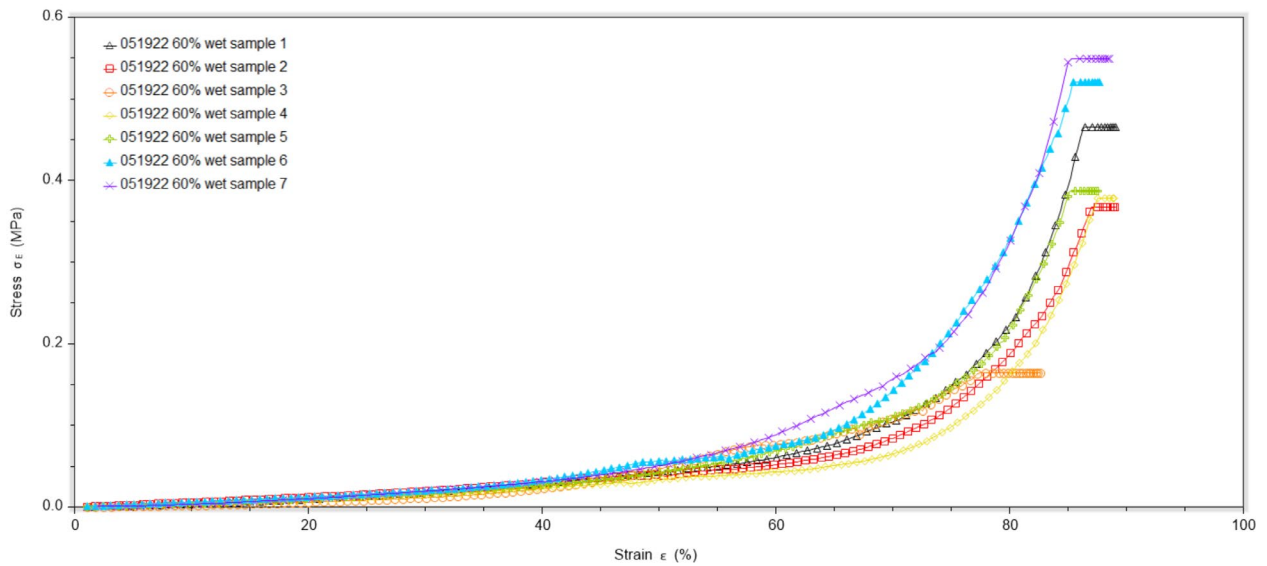


Figure A2: Stress-strain curve of 60 wt% hydrated hydrogel samples.

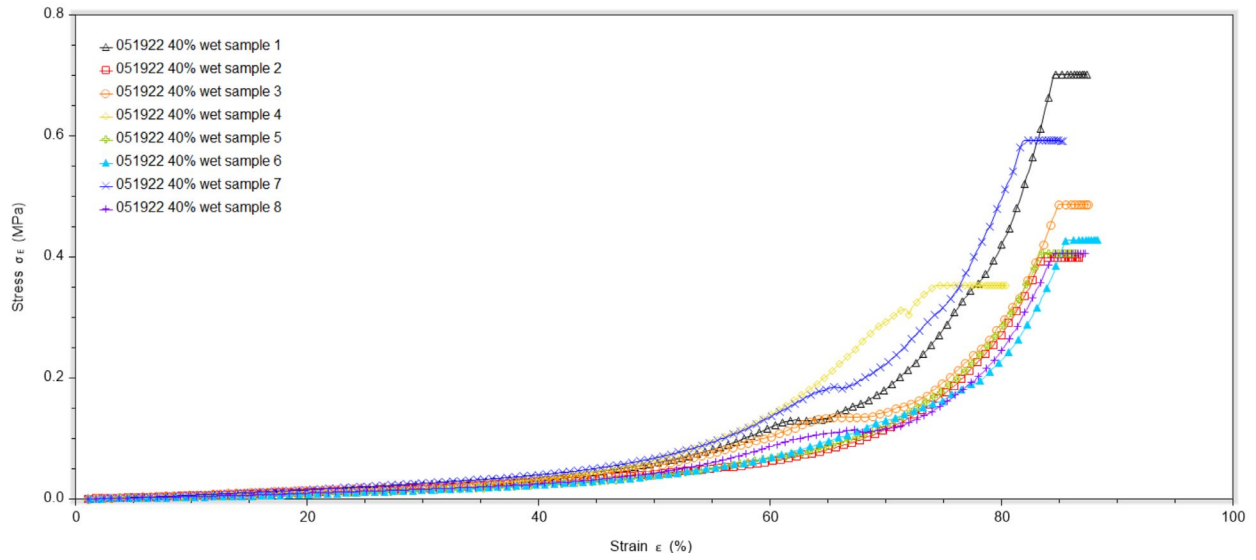


Figure A3: Stress-strain curve of 40 wt% hydrated hydrogel samples.

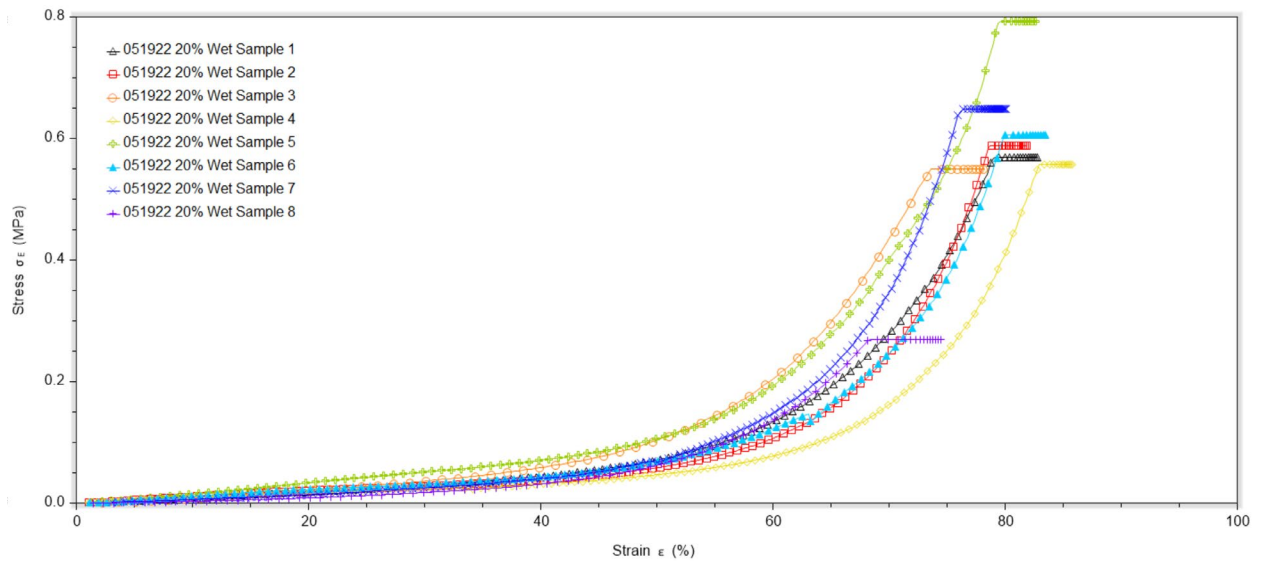


Figure A4: Stress-strain curve of 20 wt% hydrated hydrogel samples.

## Appendix B: Short Term Rehydrating Data

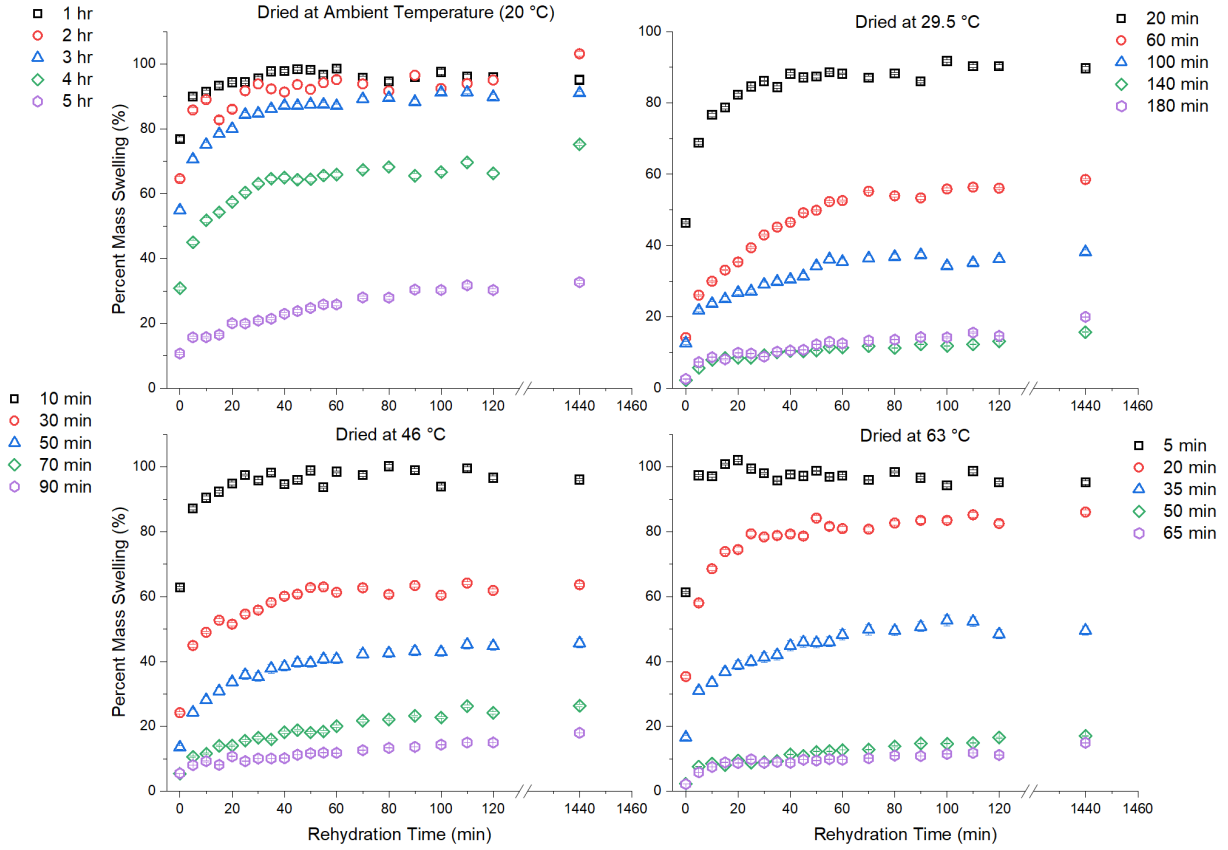


Figure B1: Short term hydrogel rehydrating percent of initial mass curves

## Appendix C: Salmon Scoring Reference Sheet

Table C1: Scoring for Visual Appearance of Abdominal Cavity

Score	Visual appearance of abdominal cavity
0	No visible lesions
1	Very slight adhesions seen as tiny fibrous tissue most frequently localized close to the injection site. Easily detached.
2	Adhesion seen as more clearly defined fibrous threads connecting different organs or viscera to peritoneum in limited areas. The adhesions are easily detached and organs are intact following detachment.
3	Firm adhesions connecting some or several organs. Viscera may be firmly attached to the peritoneum but are detached during autopsy without any damage to the different organs or peritoneum/muscle tissue. May be observed as grayish fibrous tissue film covering organs. Swim bladder may be attached to the viscera.
4	Similar to score 3 but more pronounced adhesion in and around organs. Interconnecting organs referred to as an organ package may be observed, where the organs appear as one unit, bound together by fibrous connective tissue. Smaller granulomas may be present in or around the organs. Separation of organs attached via fibrous connective tissue will result in organ damage. Viscera cannot be detached from the peritoneum without damaging it.
5	Extensive lesions affecting several organs in the abdominal cavity. In large areas, the peritoneum is thickened and opaque. Larger granulomas in viscera, together with extensive bindings between viscera and peritoneum. The peritoneum and fillet/muscle is damaged when removing the viscera. The side effects are ethically unacceptable.
6	Even more pronounced than 5. Viscera cannot be removed without severe damage to the muscle fillet. The side effects are ethically unacceptable.

Table C2: Scoring for Pigment (Melanin) for Viscera

Score	Visual appearance on the viscera
0	No melanin
1	Some faint melanin or small spots affecting small areas of the viscera
2	Moderate amounts on or within one or more organs
3	Extensive melanin deposits on viscera

Table C3: Scoring for Pigment (Melanin) for Peritoneum

Score	Visual appearance on peritoneum in the abdominal cavity
0	No melanin
1	Small amounts. Spot(s) or faint shading affecting small areas. Easy to remove.
2	Moderate amounts. The melanin can be manually removed at slaughter without severely damaging the peritoneum. May cause downgrading of final product.
3	Extensive melanin deposits on the peritoneum and into the fillet. Cannot be removed without severely damaging peritoneum/muscle/fillet. Will result in significant downgrading of the final product.

Table C4: Formulation Residues in the Abdominal Cavity

Score	Grading of product formulation residues
0	No product formulation residues.
1	Product formulation residues are enclosed in vesicles. Only small amounts of residues.
2	Larger amounts of formulation residues enclosed in vesicles and often small or moderate amounts of unbound, free flowing product.
3	Extensive quantities of unbound, free flowing product. Appears “recently vaccinated”

## **AUTHOR BIOGRAPHY**

Kora Kukk is from Brookfield, Connecticut. She started accelerating her academics when she skipped sixth grade. She graduated from Brookfield High School in the spring of 2017 before enrolling into the University of Maine. She played Division I soccer for the University of Maine from 2017-2021 while pursuing her Bachelor's in Biomedical Engineering. She was named one of the 2020-2021 America East Presidential Scholar-Athletes. Kora joined Mason labs in the summer of 2018 and fell in love with conducting research. She also was a part of the Honors College at the University of Maine and completed her creative writing honors thesis, *The Hate Within*, in the spring of 2021. In the spring of 2021, she graduated from the University of Maine with her Bachelor's in Biomedical Engineering with a 3.96 GPA and was accepted into the accelerated 4+1 Master's degree program to pursue her Masters of Science in Biomedical Engineering. She is a candidate for the Masters of Science degree in Biomedical Engineering from the University of Maine in August 2022.